SWANSEA UNIVERSITY

UNIVERSITAT POLITÈCNICA DE CATALUNYA

AN IMPROVED X-FEM SOLUTION TO ENSURE NORMAL STRESS CONTINUITY FOR TWO–PHASE FLOW PROBLEMS

Advisors

Dr. Sergio ZLOTNIK

Esther SALA LARDIES

HAYRULLAH KERİM BOZKUŞ

June 20, 2012

Acknowledgments

I would like to express my gratitude to my advisors **Dr. Sergio ZLOTNIK** and **Esther Sala LARDIES** for their help with my thesis. They have always encouraged me and supported me and this let me finish all the tasks with success. Without any hesitation, I can easily say that this work wouldn't finish without their support. It has been a great pleasure for me to be working with them.

I appreciate the full scholarship, provided to me by *The European Commission*, which allowed me to focus only on my academic work during my master degree education. This financial support has provided me not only academic achievements but also it has given me the chance to have the best moments in my life during my master degree education at **Swansea University, UNITED KINGDOM** and at **Universitat Politécnica de Catalunya, SPAIN.**

Many thanks to **Régis Cottereau** and to all the people working at *Mécanique des Sols, Structures et Matériaux* for the nice discussions on the applications of X-FEM during my 7 weeks internship in **MSSMAT (Mécanique des Sols , Structures et Matériaux) Laboratory of Ecole Centrale Paris, FRANCE.** I had a chance to see the applications of my theoretical knowledge in this laboratory.

Also thanks to all the members of **LaCáN (Laboratori de Cálcul Numéric) Laboratory of Universitat Politécnica de Catalunya, SPAIN** for sharing all the educational materials of LaCáN with me and their very friendly attitude. Without having my breaks with them, I don't think I could enjoy this work so much.

My special thanks to my parents to my uncle, **Servet SOYAÇIKGÖZ**, and to my girlfriend, **Remziye YILMAZ**, who have always supported me during my education life and and given me the strength to be successful with all this work.

Presentation of the Thesis

In this thesis, starting from the foundations of the Theory of Classical Finite Elements Method, the basic principles of Extended Finite Elements Method (X-FEM) are explained. Why X-FEM takes place in many applications in industry is also emphasized. Although X-FEM has many various applications in different disciplines of engineering, the main focus is on the numerical solutions of the two–phase flows using the method. Level Set Method (sometimes it is abbreviated as LSM) is also preferred for the tracking of the interphase position because of its easy implementation, efficiency and reliability.

After presenting the introduction and the problem definition, the Theory of Finite Elements Method is explained just before the explanation of Extended Finite Elements Method so that the difference between two methods can be noticed more easily. The advantages and disadvantages of both methods are also emphasized.The basic idea of X-FEM is to track the location of interface using a level set function and enrich the Finite Elements Method interpolation space in order to reproduce discontinuities. The elements that are cut by the interface (enriched elements) are divided into smaller cells with the aim of calculating the integral contributions coming from the enriched elements to the global system of linear system of equations accurately.

Lastly, an additional method for obtaining the accurate numerical solution in the vicinity of interface of multiphase flows is given. A MATLAB code that is able to solve the governing physical equations using the mentioned additional technique to get a better solution for the two–phase problems is also developed and submitted with the thesis. The code is written for getting the solution of a two dimensional cell growth test problem however application of the technique is straightforward for a three dimensional case. After presenting the results of the code applied to a test case a comprehensive appendix chapter is also provided with the aim of explaining the basics related to Finite Elements Method and a list of publications related to Extended Finite Elements Method is also given in the same part to give the reader a further insight related to the field.

Contents

List of Figures

List of Tables

Chapter 1

INTRODUCTION AND MOTIVATION

1.1 X-FEM And Improvement Of The Method For Two–Phase Flows

Numerical methods are extremely important for design and development of engineering systems since when used appropriately they provide very good approximations of the solutions of engineering problems. Among these methods, Extended Finite Elements Method is a versatile numerical tool for modelling singularities and discontinuities in many engineering problems in mainly Oil and Gas, Mining, Aviation, Transportation and Biomechanics Industries. In this thesis a method which is an improvement of Extended Finite Elements Method is suggested and applied on setup of cell growth problems.

It is useful to emphasize that the applications of Extended Finite Elements Method in biomechanics industry are not only limited to cell growth or tumour growth problems only. For example, the term *neuronavigation* means the computerized tools that are used by the neurosurgeons within the confines of the skull or vertebral column during surgery and in Vigneron et al. (2011) it is stated that today's neuronavigation systems can not adapt to changing intraoperative conditions over time and Extended Finite Elements Method can be used to update the preoperative brain images taken using intraoperative MRI and the article, using Extended Finite Elements Method, presents a system that is capable of updating

3D preoperative images in the presence of brain shift and successive resections. In the model described in Vigneron et al. (2011) use of X-FEM instead of FEM for modeling discontinuities makes it possible to build the biomechanical model offline before the operation starts and does not need to be remeshed during the surgery.

However, in this work we will address the application of X-FEM in biomechanics industry. This includes developing an X-FEM code and applying it on a cell growth problem experiment setup in which the main aim is to let tissues or organs to be grown from implantation and by this way it is aimed to eliminate the immunological rejection. This process is carried out in a very well controlled sterile environment (bioreactors) so that cellular biochemical and physical activity can also be enhanced by observing and controlling the conditions in bioreactors. At this point, it is useful to emphasize that the cell grows in very complex geometries that is difficult to mesh, Extended Finite Elements Method can be used to easily overcome this difficulty. The main factors that affect the cell growth and should be modelled in the process can be listed as :

- Mechanical loading of the cell culture (distribution of shear stress along the surface and the pressure distribution along the surface of the cell culture).
- Oxygen, nitrogen and glucose distribution around the cell culture
- Distribution of other chemicals around the cell culture
- Ph in the environment
- Nutrient distribution in the environment
- Temperature of the environment

In this work we are going to address the one of the most important factors in cell growth experiments. That is the stress distribution along the interface. The same factors are also important in tumour growth problems. For this reason, the mentioned factors need to be closely monitored and controlled by the scientists.

Finite Elements Method has got some problems regarding the modelling of the critical regions in the problems where singularities or discontinuities take place. For example, in the interface of the numerical models where the cell culture and the fluid flowing around the cell culture is modelled as two different fluids, handling the discontinuities due to material property changes in multiphase elements becomes possible using Extended Finite Elements Method. Although, enriching the approximation spaces used in the problem using Extended Finite Elements Method makes it possible to capture the discontinuities, it does not necessarily mean that the solution in the critical regions of the domain will satisfy the physical laws.

In this work, to satisfy the continuity of the stresses in two–phase flow problems the continuity of the stress along the interface is imposed as an extra condition to be satisfied in the numerical solution so that the quality of the results obtained in the vicinity of the interphase in a two–phase flow increases not only due to the enrichment of the approximation spaces used by Extended Finite Elements Method but also the quality also increases due to the extra imposed continuity of stress.

Chapter 2

STATE OF THE ART

2.1 Introduction And History Of X-FEM

Classical Finite Elements Method (or know as Finite Element Analysis) is a very useful numerical tool for finding numerical solutions of engineering problems and it has been used for a long time for the solution of partial differential equations and integral equations. Finite Elements Method is a good choice for design purposes in engineering since most of the real life phenomena can be expressed with differential equations and analytical solution to these equations can not be calculated except for very few simple cases.

In spite of the usefulness of Finite Elements Method (FEM) there are a number of cases where the classical FEM method imposes restrictions which makes it difficult to get a good solution to the problem. These kind of problems usually include interior boundaries, discontinuities or singularities.

Extended Finite Elements Method is a brand new numerical method that was developed by Ted Belytschko, Nicolas Möes and John Dolbow in 1999. (Möes et al. (1999)) The method is an active field of research and quite open to improvements. Also, there exists only a few commercial implementations of the method. Since its invention, Extended Finite Elements Method has been used mainly in solid mechanics for modelling strong and weak discontinuities, cracks and singularities in the problems. (Sukumar et al. (2000); Xiao and Karihaloo (2007); Wyart et al. (2007); Unger et al. (2007)) But the applications of it in other areas such as multiphase flows (Sussman and Fatemi (1999); Groß and Reusken (2007); Fries

(2009)), solidification problems also exist. In the early attempts, involved use of polynomials as test functions, they needed attention towards mesh refinement for getting reasonable results. The method has been widely developed. (Belytschko et al. (2003); Dolbow et al. (2005); Zlotnik and Diez (2009); Cottereau et al. (2010))

X-FEM is very useful if complex geometries are involved in the problems. To obtain reasonably good approximations using Classical Finite Elements Method, the edges of the elements that are used in the mesh have to coincide with geometrical features such as the boundary of the structure, material interfaces and cracks. In addition to this, the meshes must be very fine in the neighbourhood of discontinuities to be able to capture the high gradient values appearing in the applications. It is possible to use the automated meshing algorithms to satisfy this geometric conditions however there is no guarantee that these algorithms can generate the mesh with desired properties. The more geometry in the problem becomes more complex, the possibility of the automated meshing algorithms used to fail increases.

In classical Finite Elements Method for moving interface problems the condition that mesh has to conform the interface becomes very costly. This is a very big problem for simulating phenomenon like melting of materials, oceanography and flame propagation. By introducing X-FEM in the solution, the enrichment functions can be chosen to represent the geometrical features mentioned above without the necessity of remeshing. In X-FEM interpolation is enriched in order to be able to capture singularities, discontinuities in the solution. Even very simple meshes that are independent of the geometry may be used in combination with the X-FEM to get reasonable good results to the engineering problems in consideration. This is the main idea of X-FEM. In cases where Classical Finite Elements or Finite Volumes methods fail X-FEM is a useful tool for finding the reasonable approximate solution to the problem by using the partition of the unity concept. In this thesis, X-FEM is used to find solution to two–phase flows which appear in many fields of mechanics and physics. X-FEM not only improves the global solution obtained by Finite Elements Method but also it can capture the discontinuous gradients of the solution across the interface which leads getting a better solution along the interface. In most of the cases, the change in the shape of the interface is dependant on the fluxes and stress around the interface. (Knapen et al. (2007))

The contribution of this thesis is proposing a new method for improving the solution obtained by Extended Finite Elements Method in the vicinity of the interface of two–phase flows by enforcing continuity of stress along the interface while using a structured mesh and an Eulerian framework in the context of X-FEM. The results to the cell growth test problem are given in chapter 6.

2.2 Information About Discontinuity And Singularity Concepts

As it is mentioned in the previous section, one of the main difficulty when trying to calculate a numerical result is the discontinuities in the domain. By the term *discontinuity*, it is meant that there exists a rapid change of the field quantity over a length which is small enough compared to the dimensions of the problem. Some examples to these discontinuity can be stated as a list at this point:

- Boundary layers
- Shocks
- Pressure and velocity fields at the interface in a multiphase fluid flow problems
- Stresses and strains in solid interfaces
- Contact stresses at joints
- Other discontinuities due to the materials used in the system

It is also important to note that in literature the limit of the ratio of the length on which the rapid changes occur to the ratio of the problem dimensions can be considered as different in different sources.

In engineering problems there are mainly two types of discontinuities:

1. **Strong Discontinuities:** It means that the variable has a jump itself
2. **Weak Discontinuities:** It means that the gradient of the variable has a jump.

The examples of strong and weak discontinuities are plotted in Figure 2.1. In this figure the first variable has a rapid change at the unity length and this is named as a *strong discontinuity*. Only the slope of the second variable changes along the same

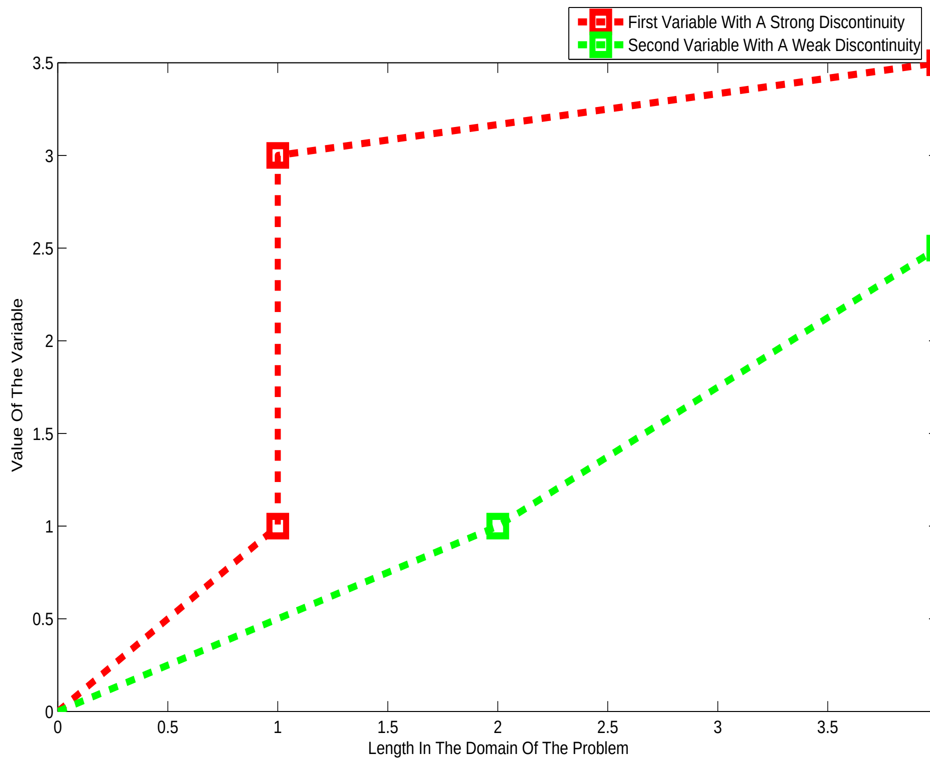

Figure 2.1: Changes of Two Different Variables Over The Same Length

length and for this reason this kind of discontinuity is named as a *weak discontinuity*.

Lastly, in mathematics *singularities* are defined as points where a mathematical object is not defined or does not well-behave. This can be exemplified by mentioning the points in the problem domain where the solution for stress tensor at that point gives an infinite component of the tensor. In solid mechanics, singularities can occur at crack tips. To deal with singularities and discontinuities in the domain, a mesh refinement in the critical region (by critical region singularities and discontinuities are meant) is needed in addition to the aligning the edges of the elements used. Extended Finite Elements Method is basically used to overcome this kind of difficulties using structured simple meshes. Optimal convergence rates can be achieved by X-FEM where there are various discontinuities and singularities in the domain. However, a tracking mechanism is needed for determining the location of places in the problem on which singularities and discontinuities exist. There are many options for this but Level Set Method is used in this thesis to achieve this goal and details are provided in section 4.5

2.3 State Of The Art And Applications Of X-FEM In Industry

There are many fields where Extended Finite Elements Method is used to solve engineering problems. For example:

In Oil and Gas Industry, there is an immense amount of interest in researching the hydraulic and mechanical properties of fractures deep well injection of liquids, CO2 sequestration and underground storage of natural gas with the aim of producing oil and gas more efficiently. Estimates of fault permeability can range over several orders of magnitude for a single location. So, the hydraulic behaviour of faults becomes one of the greatest components of uncertainty in risk assessments and cost analyses in oil and gas industry.

Faults and fractures in rocks are the main reasons for discontinuities in the displacement and strain fields during production and injection schedules in reservoirs. Generally *Hydraulic fracturing* which includes usage of pressurized water to create cracks in the rock is a technique used during oil and gas production. It is useful to emphasize that capturing of the discontinuities that occur in this process (which usually includes very complex geometries) accurately by using Standard Finite Element Analysis with a structured mesh is impossible whereas *Extended Finite Elements Method* can be used to calculate such discontinuities accurately. As it is understood from the list of references provided in Appendix B , until now X-FEM is mainly used to model the fracture/fault propagation.

The improvement of an Extended Finite Elements Method for mechanical fracture/fault evolution has a significant industrial potential. It is particularly important for the Oil and Gas Industry where the technique leads to obtaining improved predictions for porosity/permeability changes in coupled geomechanical reservoirs. So, developing efficient simulation methods with the objective of accurately predicting the three-dimensional network of hydraulic fractures considering rock self-contact, inhomogeneity, and poroelasticity is a key factor in oil and gas industry not only to reduce down the cost but also to produce oil and gas more efficiently.

In aviation industry, safety is always the most important factor in designs. Today's aircraft structures are designed using a basic load carrying shell structure reinforced by frames and longerons in the bodies and a skin stringer construction supported by spars and ribs in the surfaces. However, it is known that defects or cracks in the such structures used in aviation industry almost always exist as a result of applied forces during the operation of the aircraft. These defects or cracks grow by time. In spite of the growing defects in the structure the aim is always maintaining a safe operation of the aircraft. For this aim, engineers have to inspect the aircraft to observe the major cracks in a time interval in which a devastating failure between two inspections never happens. Various models which include simplification of the phenomenon are used at this step to guess the time of failure. This is know as *Damage Tolerance Analysis*.

Extended Finite Elements Method is mainly used to predict the crack growth and also investigate the damage tolerance of composite aircraft structures in addition to modelling the fatigue failure during the operation of the aircraft. The main advantage provided by the Extended Finite Elements Method technique is that modelling discontinuities during these simulations requires less time due to the fact that the method avoids remeshing the during the numerical simulation. This is a very important property when a complex system is considered. Also since the method introduces a local enrichment which causes a small increase in number of total degrees of freedoms in the solution better solutions can be obtained in critical regions. Last example of usage of X-FEM in aviation industry could be solution of multiphase flow problems as well as changing phase problems in fluid theory. It is even possible to apply the technique to perform multi scale analysis of the mentioned models.

In Mining Industry, crack propagation and fatigue failure are also very important in designs in the equipment that serve Mining Industry so the publication related to Extended Finite Elements Method given in Structural Mechanics and Crack Propagation subsection of Appendix B also can be considered as the examples for applications of the method for mining industry. For example, crack growth of drill pipe is a typical example of one of the discontinuous problems in this field. It is difficult to simulate this phenomenon using regular Finite Elements Analysis where as Extended Finite Elements Analysis is able to give an accurate solution by just increasing the total number of degrees of freedoms in the problem to a reasonable level.

Also plasticity is another field in which X-FEM can be used to handle the discontinuous property of the desired phenomenon.

Chapter 3

PROBLEM STATEMENT

3.1 Basics And Notation Used

Some basic information used in the thesis is given in this section to make everything clear and make the notation used in the thesis straightforward:

Fluid is a substance that flows and deforms continuously under an applied shear force. Fluids are also defined as substances that can not sustain a shear force while at rest. No matter how small the applied shear stress is fluid continues to deform as long as the force is applied. Fluids do not have a fixed shape and they take the shape of the container in which they are kept. According to this definition liquid and gases are fluids. It is known that gases and liquids are made of individual molecules. As a result the measurement of properties of the fluid medium such as density or pressure is expected to fluctuate if a very small scale is used. However, if the scale used is selected properly the properties of fluid properties become continuous. For this reason it is very important to select the length scale used. In the continuum approach, continuous fields are given by an average over a cube which has got side length L. This length L should be selected satisfying the following conditions:

$$L >> \text{average intermolecular spacing} \quad \& \quad L << \text{characteristic length of the flow}$$

At this point, it is important to state that continuum approach does not give always good results of the fluid motion. To exemplify, the cases where the average intermolecular space is larger than the characteristic length of the flow can be considered. As it will be shown later, in some cases it is possible to model solid structures as fluids that have high viscosities compared to other fluids in the problem.

a is a scalar variable and $\overrightarrow{\mathbf{a}}$ is a vector and it has got components a_i .

For a three dimensional space $\overrightarrow{\mathbf{a}} = \begin{bmatrix} a_1 \\ a_2 \\ a_3 \end{bmatrix}$

Tensor is a indexed array and the rank of a tensor is total number of indices required to represent that tensor. In solution of fluid flow problems rank 2 tensors are widely used.

$\underline{\underline{\mathbf{S}}}$ is a rank two tensor which has got components S_{ij}

$\underline{\underline{\mathbf{S}}}$ can be written explicitly as $\underline{\underline{\mathbf{S}}} = \begin{bmatrix} S_{11} & S_{12} & S_{13} \\ S_{21} & S_{22} & S_{23} \\ S_{31} & S_{32} & S_{33} \end{bmatrix}$

Gradient of a scalar field ϕ is shown as $\nabla\phi$ and it can explicitly be written as:

$$\nabla\phi = \frac{\partial\phi}{\partial x_1}\overrightarrow{\mathbf{i}} + \frac{\partial\phi}{\partial x_2}\overrightarrow{\mathbf{j}} + \frac{\partial\phi}{\partial x_3}\overrightarrow{\mathbf{k}} \tag{3.1}$$

where $\overrightarrow{\mathbf{i}}$, $\overrightarrow{\mathbf{j}}$, $\overrightarrow{\mathbf{k}}$ are unit vectors in direction of axes x_1, x_2 and x_3.

Gradient of a vector $\overrightarrow{\mathbf{v}}$ is shown as $\nabla\overrightarrow{\mathbf{v}}$ and can explicitly be written as:

$$\nabla\overrightarrow{\mathbf{v}} = \begin{bmatrix} \frac{\partial v_1}{\partial x_1} & \frac{\partial v_1}{\partial x_2} & \frac{\partial v_1}{\partial x_3} \\ \frac{\partial v_2}{\partial x_1} & \frac{\partial v_2}{\partial x_2} & \frac{\partial v_2}{\partial x_3} \\ \frac{\partial v_3}{\partial x_1} & \frac{\partial v_3}{\partial x_2} & \frac{\partial v_3}{\partial x_3} \end{bmatrix} \tag{3.2}$$

Divergence of a vector $\overrightarrow{\mathbf{v}}$ **(velocity vector)** is shown as $\nabla \cdot \overrightarrow{\mathbf{v}}$ and it can explicitly be written as:

$$\nabla \cdot \overrightarrow{\mathbf{v}} = \frac{\partial \mathrm{v}_1}{\partial x_1} + \frac{\partial \mathrm{v}_2}{\partial x_2} + \frac{\partial \mathrm{v}_3}{\partial x_3} \tag{3.3}$$

Any tensor can be decomposed into its symmetric and skew symmetric parts. In case the tensor to be decomposed is the gradient of the velocity field shown as $\nabla\overrightarrow{\mathbf{v}}$ of which components are explicitly written in equation 3.2 :

$$\nabla\overrightarrow{\mathbf{v}} = \frac{\partial\ \mathrm{v}_i}{\partial\ x_j} = 0.5 \times \frac{\partial\ \mathrm{v}_i}{\partial\ x_j} + 0.5 \times \frac{\partial\ \mathrm{v}_i}{\partial\ x_j} \tag{3.4}$$

Equation 3.4 can be restated adding and subtracting the same term as:

$$\nabla\overrightarrow{\mathbf{v}} = \frac{\partial\ \mathrm{v}_i}{\partial\ x_j} = \underbrace{0.5 \times \left(\frac{\partial\ \mathrm{v}_i}{\partial\ x_j} - \frac{\partial\ \mathrm{v}_j}{\partial\ x_i}\right)}_{A} + \underbrace{0.5 \times \left(\frac{\partial\ \mathrm{v}_i}{\partial\ x_j} - \frac{\partial\ \mathrm{v}_j}{\partial\ x_i}\right)}_{B} \tag{3.5}$$

Terms in equation 3.5 :

$$\text{term A} = \nabla^s\overrightarrow{\mathbf{v}} = \varepsilon \rightarrow \text{is named as } \textit{strain rate tensor} \tag{3.6}$$

$$\text{term B} = \nabla^w\overrightarrow{\mathbf{v}} \rightarrow \text{is named as } \textit{vorticity tensor} \tag{3.7}$$

In fluid mechanics, strain rate tensor includes information related to the local velocity of strain. The vorticity tensor gives information on local rotation velocity.

Divergence of rank-2 tensor $\underline{\underline{\boldsymbol{\sigma}}}$ is a vector and shown as $\nabla \cdot \underline{\underline{\boldsymbol{\sigma}}}$ of which i^{th} component can be written using Einstein's notation as :

$$\left[\nabla \cdot \underline{\underline{\boldsymbol{\sigma}}}\right]_i = \sigma_{ij,j} \tag{3.8}$$

Level Surface is the union of the spatial positions in which a scalar has the same value and in two dimensional space it is named as *Contour Line.* If the scalar function is shown with symbol ϕ the unit normal vector to the Level Surface or Contour Line of ϕ is stated using the formula:

$$\overrightarrow{\mathbf{n}} = \frac{\nabla\phi}{\parallel \nabla\phi \parallel} \tag{3.9}$$

Equation 3.9 also gives the direction in which the maximum rate of change of ϕ

at that point exists.

Kronecker delta is a function defined as:

$$\delta_{ij} = \begin{cases} 1 & \text{if } i = j \\ 0 & \text{if } i \neq j \end{cases} \tag{3.10}$$

where the range of i and j changes from one to the dimensional space of the problem.

Before finishing the section, note that all the basics related to the Finite Elements Method is given in Appendix A.

3.2 Governing Equations Of Stokes Flow

Stokes flow, in other words *creeping flow* is a flow type in which the internal forces are small enough compared to the viscous forces. This means that Reynolds number is low. Reynolds number is defined as:

$$Re = \frac{\rho v L}{\mu} \tag{3.11}$$

where:

- ρ is the density of the fluid
- v is the mean velocity of the flow
- L is the characteristic length of the flow
- μ is the dynamic viscosity of the fluid.

Consequently, the flow can include very low velocities or very high viscosities, the third possibility is that the length scale of the flow is very small.

Starting from the form of momentum equation, which is derived in Appendix A.6.2, written for a fluid with constant material properties:

$$\rho \left(\overrightarrow{\mathbf{V}}_t + \left(\overrightarrow{\mathbf{V}} \cdot \nabla \right) \overrightarrow{\mathbf{V}} \right) = \nabla \cdot \underline{\underline{\boldsymbol{\sigma}}} + \underline{\mathbf{b}} \tag{3.12}$$

where :

- $\underline{\underline{\boldsymbol{\sigma}}}$ is Cauchy stress

- $\overrightarrow{\mathbf{V}}$ is velocity field

- $\underline{\mathbf{b}}$ is the force acting on unit volume of the material

For the Stokes flow, the term in equation 3.12 $((\overrightarrow{\mathbf{V}} \cdot \nabla) \overrightarrow{\mathbf{V}})$ is negligible since the effect of inertia is negligible. Assuming there is no time dependency, time derivative also disappears. So, the equation 3.12 reduces to :

$$\nabla \cdot \underline{\underline{\boldsymbol{\sigma}}} + \underline{\mathbf{b}} = 0 \tag{3.13}$$

This is equation represents the conservation of momentum in the time independent Stokes flow problem. Stokes flow momentum equation includes the balance of dynamical effect of externally applied forces and internal forces of a fluid. Here the sources of the internal forces are pressure and the viscosity of the fluid and external forces are body and surface forces applied to the fluid. Actually, Stokes flow equations are identical to the equations of isotropic incompressible elasticity. The only difference is the physical interpretation of the variables.

Because of the conservation of mass as explained in Appendix A.6.1, equation A.18 gives us a divergence free velocity in domain:

$$\nabla \cdot \overrightarrow{\mathbf{v}} = 0 \tag{3.14}$$

For a two–phase flow the equations 3.14 and 3.13 should be satisfied in both of the subdomains. In addition to this jump of the normal component of stress across the interface should also be zero:

$$[\![\underline{\underline{\boldsymbol{\sigma}}} \overrightarrow{\mathbf{n}}]\!] = 0 \qquad\qquad on\ \boldsymbol{\Gamma} \tag{3.15}$$

Next section includes information about the constitutive relations. It is important to note that the fluids used in our problem are all Newtonian fluids before giving the details.

3.3 Constitutive Relations

Viscosity is the most important property of a fluid which directly characterize the fluid-mechanical behaviour of the fluid in consideration. In another words, viscosity relates the stress acting on a fluid with the strain rate. Viscosity is also a measure of the resistance of the fluid to deform under applied shear stress. See figure 3.1 which is taken from White (2006). In the figure a fluid element sheared in one plane by a shear stress $\boldsymbol{\tau}$ takes place. The shear strain angle $\partial\theta$ will continuously grow with time as long as the shear stress is applied to the fluid element as shown in the figure. The upper surface moving at a speed ∂u larger than the lower. Such common fluids such as water, oil and air show a linear relation between applied shear and resulting strain rate.

$$\boldsymbol{\tau} \propto \frac{\partial\theta}{\partial t} \tag{3.16}$$

From the geometry in figure 3.1 the following relation can be written :

$$\tan \partial\theta = \frac{\partial u \, \partial t}{\partial y} \tag{3.17}$$

In the limit of infinitesimal changes this becomes:

$$\frac{d\theta}{dt} = \frac{du}{dy} \tag{3.18}$$

It is known from the equation 3.16 that the applied shear is also proportional to the velocity gradient for the common linear fluids. The constant of the proportionality is called the viscosity and shown by the symbol μ:

$$\tau = \mu \frac{d\theta}{dt} = \mu \frac{du}{dy} \tag{3.19}$$

The linear fluids which obeys the given formula in equation 3.19 is called *Newtonian Fluids.* (White (2006))

Constitutive relations in fluid mechanics give the relation between stress, velocity and strain rate. *Rheology* is the branch which researches this relation for different kinds of materials. The term is most commonly applied to liquids or liquid-like materials such as paint, catsup, oil well drilling mud, blood, polymer and molten

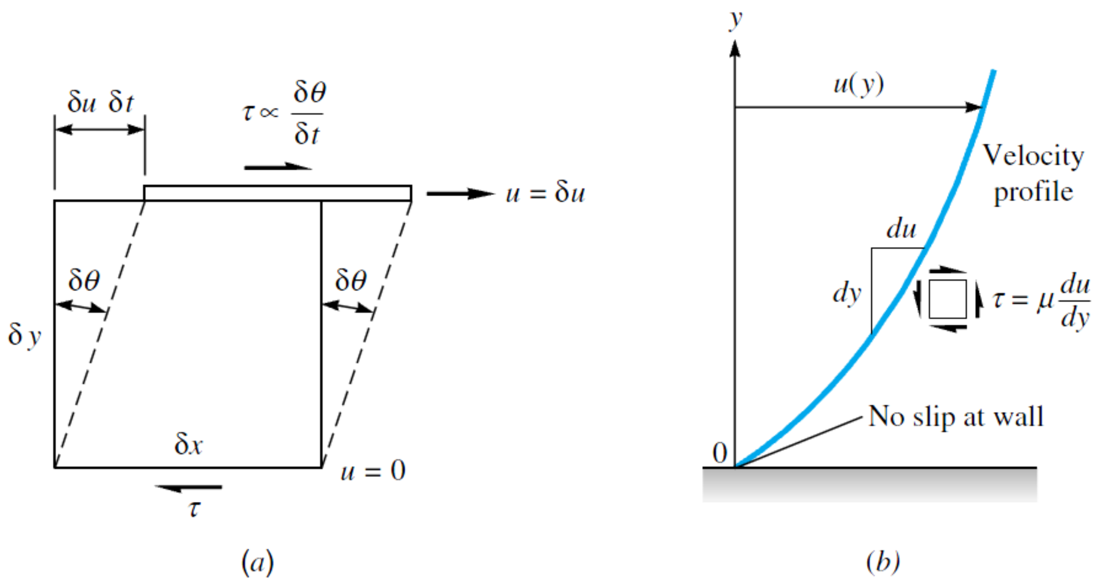

Figure 3.1: A Fluid Element Straining At A Rate $\partial\theta/\partial t$

plastics although it also includes the deformation of solids such as in metal forming or stretching of rubber. For more a detailed definition of rheology refer to Dealy and Wissbrun (1990).

Although for non-Newtonian fluids like polymers and some kind of oil there can be very complicated relations which also can change according to the history of deformation of the material for Newtonian fluids the relation between the stress and the rate of strain is linear. Since this is a reasonable assumption for many fluids in practice only Newtonian fluids are considered for the model in this thesis. The stress strain rate relationship for a Newtonian fluid can be written as:

$$\sigma_{ij} = -p\,\delta_{ij} + \tau_{ij} = \underbrace{-p\,\delta_{ij}}_{\text{Isotropic Part of Stress}} + \underbrace{2\mu\dot{\varepsilon}_{ij} + \lambda\dot{\varepsilon}_{kk}\delta_{ij}}_{\text{Deviatoric Part of Stress}} \tag{3.20}$$

where:

- μ is the dynamic viscosity of the fluid
- ε_{ij} is strain rate tensor defined in equation 3.6
- λ is bulk elasticity
- δ_{ij} is the Kronecker delta

Assuming that the fluid in consideration is incompressible the velocity field becomes divergence free ($\dot{\varepsilon}_{kk} = 0$). For this reason equation 3.20 reduces to the *Stokes law* defined as :

$$\sigma_{ij} = -p\,\delta_{ij} + \tau_{ij} = -p\,\delta_{ij} + 2\mu\dot{\varepsilon}_{ij} \tag{3.21}$$

Equation 3.21 can also be expressed in matrix form for an isotropic, incompressible Newtonian fluid as :

$$\underline{\underline{\boldsymbol{\sigma}}} = -p\,\underline{\underline{\mathbf{I}}} + 2\,\mu\nabla^s\overrightarrow{\mathbf{u}} \tag{3.22}$$

where:

- $\underline{\underline{\mathbf{I}}}$ is identity tensor
- $\overrightarrow{\mathbf{u}}$ is assumed to be the fluid velocity

Where the definition of the symmetric gradient operator ∇^s is defined as :

$$\nabla^s = 0.5 \times (\nabla + \nabla^T) \tag{3.23}$$

3.4 Boundary Conditions

In addition to the information provided so far, the problem must be completed using the appropriate boundary conditions. Typically the velocity is defined as Dirichlet boundary condition on Dirichlet part $\boldsymbol{\Gamma_D}$ of the boundary:

$$\overrightarrow{\mathbf{v}}(\overrightarrow{\mathbf{x}}) = \overrightarrow{\mathbf{v}}_D(\overrightarrow{\mathbf{x}}) \quad \text{where} \quad \overrightarrow{\mathbf{x}} \in \boldsymbol{\Gamma}_D \tag{3.24}$$

also a boundary traction $\overrightarrow{\mathbf{t}}$ is given as Neumann boundary condition on the Neumann part of the boundary represented with $\boldsymbol{\Gamma_N}$:

$$\underline{\underline{\boldsymbol{\sigma}}}(\overrightarrow{\mathbf{x}})\overrightarrow{\mathbf{n}} = \overrightarrow{\mathbf{t}}(\overrightarrow{\mathbf{x}}) \quad \text{where} \quad \overrightarrow{\mathbf{x}} \in \boldsymbol{\Gamma}_N \tag{3.25}$$

Pressure exist only by its gradient in Stokes problem for this reason a restriction of pressure is needed. One option is giving the value of the pressure at one position as a reference in cases where all boundary is only full of Dirichlet boundary conditions defined as velocities.

Chapter 4

FEM AND X-FEM SOLUTION OF STOKES FLOW

4.1 Extended Finite Elements Method

X-FEM method was developed in a research by the computational mechanics group at Northwestern University directed by Ted Belytschko. The main advantage of Extended Finite Elements Analysis as compared to Classical Finite Elements Analysis is that the features of interest such as fluid structure interface, phase boundaries and crack surfaces are represented independently from the mesh and using an Eulerian framework so that the solution can be easily obtained using a reasonable extra computational resources compared to Classical Finite Elements Analysis.

It is widely known that meshing is the biggest problem in design stage of complex industrial applications such as designing cars, bridges or machines for specific purposes. In a complex designs in industry, for an average company it is considered to be normal to spend more than % 60 of the total time of the design stage to have a good mesh. Since the computational mesh used in the numerical analysis directly effects the errors associated to the numerical solution it is very important indeed. However, remeshing the whole computational domain in every time step is a very time consuming process. This becomes extremely important especially in applications where the deformations in the problem is big. Meshing is not only a time consuming process but also its computational cost is very high. Since

Extended Finite Elements Method does not require remeshing in the solutions of the problems and can calculate the solution where there are moving interfaces involved in the problem Extended Finite Elements Method becomes a versatile tool for getting solution in this kind of problems. When Extended Finite Elements Method is used even in complex applications, just using a structured mesh is enough.

Extended Finite Elements Method is specifically handy in cases where the strain rate is discontinuous due to the continuity of stresses and a change in material properties. Extended Finite Elements Method adds the extra degrees of freedoms to the critical locations that is determined by using a level set function. By the usage of this Level Sets in Extended Finite Element Analysis technique it becomes possible to describe and accurately solve multiphase problems using an Eulerian framework.

4.2 Derivation Of The Weak Form

In Finite Elements Analysis weak form (in another words variational form) is used before replacing the functions with their approximations with the aim of reducing the continuity constraint on the approximation that are going to be used in the numerical solution. Writing the previously derived form of the Stokes flow given in section 3.2, it has to be written for a flow domain $\mathbf{\Omega} \in R^n$ with a closed boundary $\mathbf{\Gamma}$ sufficiently regular with Neumann and Dirichlet boundaries shown as $\partial\,\mathbf{\Gamma}_N$ and $\partial\,\mathbf{\Gamma}_D$ where $\partial\,\mathbf{\Gamma}_N \cap \partial\,\mathbf{\Gamma}_N = 0$:

$$\nabla \cdot \underline{\underline{\boldsymbol{\sigma}}} + \underline{\mathbf{b}} = 0 \qquad \text{in} \quad \mathbf{\Omega} \tag{4.1}$$

Since the flow is incompressible, as explained in equation A.18 flow field has to be divergence free, for convenience the equation is written with a minus in front:

$$-\nabla \cdot (\overrightarrow{\mathbf{v}}) = 0 \qquad \text{in} \quad \mathbf{\Omega} \tag{4.2}$$

For the derivation of the weak formulation of the problem the following definitions for mathematical convenience are required:

A function u is called *square-integrable* on a domain $\mathbf{\Omega}$ if the function u satisfies the following condition :

$$\int_{\Omega} u^2 \quad \mathrm{d}\Omega < \infty \tag{4.3}$$

where ∞ is infinity. If equation 4.3 is satisfied we write $u \in \mathcal{L}^2(\Omega)$. $\mathcal{H}^k(\Omega)$ is the set of functions of which derivatives up to order k are in $\mathcal{L}^2(\Omega)$.

Four collections of functions are required in the derivation of the weak form of the problem. They are the *trial functions* and the *test functions*, both for the pressure field and the velocity field. $\mathcal{S}$ is the space of velocity trial functions. This collection of functions includes all the functions which are square–integrable, also have square integrable first derivatives over the computational domain Ω and satisfy the Dirichlet boundary conditions on Γ_D defined in 3.24. This collection of functions is given by :

$$\mathcal{S} = \left\{ u \in \mathcal{H}^1(\Omega) \,|\, u = u_D \text{ on } \Gamma_D \right\}.$$

This space contains vector functions of which all components are in the corresponding space of scalar functions.

The test functions for velocity belong to space $\mathcal{V}$. Functions in this class have the same characteristics with the ones in $\mathcal{S}$, except that they are required to become zero on Γ_D where the velocity is prescribed as a Dirichlet boundary condition . The definition of space $\mathcal{V}$ is :

$$\mathcal{V} = \left\{ w \in \mathcal{H}^1(\Omega) \,|\, w = 0 \text{ on } \Gamma_D \right\}.$$

Lastly, space of functions shown by the symbol $\mathcal{Q}$ are introduced for the pressure field. Because of the fact that the space derivatives of pressure do not appear in the weak form of the Stokes problem, the functions that are in $\mathcal{Q}$ are require only the following condition :

$$\mathcal{Q} = \left\{ q \in \mathcal{L}^2(\Omega) \right\}.$$

This space is both the trial space and the test function space.

Equations 4.1 and 4.2 are the governing equations that have to be satisfied in Stokes flow. So, the weighted residuals that has to be forced to become averagely zero over the problem domain with the aim of finding a good solution to the problem. By the term residuals the left-hand sides of equations 4.1 and 4.2 are meant.

To obtain the weak formulation of the problem, the governing equation 4.1 is multiplied by a velocity test function $\overrightarrow{\mathbf{w}} \in \mathcal{V}$ and integrated over the domain $\mathbf{\Omega}$. Similarly, the incompressibility condition 4.2 is multiplied by the pressure test function $q \in \mathcal{Q}$ and integrated over the domain Ω. Hence, using the mentioned weighting functions $\overrightarrow{\mathbf{w}}$ and q for the equations 4.1 and 4.2 and integrating the functions over the domain of the problem $\mathbf{\Omega}$ the weighted residual integral equations that are forced to be zero can be expressed as:

$$\int_{\mathbf{\Omega}} \overrightarrow{\mathbf{w}} \cdot \left(\nabla \cdot \underline{\underline{\boldsymbol{\sigma}}} + \underline{\mathbf{b}}\right) \ \mathbf{d\Omega} = 0 \tag{4.4}$$

$$-\int_{\mathbf{\Omega}} q \left(\nabla \cdot (\overrightarrow{\mathbf{v}})\right) \ \mathbf{d\Omega} = 0 \tag{4.5}$$

The first equation (4.4):

$$-\int_{\mathbf{\Omega}} \overrightarrow{\mathbf{w}} \cdot \left(\nabla \cdot \underline{\underline{\boldsymbol{\sigma}}}\right) \ \mathbf{d\Omega} = \int_{\mathbf{\Omega}} \overrightarrow{\mathbf{w}} \cdot \overrightarrow{\mathbf{b}} \ \mathbf{d\Omega} \tag{4.6}$$

Using the integration by parts and divergence theorem, equation 4.6 can be stated as:

$$\int_{\mathbf{\Omega}} \nabla \overrightarrow{\mathbf{w}} : \underline{\underline{\boldsymbol{\sigma}}} \ \mathbf{d\Omega} - \int_{\mathbf{\Gamma}} \overrightarrow{\mathbf{w}} \cdot \left(\underline{\underline{\boldsymbol{\sigma}}} \cdot \overrightarrow{\mathbf{n}}\right) \ \mathbf{d\Gamma} = \int_{\mathbf{\Omega}} \overrightarrow{\mathbf{w}} \cdot \overrightarrow{\mathbf{b}} \ \mathbf{d\Omega} \tag{4.7}$$

where:

- $\mathbf{\Gamma}$ is the surfaces in the problem domain $\mathbf{\Omega}$
- $\overrightarrow{\mathbf{n}}$ is the outward unit normal vector to $\mathbf{\Gamma}$

The first term in equation 4.7, the definition of Cauchy stress tensor can be used from equation 3.22 considering the definition of the symmetric gradient defined in equation 3.23. Therefore, the first term in equation 4.7 can be written as :

$$= \int_{\mathbf{\Omega}} \nabla \overrightarrow{\mathbf{w}} : \left(-p\,\underline{\underline{\mathbf{I}}} + 2\,\mu \nabla^{s} \overrightarrow{\mathbf{v}}\right) \ \mathbf{d\Omega} \tag{4.8}$$

$$= -\underbrace{\int_{\mathbf{\Omega}} \nabla \overrightarrow{\mathbf{w}} : \left(p\,\underline{\underline{\mathbf{I}}}\right) \ \mathbf{d\Omega}}_{\text{term B}} + \int_{\mathbf{\Omega}} \nabla \overrightarrow{\mathbf{w}} : \left(2\mu \nabla^{s} \overrightarrow{\mathbf{v}}\right) \ \mathbf{d\Omega} \tag{4.9}$$

where the double contraction of two rank-two tensors $\underline{\underline{\boldsymbol{K}}}$ and $\underline{\underline{\boldsymbol{L}}}$ is defined as :

$$\underline{\underline{\boldsymbol{K}}} : \underline{\underline{\boldsymbol{L}}} = K_{ij} L_{ij} \tag{4.10}$$

thus term B defined in the first term in equation 4.7 can be written in an equivalent form :

$$\nabla \overrightarrow{\mathbf{w}} : \left(p\, \underline{\underline{\mathbf{I}}}\right) = \frac{\partial w_1}{\partial x} \times p + \frac{\partial w_2}{\partial y} \times p + \frac{\partial w_3}{\partial z} \times p = \nabla \cdot \overrightarrow{\mathbf{w}}\ p \tag{4.11}$$

Finally the weak form of the problem can be stated as :

$$\int_{\boldsymbol{\Omega}} \nabla^s \overrightarrow{\mathbf{w}} : 2\mu \nabla^s \overrightarrow{\mathbf{v}}\ \mathbf{d\Omega} - \int_{\boldsymbol{\Omega}} \nabla \cdot \overrightarrow{\mathbf{w}}\ p\ \mathbf{d\Omega} = \int_{\boldsymbol{\Omega}} \overrightarrow{\mathbf{w}} \cdot \overrightarrow{\mathbf{b}}\ \mathbf{d\Omega} + \int_{\boldsymbol{\Gamma}} \overrightarrow{\mathbf{w}} \cdot \left(\underline{\underline{\boldsymbol{\sigma}}} \cdot \overrightarrow{\mathbf{n}}\right)\ \mathbf{d\Gamma} \tag{4.12}$$

$$-\int_{\boldsymbol{\Omega}} q\left(\ \nabla \cdot (\overrightarrow{\mathbf{v}})\right)\ \mathbf{d\Omega} = 0 \tag{4.13}$$

In equation 4.12 it is worth to note that the surface term $\underline{\underline{\boldsymbol{\sigma}}} \cdot \overrightarrow{\mathbf{n}}$ on the right-hand side is the physical traction on the boundary of the domain.

The proof that shows the strong and the weak formulations of the problem are equivalent can be found also in Hughes (2000), Zienkiewicz and Taylor (2000) or Donea and Huerta (2002).

4.3 Finite Elements Method Solution Of The Stokes Problem

Finite Elements method is a very good choice for solving an engineering problem but it is useful to state that the simplest way for solving the same problems is the Finite Difference Method rather than Finite Elements Method. Both Finite Elements Method and Finite Difference Methods are based on a discretization of the domain. In another words, in both techniques a mesh is needed. Standard version of Finite Difference Method includes using a structured mesh. As a natural result, it becomes impossible to control the density of the mesh in different regions of the domain. In contrast, Finite Elements Method uses an unstructured mesh which gives the opportunity to change the density of the mesh in different regions of the domain. So, it becomes possible to get a better solution in critical areas using more elements per area (increasing the density of the mesh in that region only). It is always better to use a coarse mesh for the regions where the solution is simpler with the aim of using computational resources efficiently. Furthermore, complex or curved boundaries and boundaries that are not parallel to the cartesian axes are very hard to handle with Finite Difference Method whereas handling them is straightforward with Finite Elements Method.

The main technique that is used in this thesis is *Extended Finite Element Method* for the solution of the given basic differential equations that are used in the analysis of fluid flow problems (main equations used in the definitions of the problem are provided in section A.6 of Appendix A). Finite Elements Analysis is a robust technique and capable of modelling complex geometries. Because of this, Finite Elements Analysis has been used for many years in many engineering problems. In addition to this, Finite Elements Analysis lets modelling the problem in spherical or cartesian domains without reformulating the equations and this shows that the method has got flexibility as well. Extended Finite Elements Method improves this technique by adding a local enrichment in the solution.

With the aim of comparing Classical Finite Element Method with Extended Finite Element Method, Classical Finite Elements Method derivations of the problem is also given in this section. In the beginning of section 4.2, it is already mentioned that weak formulation is used in Finite Elements Analysis. The next step includes replacing the unknown functions with their approximations which uses the values of the unknowns in the nodes of the elements of the computational mesh used in the solution. By the term mesh it is meant a division of the domain Ω into subdomains Ω_k where k goes from one to total number of elements in the mesh $(k = 1 \ldots n)$ where $\Omega_k \cap \Omega_{\overline{k}} = 0$ if $k \neq \underline{k}$. The approximation mentioned leads to a linear system of equations to be solved with the aim of calculating the the unknowns. For this purpose, a Standard Finite Elements Method approximation of the function $u(\overrightarrow{\mathbf{x}})$ which is represented as $u^h(\overrightarrow{\mathbf{x}})$ can be stated as :

$$u^h(\overrightarrow{\mathbf{x}}) = \sum_{i \in I} N_i(\overrightarrow{\mathbf{x}}) * u_i \tag{4.14}$$

In equation 4.14 :

- i is the nodes in the finite elements mesh
- N is the shape functions used in classical finite elements
- u_i is the values of the unknown at the nodes of the mesh
- $\overrightarrow{\mathbf{x}}$ is the position

For stability reasons, a mixed Finite Elements Method is used since some numerical difficulties that arises because of the *saddle point* nature of the resulting variational problem exist in the solution of incompressible flow problems. By mixed Finite Element Method, it is meant that the meshes that are used to interpolate the pressure and velocity unknowns are selected as different meshes since if the same mesh is used the numerical solution becomes unstable. The incompressibility condition given in equation 4.2 is actually a constraint on the velocity field in the flow. The existence of pressure in momentum equation has the aim of introducing an additional degree of freedom needed to satisfy the incompressibility constraint. In this sense, the role of the pressure variable in the problem is to adjust itself in order to satisfy the condition of having a divergence free velocity field. This means, the pressure is acting as a Lagrangian multiplier of the incompressibility constraint and thus there is a coupling between the velocity and pressure unknowns. (Donea and Huerta (2002)).

Replacement of the unknown functions with their approximations in equations 4.12 and 4.13 should be done in order to get a system equations to be solved. The approximated values of the velocity and pressure fields using the discretization for the Galerkin formulation of the Stokes problem are defined as $\mathbf{v}^h$ and p^h for velocity and pressure fields. The related test functions $\overrightarrow{\mathbf{w}}$ and q are also discretized as $\mathbf{w}^h$ and q^h. $\mathcal{V}^h$ and $\mathcal{S}^h$ are used to represent the finite dimensional subspaces of $\mathcal{V}$ and $\mathcal{S}$, and the finite dimensional subspace of $\mathcal{Q}$ is $\mathcal{Q}^h$. The computational domain Ω is partitioned into element domains Ω^e. This discretization or mesh is composed by elements and nodes.

Each unknown functions are approximated using the shape functions and associated nodal values of the value of the unknown function. We denote I the set of velocity nodes in the mesh. The subset I_D of I is the subset of velocity nodes corresponding to the Dirichlet boundary conditions, where the velocity is prescribed. The velocity is can be written as:

$$\overrightarrow{\mathbf{v}}^h = \overrightarrow{\mathbf{v}}^h + \overrightarrow{\mathbf{v}}_D^h \tag{4.15}$$

$$\overrightarrow{\mathbf{v}}^h = \sum_{i \in I} N_i(\overrightarrow{\mathbf{x}})\ \overrightarrow{\mathbf{v}}_i \tag{4.16}$$

$$\overrightarrow{\mathbf{v}}_D^h = \sum_{i \in I_D} N_i(\overrightarrow{\mathbf{x}})\ \overrightarrow{\mathbf{v}}_{Di} \tag{4.17}$$

where the shape function associated with the node number i is represented by N_i and $\overrightarrow{\mathbf{v}}_i$ is the value of $\overrightarrow{\mathbf{v}}^h$ at node i. The interpolation of the pressure field is done using a different set of pressure nodes denoted by I_p and shape functions $\hat{N}_i$:

$$p^h \ = \ \sum_{i \in I_p} \hat{N}_i(\mathbf{x})\, p_i \tag{4.18}$$

where p_i is the pressure value at node i in of the pressure mesh used.

Replacing the unknown functions with their approximations in the end gives a linear equation system as:

$$\begin{pmatrix} \mathbf{K} & \mathbf{G} \\ \mathbf{G}^T & \mathbf{0} \end{pmatrix} \begin{pmatrix} \overrightarrow{\mathbf{v}} \\ \overrightarrow{\mathbf{p}} \end{pmatrix} = \begin{bmatrix} \overrightarrow{\mathbf{f}} \\ \overrightarrow{\mathbf{h}} \end{bmatrix} \tag{4.19}$$

The first line of equation 4.19 is the conservation of momentum and the second line is the conservation of mass after discretization of the system of equations. Because of the fact that the right-hand side of mass conservation equation (given in equation 3.14) is zero, in equation 4.19 $\overrightarrow{\mathbf{h}}$ is defined as a zero vector. Using the derivation provided in Liu and Li (2006) the viscosity term $\mathbf{K}$ can also be expresses as:

$$\mathbf{K} = \int_\Omega \mathbf{B}^T\,\mathbf{C}\,\mathbf{B}\ \mathrm{d}\boldsymbol{\Omega} \tag{4.20}$$

where matrix form of the tensor $\mathbf{C}$ is defined as:

$$\mathbf{C} = \begin{bmatrix} 2v & 0 & 0 \\ 0 & 2v & 0 \\ 0 & 0 & v \end{bmatrix} \tag{4.21}$$

here v is the kinematic viscosity of the fluid defined as $v = \mu/\rho$ and the gradient matrix $\mathbf{B}$ is defined by equations 4.22 and 4.23:

$$\mathbf{B} = [\mathbf{B}_1, \mathbf{B}_2, \ldots, \mathbf{B}_{n_v}] \tag{4.22}$$

$$\mathbf{B}_i = \begin{bmatrix} \frac{\partial N_i}{\partial x_1} & 0 \\ 0 & \frac{\partial N_i}{\partial x_2} \\ \frac{\partial N_i}{\partial x_2} & \frac{\partial N_i}{\partial x_1} \end{bmatrix} \tag{4.23}$$

The system of equations obtained in equation 4.19 after replacing the unknown functions with their approximations in equations 4.12 and 4.13 gives a partitioned matrix with a null submatrix on the diagonal. An appropriate choice of the finite element spaces for velocity and pressure interpolation is crucial since it effects the solvability of such a system. In this thesis, the element used is called *mini-element*. It is illustrated in figure 4.1.

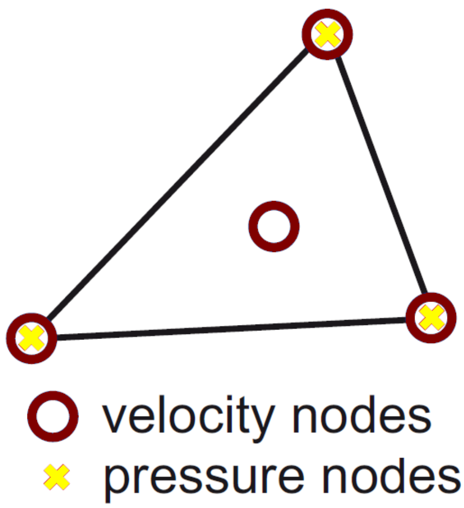

Figure 4.1: Mini Element Used In The Numerical Solution

Mini Element is a triangular element in which there are three pressure nodes at the vertices of the element and four velocity nodes (three of them are at the vertices of the element whereas the fourth one is in the center). This lets pressure values to be linearly interpolated. Mini element satisfies the LBB compatibility condition which guarantees the solvability of the system. (after Ladyzhenskaya (1969), Babuka (1971), Brezzi (1974)).

To complete the statement of the space discretization the technique used to track the location of the material phases should also be stated. This is done in the section 4.5.

4.4 Derivation Of X-FEM For Two–Phase Stokes Flow

Standard Finite Elements method approximation of the function $u(\overrightarrow{\mathbf{x}})$ which is represented as $u^h(\overrightarrow{\mathbf{x}})$ is:

$$u^h(\overrightarrow{x}) = N_i(\overrightarrow{x}) * u_i \tag{4.24}$$

In equation 4.24:

- i is the nodes in the finite elements mesh
- N is the shape functions used in classical finite elements
- u_i is the values of the unknown at the nodes of the mesh

Adding the local enrichment to this approximation given in 4.24 it is possible to obtain the approximation used by the Extended Finite Elements Method as:

$$u^h(\overrightarrow{x}) = \sum_{i \in I} \underbrace{N_i(\overrightarrow{x}) * u_i}_{\text{Standard Finite Elements Part}} + \sum_{j \in I^+} \underbrace{M_j(\overrightarrow{\mathbf{x}}) * a_j}_{\text{Extended Finite Elements Part}} \tag{4.25}$$

in equation 4.25 :

- N is the shape functions used in classical finite elements
- u_i is the values of the unknown of the standard finite elements part at the nodes of the mesh
- a_j is the extra degrees of freedoms that is assigned only to the enriched elements
- M_j is the local enrichment function used with the aim of getting a better solution where there is a discontinuity or singularity

In equation 4.25, it is important to note that I^{+} here represents the enriched nodes only. When equation 4.25 is used the Extended Finite Elements part of the equation written modifies the approximation using Classical Finite Elements Method at the positions defined by the scalar level set function. For a multiphase flow this corresponds to the elements which include more than one phases.

To exemplify this in one dimension, it is appropriate to give an example which includes both the solution using Classical Finite Elements Method and Extended Finite Elements method. See the figure 4.2 where solutions in one dimensional case using FEM and X-FEM are illustrated. X-FEM allows a discontinuous solution across the interface of the problem.

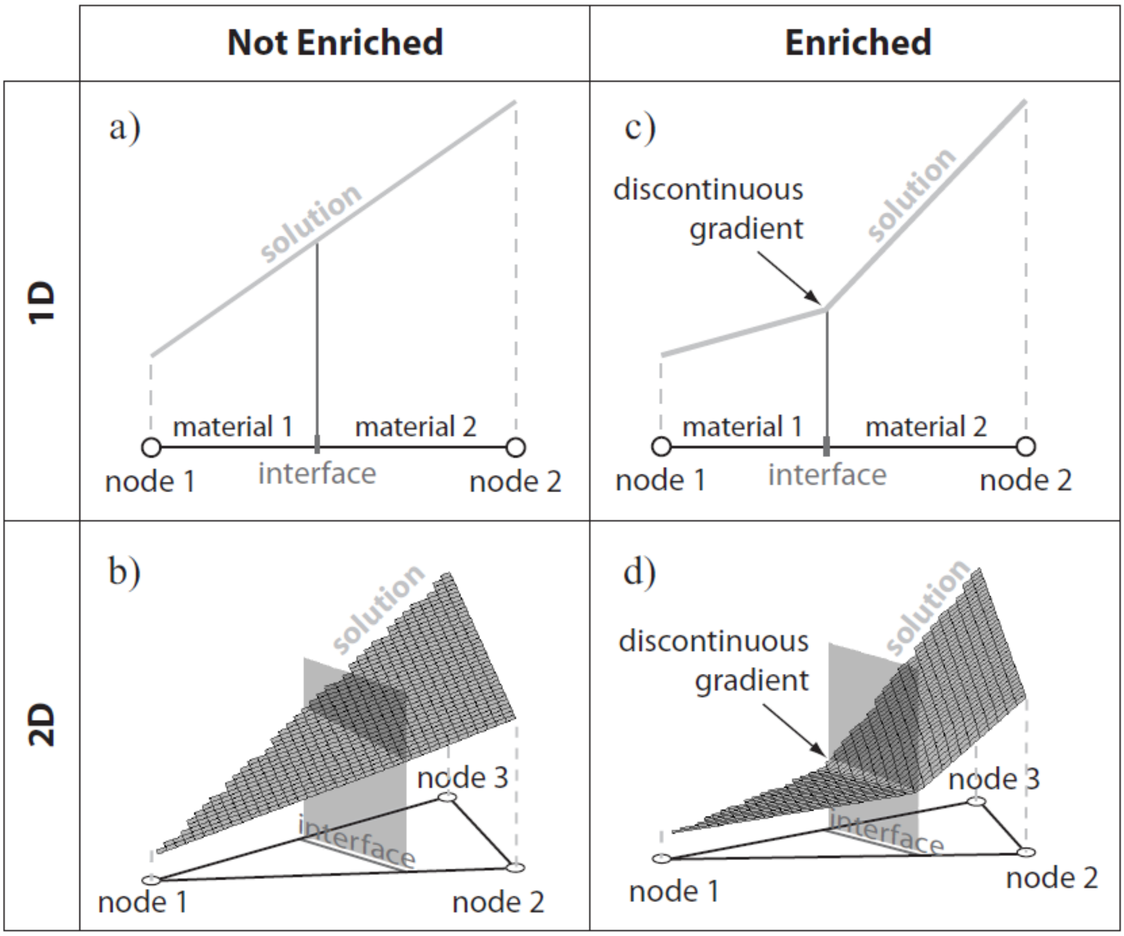

Figure 4.2: Comparison Of Different Solution Techniques In One And Two Dimensional Case

In the thesis to get a better numerical solution across the interface of the multiphase Stokes flow the local enrichment function to be used in order to improve the ability of the interpolation to include the gradient discontinuities across the interface includes a ridge function (R given in equation 4.26) defined by Moës et al. (2003). In the literature there are other ridge functions defined as well for example see Chessa and Belytschko (2003a). In the solution, the interpolation of the pressure and velocity are also enriched using a partition of the unity concept.

$$R(\overrightarrow{\mathbf{x}}) = \sum_{j\in I^+} |\phi_j|\, N_j(\overrightarrow{\mathbf{x}}) - \left| \sum_{j\in I^+} \phi_j\, N_j(\overrightarrow{\mathbf{x}}) \right| \tag{4.26}$$

in equation 4.26 ϕ_j represents the nodal values of the Level Set function.

The Ridge function given in equation 4.26 is defined in such a way that it vanishes in all the elements except the ones which contain a part of the interface. In equation 4.26 the definition of j only includes the nodes that are on the vertex nodes of the elements. As a natural result, the enrichment included in the solution using equation 4.26 only affects the degrees of freedoms that are on the vertex nodes of the enriched elements.

Using the main idea of Extended Finite Elements Method the enriched version of interpolations of velocity and pressure can be written using the information provided in equation 4.25 :

$$\overrightarrow{\mathbf{v}}^h(\overrightarrow{\mathbf{x}}) = \sum_{i\in I} \overrightarrow{\mathbf{v}}_i \times N_i(\overrightarrow{\mathbf{x}}) + \sum_{j\in I^+} \overrightarrow{\mathbf{a}}_j \times M_j(\overrightarrow{\mathbf{x}}) \tag{4.27}$$

$$p^h(\overrightarrow{\mathbf{x}}) = \sum_{k\in I_p} p_k \times N_k(\overrightarrow{\mathbf{x}}) + \sum_{j\in I^+} b_j \times M_j(\overrightarrow{\mathbf{x}}) \tag{4.28}$$

where:

- I is the set of velocity nodes
- I^+ is the vertex nodes of the enriched elements
- I_p is the set of pressure nodes
- M_j is the enrichment function
- $\overrightarrow{\mathbf{a}}_j$ is the extra velocity degree of freedoms added to the solution by X-FEM
- b_j is the extra pressure degree of freedoms added to the solution by X-FEM

here enrichment function M is defined as :

$$M_j(\overrightarrow{\mathbf{x}}) = R(\overrightarrow{\mathbf{x}})\ N_j(\overrightarrow{\mathbf{x}}) \tag{4.29}$$

where R is the ridge function defined in equation 4.26.

Using the information provided in equations 4.27 and 4.28 for fluid velocity and pressure distribution can be approximated by using the vectorial form as :

$$\overrightarrow{\mathbf{v}}^h(\overrightarrow{\mathbf{x}}, t) = \mathbf{N}_v\ \overrightarrow{\mathbf{V}} \tag{4.30}$$

$$p^h(\overrightarrow{\mathbf{x}}, t) = \mathbf{N}_p\ \overrightarrow{\mathbf{P}} \tag{4.31}$$

where the terms in equations can be explicitly written as:

$$\begin{aligned}
\overrightarrow{\mathbf{N}}_v &= [N_1, N_2, \ldots, N_{n_v}, M_1, \ldots, M_{n_e}] \\
\mathbf{V} &= [\overrightarrow{\mathbf{v}}_1, \overrightarrow{\mathbf{v}}_2, \ldots \overrightarrow{\mathbf{v}}_{n_v}, \overrightarrow{\mathbf{a}}_1, \ldots, \overrightarrow{\mathbf{a}}_{n_e}]^\top \\
\overrightarrow{\mathbf{N}}_p &= [N_1, N_2, \ldots, N_{n_p}, M_1, \ldots, M_{n_e}] \\
\overrightarrow{\mathbf{P}} &= [p_1, p_2, \ldots, p_{n_p}, b_1, \ldots b_{n_e}]^\top
\end{aligned}$$

It is important to emphasize here that n_v and n_p are the total number of nodes used in velocity and pressure meshes. Since in a two dimensional problem there are two degrees of freedom in one node of the velocity mesh. These unknowns in the same node have to be written explicitly as well. The new vector of unknowns which includes the velocities is shown as $\overrightarrow{\mathbf{V}}^{rs}$ to emphasize that this is the reshaped form of the vector $\overrightarrow{\mathbf{V}}$. For example the velocity degree of freedoms in x and y direction in global node number 17 are represented by v_{17}^x and v_{17}^y. Explicitly writing these unknowns requires also reshaping $\mathbf{N}_v$ accordingly and calling it $\mathbf{N}_v^{rs}$:

$$\mathbf{N}_v^{rs} = \begin{bmatrix} N_1 & 0 & N_2 & 0 & \ldots & N_{n_v} & 0 & M_1 & 0 & \ldots & M_{n_e} & 0 \\ 0 & N_1 & 0 & N_2 & \ldots & 0 & N_{n_v} & 0 & M_1 & \ldots & 0 & M_{n_e} \end{bmatrix}.$$

$$\overrightarrow{\mathbf{V}}^{rs} = [v_1^x, v_1^y, v_2^x, v_2^y, \ldots, v_{n_v}^x, v_{n_v}^y, a_1^x, a_1^y, \ldots, a_{n_e}^x, a_{n_e}^y]^\top$$

Using the same logic of Galerkin Finite Elements with the one that is used in section 4.3 to derive the Classical Finite Elements Method Solution of Stokes Flow, replacing the unknown functions with their approximations in the weak form of the problem derived in section 4.2 and using the weighting functions as the shape functions used in the interpolation of unknowns the linear system of algebraic equations obtained can be written in a neat form as :

$$\mathbf{K}\overrightarrow{\mathbf{V}}^{rs} + \mathbf{G}^{T}\overrightarrow{\mathbf{P}} = \overrightarrow{\mathbf{f}} \tag{4.33}$$

$$\mathbf{G}\,\overrightarrow{\mathbf{V}}^{rs} = \mathbf{0} \tag{4.34}$$

where the matrices $\mathbf{K}$, $\mathbf{G}$ and vector $\overrightarrow{\mathbf{f}}$ can be explicitly written as :

$$\begin{aligned}
\mathbf{K} &= \int_{\Omega} \mathbf{B}^{\top}\mathbf{C}\,\mathbf{B}\ \mathrm{d}\Omega \\
\mathbf{G} &= -\int_{\Omega} \overrightarrow{\mathbf{N}}_{p}^{\top}\,(\nabla\cdot\overrightarrow{\mathbf{N}}_{v}^{rs}\ \mathrm{d}\Omega \\
\overrightarrow{\mathbf{f}} &= \int_{\Omega} (\overrightarrow{\mathbf{N}}_{v}^{rs})^{\top}\rho\,\overrightarrow{\mathbf{b}}\ \mathrm{d}\Omega
\end{aligned}$$

where:

- $\mathbf{C}$ is defined in equation 4.21
- The gradient matrix $\mathbf{B}$ is defined as:

$$\mathbf{B} = [\mathbf{B}_1, \mathbf{B}_2, \ldots, \mathbf{B}_{n_v}, \acute{\mathbf{B}}_1, \ldots, \acute{\mathbf{B}}_{n_e}]$$

$$\mathbf{B}_i = \begin{bmatrix} \frac{\partial N_i}{\partial x_1} & 0 \\ 0 & \frac{\partial N_i}{\partial x_2} \\ \frac{\partial N_i}{\partial x_2} & \frac{\partial N_i}{\partial x_1} \end{bmatrix} \text{ and } \acute{\mathbf{B}}_i = \begin{bmatrix} \frac{\partial M_i}{\partial x_1} & 0 \\ 0 & \frac{\partial M_i}{\partial x_2} \\ \frac{\partial M_i}{\partial x_2} & \frac{\partial M_i}{\partial x_1} \end{bmatrix}$$

Note that the spatial derivatives of M_i contained in matrices $\tilde{\mathbf{B}}_i$, for $i = 1, \ldots, n_e$ account for the enrichment and depend on the level set ϕ. Therefore, the chain rule must be employed to evaluate the material those functions.

Lastly, the system of linear equations to be solved for the solution of multiphase flow can be expressed as :

$$\begin{bmatrix} \mathbf{K} & \mathbf{G}^T \\ \mathbf{G} & \mathbf{0} \end{bmatrix} \begin{bmatrix} \overrightarrow{\mathbf{V}}^{rs} \\ \overrightarrow{\mathbf{P}} \end{bmatrix} = \begin{bmatrix} \overrightarrow{\mathbf{f}} \\ \mathbf{0} \end{bmatrix}$$

Also a Matlab code that calculates the elements of the system is submitted with the thesis and results of the code are presented in chapter 6.

4.5 Explanation Of Level Set Method For Multiphase Problems Interface Tracking

Eulerian framework is usually used for the solution of fluid flow problems. In this approach computational mesh is fixed and fluid moves with respect to this fixed mesh. As a result, the position of interface should be updated throughout the solution. When Eulerian framework is used the tracking of the interface of multiphase flow problems becomes a problem and the tracking of the interface should be done using an additional method because of the fact that the physical properties belonging to each specific point will change throughout the solution in case interface moves.

Level Set Method includes the implicit representation of the interface and is used to decide where to apply the local enrichment of approximation spaces in the domain to get a solution with a better quality. From the invention of the technique by Osher and Sethian (1988) and application of it on the solution of two–phase flows (Sussman et al. (1994)) there has been many articles written using the method. For example see these papers: Sethian and Smereka (2003); Osher and Fedkiw (2001). Level Set Method is widely used to track the interface location such as in Chessa and Belytschko (2003a); Moës et al. (2003) and crack propagation (Belytschko and Black (1999); Stolarska et al. (2001)) and permeability calculations in reservoir simulations (Karlsen et al. (2000); Nielsen et al. (2008)). Its power to track the changes in the topology of the problem is well known. (Mulder et al. (1992)) Also there are other fields where the method is used such as grid generations and computer vision.

Level Set Method, actually, is a scalar function that is introduced to the problem and it is used to track the location of singularities and discontinuities. This can be considered as a factor that slows down the calculations since Level set Technique add another dimension to the problem in consideration. However, this property gives the technique a great generality and makes it possible to deal with problems in which the front is not only moving forward or backwards. This is the main reason why Level Set Method is usually coupled with Extended Finite Elements Method to solve problems. Level set function is capable of representing the changes in the topology of the different phases that exist in the problem. So, representing merging bubbles, breaking sets ,detaching drops or cracks with this technique is not a problem at all.

It is advantageous compared to other methods. For example comparing it to the *fast marching* methods it can be concluded that fast marching methods are designed to track the front velocity that never changes sign which means that the front is going always forward or backward only. To deal with the front which is moving forward in some places and backwards in some places depending on the location *Level set Methods* are designed to track the front in which the speed can be negative or positive depending on the location.

Hereby, we emphasize that other techniques to track the location of the discontinuities and singularities in engineering problems can be used with Extended Finite Elements Method. For a quick comparison of Level Set Method with Markers method it is possible to state that using Level Set Method compared to using markers method is very advantageous because it uses the same same number of points in the mesh to describe the location of the interface. In addition to this, Level Set method does not require averaging the material properties from markers to nodes. This is a very nice computational property.

In Level Set Method, the zero level of the Level Set Function is considered to be the location of discontinuities. As a result, the domain Ω is divided into two subregions in one of which the Level Set function takes the positive values in material one and in the other region the Level Set Function takes negative values in second material. So, it can be concluded that Level Set Method is used to handle the multiphase character of the multiphase problems. The beauty of using the Level Set Method is that it allows to find the location of the interface without requiring it to conform with the mesh. When used with Extended Finite Elements Method the solution obtained is expected to have a discontinuous gradient on the interface. The reason for the discontinuity is the change of material properties across the interface.

In many researches the Level Set Function is considered to be the signed distance to the interface which can be defined as in the equation 6.1 :

$$\phi(\overrightarrow{\mathbf{x}}) = \pm \quad \min \parallel \overrightarrow{\mathbf{x}} - \overrightarrow{\mathbf{x_\Gamma}} \parallel, \quad \forall \mathbf{x} \in \Omega \tag{4.36}$$

Here in equation 6.1 :

- $\phi(\overrightarrow{\mathbf{x}})$ is the Level Set function
- $\overrightarrow{\mathbf{x}}$ is the position of the point in the domain
- $\overrightarrow{\mathbf{x_\Gamma}}$ is the positions of the points on the interface
- $\parallel \cdot \parallel$ is the norm of the vector

It is also a common practice to truncate the level set function at positions that are considered to be far enough from the interface. According to the definition of the Level Set Function the sign of it gives the information about in which subdomain the point under consideration is so that the material in each point in the domain can be determined easily :

$$\phi(\overrightarrow{\mathbf{x}}) = \begin{cases} > 0 & \text{for } \overrightarrow{\mathbf{x}} \in \Omega_1 \\ = 0 & \text{for } \overrightarrow{\mathbf{x}} \in \Gamma \\ < 0 & \text{for } \overrightarrow{\mathbf{x}} \in \Omega_2 \end{cases} \tag{4.37}$$

where $\overrightarrow{\mathbf{x}}$ is the point under consideration in the domain. What equation 4.37 tells is that the discontinuity in a problem (it is the interface in a two–phase flow problem) can be expressed as :

$$\boldsymbol{\Gamma} = \{\overrightarrow{\mathbf{x}} \in \mathbf{R}^d \mid \phi(\overrightarrow{\mathbf{x}}) = 0\} \tag{4.38}$$

In equation 4.38 the interface is stated as the isocontour ($\phi = 0$) of the Level Set function. In figure 4.3 an example Level Set function for a two dimensional problem (so that the plot is a 3D plot) is illustrated.

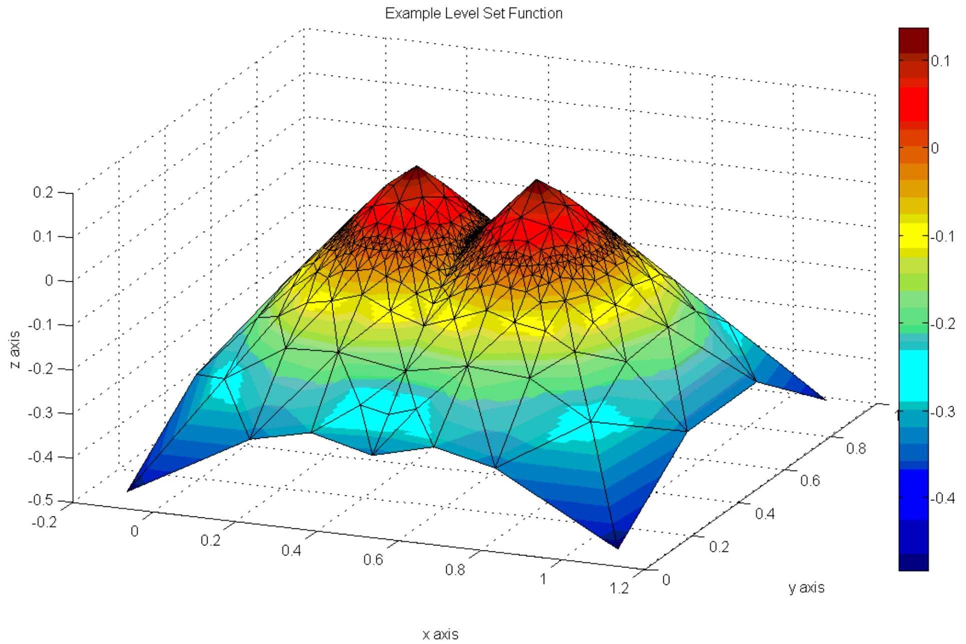

Figure 4.3: An Example Level Set Function

In Finite Elements Analysis values of the functions are approximated using the values of the functions in the nodes of the elements used. Consequently, it is also possible to write the approximation of the Level Set function as in equation 4.39 :

$$\phi^h(\overrightarrow{\mathbf{x}}) = \sum_i N_i \ \phi_i \tag{4.39}$$

where i is the nodes to which the Level Set function is assigned and N_i is the linear shape functions that are used to interpolate the Level Set values.

In this thesis, the same mesh for the pressure and Level Set function is used. It is a common practice to use the mechanical computational mesh used in the numerical solution for the Level Set function. It makes sense because in the end same resolution is obtained for approximation of interface and the factors that effect how this interface evolves. So, the quality of the approximated interface is dependant on the quality of mesh used for the pressure. The same mesh for the Level Set can be used throughout the whole simulation the reason is it represents interface which does not necessarily coincide with element edges.

At any location on the interface the unit normal vector, in case it is needed, can be calculated using the equation given in equation 3.9. Lastly, before giving the evolution of the Level Set function it is important to state that using smaller elements at the positions near the interface makes it possible to get a better solution for the location of the interface.

Lastly, some of the publications that can give further insight on Level Set Method is also listed in Appendix B.5.4.

4.6 Accurate Numerical Integration Of Enriched Elements

Gauss Quadrature Method is the most preferred numerical integration scheme in Finite Element Analysis because of the fact that this method can calculate the results exactly when the integrand is a polynomial as it is the case for most of the Finite Elements Method applications. See Appendix A.3 for more details.

Now imagine a case where there is a discontinuity in material properties in the domain and the integral that is to be calculated include this material property. In our problem, it is the viscosity. The viscosity of two fluids are different and this introduces a discontinuity in the gradient of the solution in elements that are crossed by the interface.

See the figure 4.4 where how the real interface (Γ) and the approximation of the interface shown using the symbol Γ^h divides a triangular element into two pieces. In the same figure, the area colored in pink belongs to the first domain. However, since linear shape functions are used to interpolate the interface in the code assumes that this area is belongs to domain 2. In the numerical calculation of the integral terms in case there is a gauss point in this area the contribution will be calculated wrong. To fix this error a higher order approximation space can be used or the number of elements used in the Level Set mesh can be increased until the error becomes negligible.

For numerical calculation of a general integral stated in equation 4.40 on an element which is cut by the interface as stated picture 4.4 different material properties depending on the spatial position of the each Gauss point used should be used. However, this approach does not give the accurate result since the integrand in this case is not a polynomial and has got a discontinuity. Writing the general integral to be calculated where Ω^e represent the elemental area of the element given

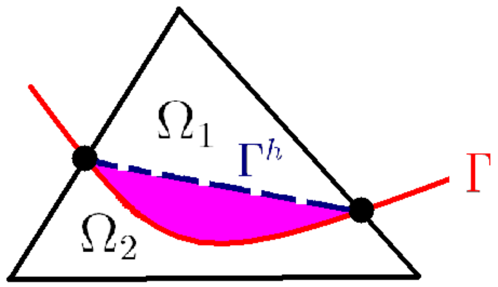

Figure 4.4: Real Interface Γ And The Approximation Of The Interface Γ^h When Linear Shape Functions Are Used

in the same figure :

$$\int_{\Omega^e} \nu(\overrightarrow{\mathbf{x}}) f(x,y)\, \mathrm{d}\Omega \tag{4.40}$$

To fix this problem what is suggested is the division of the enriched elements into smaller integration cell elements which have the only one value of the material properties on them and calculating the contributions coming from these smaller elements. It should be emphasized that the aim of this division is obtaining smaller elements with the same material properties so that the position of the interface becomes very important. The positions of the points where the interface cuts the interface has to be stored and used.

Also in this approach, according to how the interface cuts the elements the number of subelements used will differ and how many subelements will be used should be determined for every element that is cut by the interface. Figure 4.5 explains this in color where the green color represent the first material used and the grey color corresponds to the second material. Blue line is the extra border added to the problem.

As it is seen in the figure 4.5, there are two different cases for a triangular element: when the interface crosses one of the nodes using two subelements is enough whereas if the interface cuts the edges of the elements an extra subelement has to be created to create areas which have the same material properties so that all the Gauss points on the same element uses the properties of the same material. Accordingly, the written integral is dived into two or three domains depending how the interface cuts the element. Assuming it is divided into two subelements rewriting equation 4.40 in

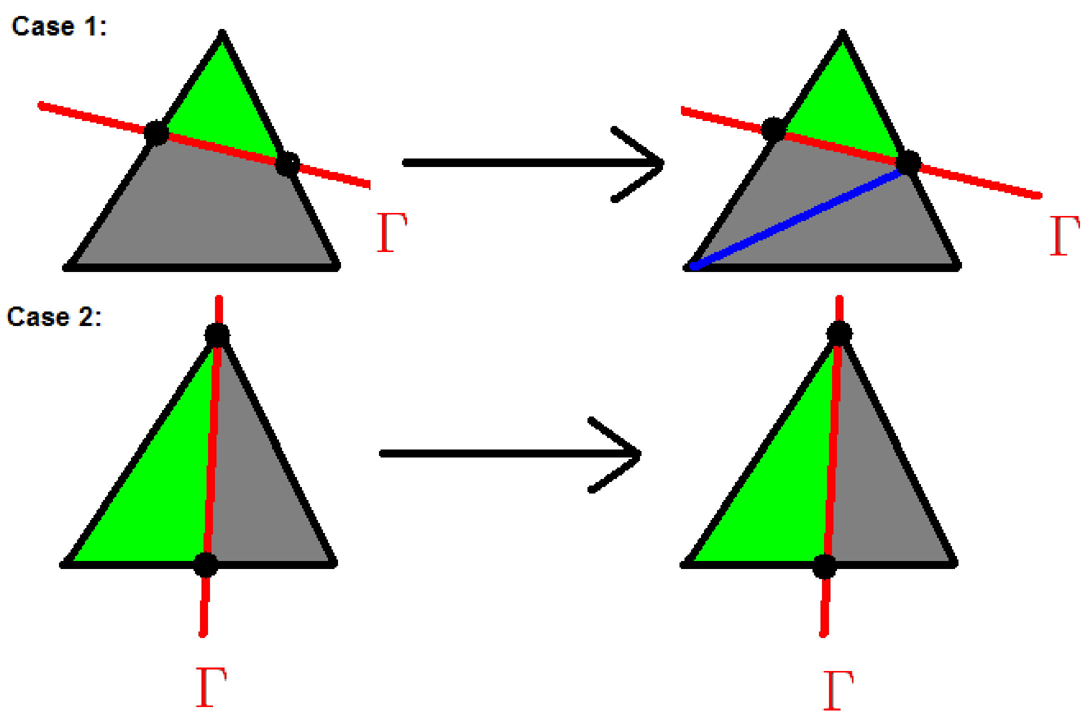

Figure 4.5: Different Division Of The Multiphase Elements According To How Interface Cuts Them

two terms showing the the subelements domains as Ω^{e1} and Ω^{e2}:

$$\int_{\Omega^e} \nu(\overrightarrow{\mathbf{x}}) f(x,y)\ \mathrm{d}\Omega^e = \int_{\Omega^{e1}} \nu(\overrightarrow{\mathbf{x}}) f(x,y)\ \mathrm{d}\Omega + \int_{\Omega^{e2}} \nu(\overrightarrow{\mathbf{x}}) f(x,y)\ \mathrm{d}\Omega \quad (4.41)$$

The key point here is, when mapping the x-y coordinate system to the master element the positions of the Gauss points of the subelement according to the main element in the master coordinate system should be determined and used as it is done in the code to calculate the integrals numerically. Also, the Jacobian matrixes of the subelements should be used since determinant of Jacobian is a ratio of the area between the master element and the element in x-y coordinate system and the contributions coming from the subelements are only calculated in their own areas.

Chapter 5

CONTINUITY OF STRESS ON THE INTERFACE

5.1 Why X-FEM Needs To Be Improved?

Classical Finite Elements Method is not able to capture the discontinuous gradients in the element if the used computational mesh is not aligned with interface in two–phase problems. In addition to the Classical Finite Elements Method Theory, Extended Finite Elements Method includes introducing an enrichment technique via partition of the unity concept to obtain a solution with discontinuous gradient across the interfaces in two–phase flows or in problems where discontinuities or singularities exist in the problem domain. This means, for our two–phase problem it becomes possible to get a better solution with discontinuous gradient inside the elements crossed by the interface and also this enrichment that Extended Finite Elements Method makes it possible to enforce other equations.

The main problem mentioned above related to Finite Elements Analysis can be expressed in another words as using a general point P defined on the interface of a two–phase flow. Refer to figure 5.2b for the illustration of the point mentioned. Writing the fluxes for the first domain and second domain in a case where a mesh that doesn't conform the interface:

$$\overrightarrow{\mathbf{q}}_1 = -\nu_1 \nabla \overrightarrow{\mathbf{v}}|_{\Omega_1} \tag{5.1}$$

$$\overrightarrow{\mathbf{q}}_2 = -\nu_2 \nabla \overrightarrow{\mathbf{v}}|_{\Omega_2} \tag{5.2}$$

In equations 5.1 and 5.2, the gradient of the velocity function $\overrightarrow{\mathbf{v}}$ calculated at the general point P on the interface is the same when Classical Finite Elements approximation spaces is used. The flux jump at this point reads:

$$-\nu_1 \nabla \overrightarrow{\mathbf{v}}|_{\Omega_1} + \nu_2 \nabla \overrightarrow{\mathbf{v}}|_{\Omega_2} \neq 0 \tag{5.3}$$

as long as $\nu_1 \neq \nu_2$ or $\nabla \overrightarrow{\mathbf{v}} \neq 0$ this happens. Because of the fact that Classical Finite Elements Method gradient of velocity has the same in an enriched element. So equation 5.3 can be rewritten also as in the form:

$$(\nu_2 - \nu_1) \nabla \overrightarrow{\mathbf{v}}|_{x=P} \neq 0 \tag{5.4}$$

In our two–phase problem this is the continuity of the normal component of stress which (as it is stated before in equation 3.15) is:

$$[\![\underline{\underline{\boldsymbol{\sigma}}} \, \overrightarrow{\mathbf{n}}]\!] = 0 \qquad \text{on} \quad \boldsymbol{\Gamma} \tag{5.5}$$

that is desired to be satisfied to make the stress continuous along the interface of two–phase problem. But as it explained before it is not possible using only Finite Elements Analysis. According to the results obtained in section 6, equation 5.5 is not still satisfied even when X-FEM is used as the solution technique. So Using X-FEM the continuity of the normal component of stress along the interface should be enforced in the global solution. The details related to this process is given in section 5.3. It is useful to emphasize that it is not possible to get such a solution using Classical Finite Elements Method only if the mesh used does not conform the interface in the domain. So, in this part the different part of the Extended Finite Elements Method from the Classical Finite Elements is emphasized assuming that the derivation for the Classical Finite Elements part is the same with the one derived in section 4.3 using also the basics provided in Appendix A.

5.2 Imposing The Continuity Of Fluxes Along The Interface

In order to introduce the ideas that will be used next to impose the normal stress continuity across the interface, we describe here the solution of a simpler problem: The continuity of fluxes in a two–phase Poisson problem. It is mentioned before that for cases where a discontinuous solution exist across the interface Classical Finite Elements Method can not capture the solution if the mesh is not aligned with the interface but X-FEM can capture these discontinuities. However still when the results are checked it is seen that the continuity of fluxes are not still satisfied and an additional enforcement of continuity of across the interface is needed. The general form of bimaterial Poisson problem after imposing the continuity of fluxes along the interface can be stated as :

$$\nabla \cdot (-\nu_i \nabla u) = f \qquad \text{in} \qquad \Omega_i \tag{5.6}$$

$$-\nu_i \nabla u \cdot \overrightarrow{\mathbf{n_1}} = g_n \qquad \text{on} \qquad \Gamma_N \tag{5.7}$$

$$u = u_D \qquad \text{on} \qquad \Gamma_D \tag{5.8}$$

$$[\![\nu \nabla u]\!] \overrightarrow{\mathbf{n_2}} = 0 \qquad \text{on} \qquad \Gamma \tag{5.9}$$

Where:

- The variable that represent different subdomains (i) goes from one to two for a bimaterial problem
- $[\![\ ]\!]$ is the jump term
- $\overrightarrow{\mathbf{n_1}}$ is the unit outwards normal vector to the domain Ω_i
- $\overrightarrow{\mathbf{n}}_2$ is the normal vector to the interface

It becomes possible to get a discontinuous solution when X-FEM is used. However according to the results obtained it is still needed to enforce the continuity of fluxes across the interface. The condition enforced to get a continuous flux solution in the problem in this case is given in 5.9. The results obtained from the paper in preparation Diez et al. (2011) are given in figure 5.1. See the continuity of the fluxes across the interface when the continuity of fluxes along the interface are enforced.

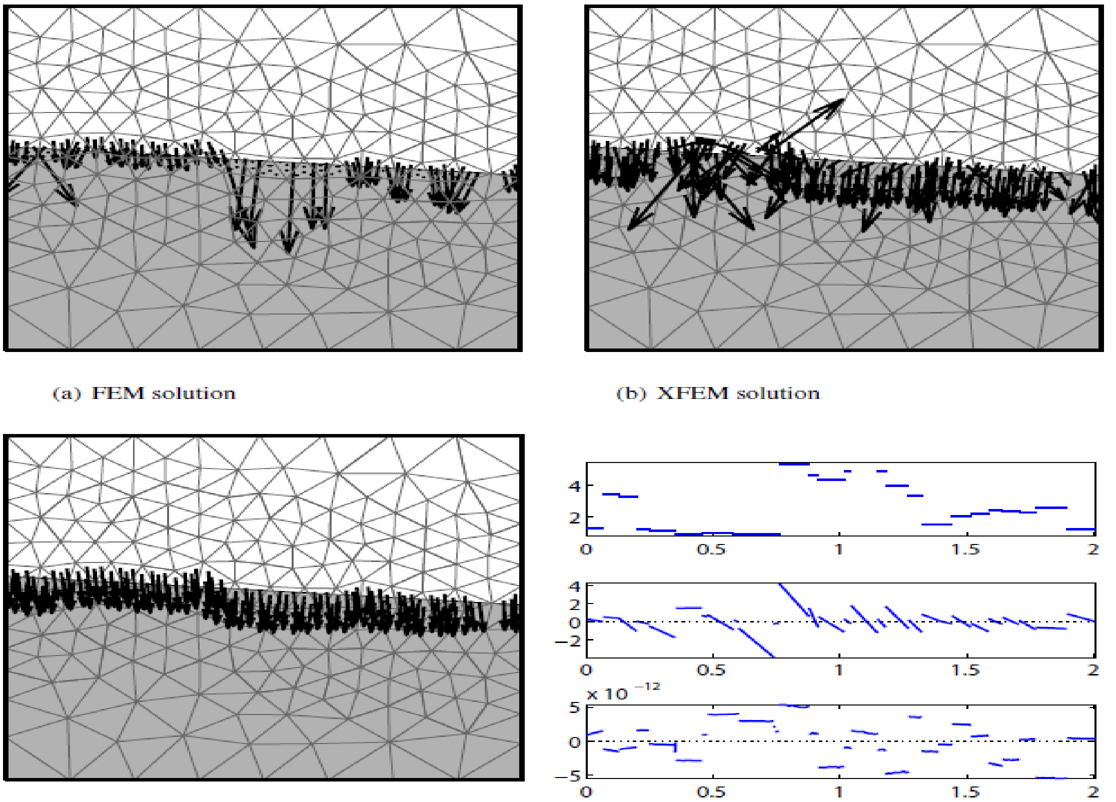

(a) FEM solution

(b) XFEM solution

(c) XFEM+ solution

(d) Flux jump along the interface for FEM (up), XFEM (middle) and XFEM+ (bottom)

Figure 5.1: Comparison Of Different Solution Techniques For Two Dimensional Poission's Problem

Notice in the figure that the derivatives of the solution are plotted and they are inaccurate in the vicinity of the interface when extra condition is not enforced.

5.3 Enforcing Continuity of Normal Component Of Stress Across The Interface

The same concept to get a more accurate numerical solution is applied here to a two–phase flow problem. The representation of a random point on the interface in a two–phase flow is given in picture 5.2. The stresses at this general point P on the interface for the first and the second fluid can be expressed as:

$$\overrightarrow{\boldsymbol{\sigma}}_1 = -p|_{\Omega_1}\, \underline{\underline{\mathbf{I}}} - \nu_1 \nabla^s \overrightarrow{\mathbf{v}}|_{\Omega_1} \tag{5.10}$$

$$\overrightarrow{\boldsymbol{\sigma}}_2 = -p|_{\Omega_2}\, \underline{\underline{\mathbf{I}}} - \nu_2 \nabla^s \overrightarrow{\mathbf{v}}|_{\Omega_2} \tag{5.11}$$

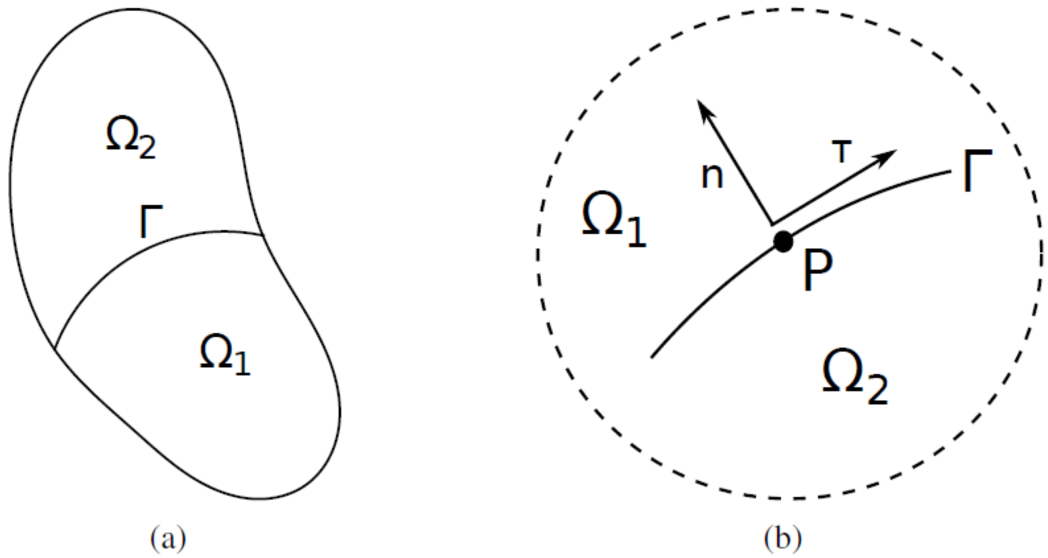

Figure 5.2: a)Problem Domain, b) A Random Point Taken On The Interface Of A Two–Phase Flow With Definition Of Normal And Tangential Vectors

Because of the fact that pressure is continuous across the interface, only enforcing the rest in equations 5.10 and 5.11 will make it possible to get a continuous normal component of stress on the interface. At this point the reason why only the values of one part of the stress is traced in results section (section 6) is given. In addition to this, imposing the normal component of stress continuity reads:

$$\left(\nu_1\, \nabla^s \overrightarrow{\mathbf{v}}|_{\Omega_1} - \nu_2\, \nabla^s \overrightarrow{\mathbf{v}}|_{\Omega_2}\right) \overrightarrow{\mathbf{n}} = \overrightarrow{\mathbf{0}} \tag{5.12}$$

where $\overrightarrow{\mathbf{n}}$ is the unit normal vector to the interface. Since the right-hand side here is a zero vector, the normal vector to the interface can be taken as vectors facing outward of the first domain or the second domain, namely $\overrightarrow{\mathbf{n_1}}$ or $\overrightarrow{\mathbf{n_2}}$. Multiplying equation 5.12 with a weighting function and integrating along the interface the equation that will be added to the equation system is obtained:

$$\int_\Gamma t_i \cdot \left(\nu_1\, \nabla^s \overrightarrow{\mathbf{v}}|_{\Omega_1} - \nu_2\, \nabla^s \overrightarrow{\mathbf{v}}|_{\Omega_2}\right) \overrightarrow{\mathbf{n}}\, \mathrm{d}\Gamma = \overrightarrow{\mathbf{0}} \tag{5.13}$$

where t_i is the linear weighting function used in the analysis which takes the value unity at the locations where interface cuts the elements. See figure 5.3 where the points that are cut by the interface is named as 1 and 2. Notice that t_i is discontinuous between different elements. The figure shows the values of the two weighting functions for the enriched elements with different colors along the approximation of the real interface.

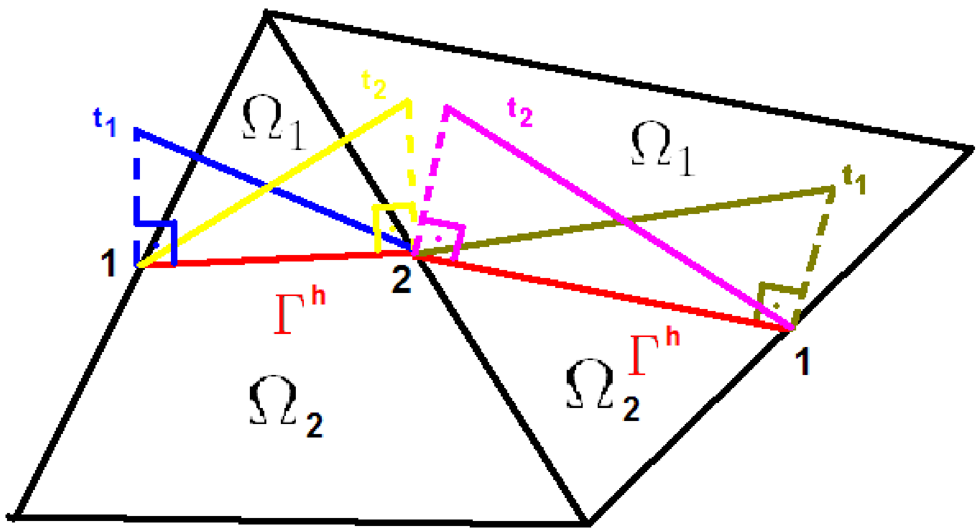

Figure 5.3: Illustration of the Shape Function Used to Enforce Continuity of Normal Component Of Stress Along The Interface

Equation 5.13 is the equation that forces stresses across the interface to be continuous in the numerical solution. The next step is replacing the velocity with its Extended Finite Elements approximation as in section 5.1.

The normal vector here can be calculated using the values of the Level Set Function in the vertex nodes using the formula given in equation 3.9. Lastly, it should be emphasized that for numerical calculation of the integral when the interface on the enriched element is mapped onto a master element of [-1,1] the linear shape functions are selected as :

$$t_1 = (1-\xi)/2 \tag{5.14}$$

$$t_2 = (1+\xi)/2 \tag{5.15}$$

So according to the information provided in this section totally four equations are added to the global system of equation for one enriched element. This slows the computation but gives a solution in which continuity of normal component of stress is weakly satisfied.

Chapter 6

NUMERICAL RESULTS

In the previous chapters the basic numerical techniques that are used to obtain solution to the coupled equations of multiphase fluid flow problem are described. The proposed numerical approach is tested in this section on a test case using MATLAB.

6.1 Definition Of The Test Problem

The problem is the setup of a cell growth experiment where the a group of cells (cell culture) is attached to the one of the walls and a fluid is flowing around them. The aim is increasing the shear stress on the cell culture to trigger an increase in the rate of proliferation. Domain is considered as a square which has got sides of unity length. The flow into the domain is defined with a unity length vertical velocity defined only in the bottom side of the square domain. Left and right sides are assumed to have a no-slip condition. Left bottom corner of the domain is assumed to be origin. In addition to this, only the pressure value of the node at the left bottom corner is given as zero with the aim of finding the relative pressure distribution in the domain.

Cell culture is modelled as another fluid which has got 10 times of viscosity of water and water is assumed to be the fluid flowing around the cells. Cell culture is modelled as a half circle attached to the left wall (The Level Set and the problem set up is shown in figures 6.1 and 6.2) using the Level Set function :

$$\phi(\overrightarrow{\mathbf{x}}) = x^2 + (y - 0.5)^2 - 0.25^2 \tag{6.1}$$

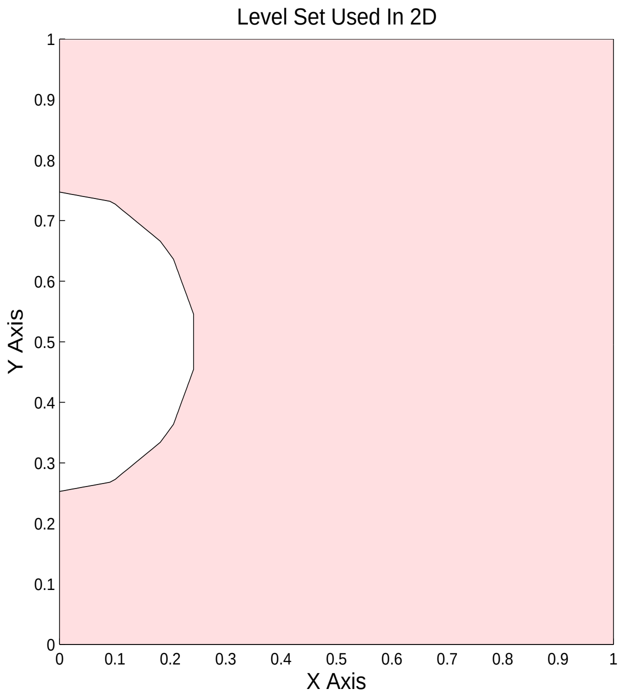

Figure 6.1: Level Set Used In 2D

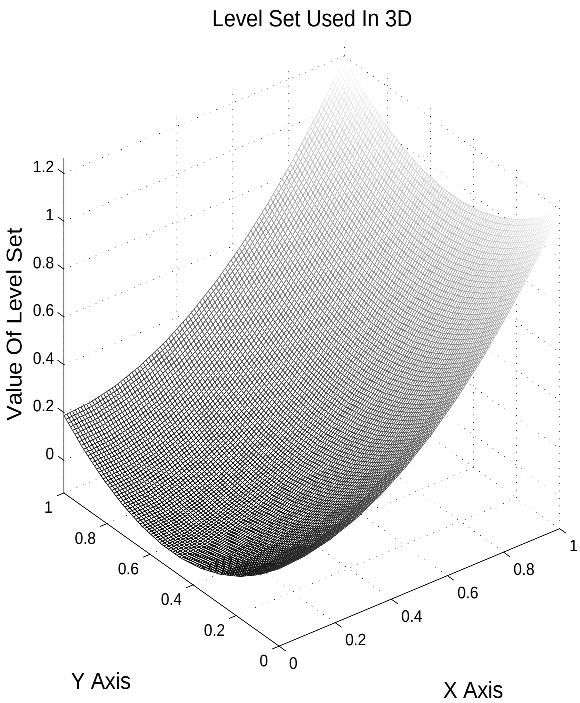

Figure 6.2: Level Set Used In 3D

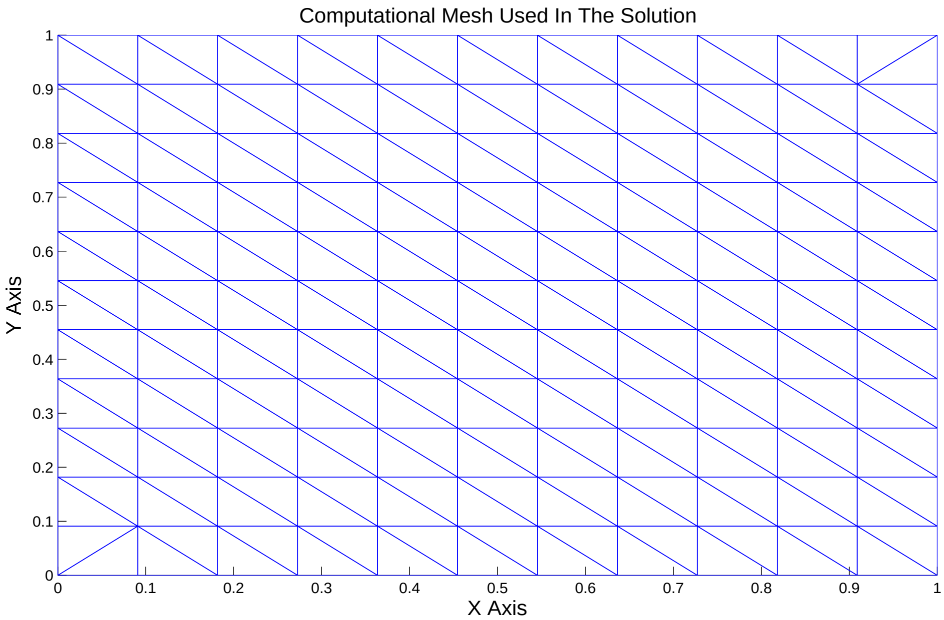

Figure 6.3: Computational Mesh Used In Numerical Solution

The computational mesh used in the solution is shown in figure 6.3.

6.2 Results

The velocity distribution when the continuity of normal component of stress across the interface is not enforced is illustrated in figure 6.4

To show that the scheme could enforce the continuity of the stress along the interface in the problem defined in section 6.1, a comparison of the jump of stresses along the interface is given in this section. For this purpose a function is written with the aim of checking the values of norm of normal component of stress jump on Gauss points on the interface and maximum element of absolute of the weighted continuity of stress condition. It is mentioned in section 5.3 that since the pressure is continuous only the deviatoric part of the stress on the interface is taken into consideration. (In other words stress jump in the graphs given in this section is calculated using the formula $2\times(\nu_1\nabla^s\overrightarrow{\mathbf{v}}|_{\Omega_1} - \nu_2\nabla^s\overrightarrow{\mathbf{v}}|_{\Omega_2})\overrightarrow{\mathbf{n}}$).

When the continuity of normal component of stress is not enforced the jump of norm of normal component of stress on Gauss points on the interface are illustrated in 6.5 and the maximum element of the weighted continuity of stress condition (calculated value of expression in equation 6.3) is illustrated in 6.6. Note that figure

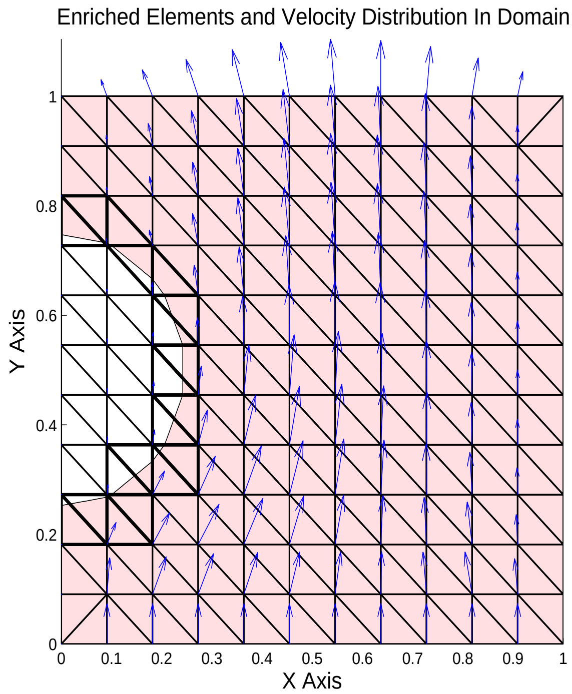

Figure 6.4: Enriched Elements and Velocity Distribution In Problem Domain When Continuity of Normal Component Of Stress Condition Is Not Enforced

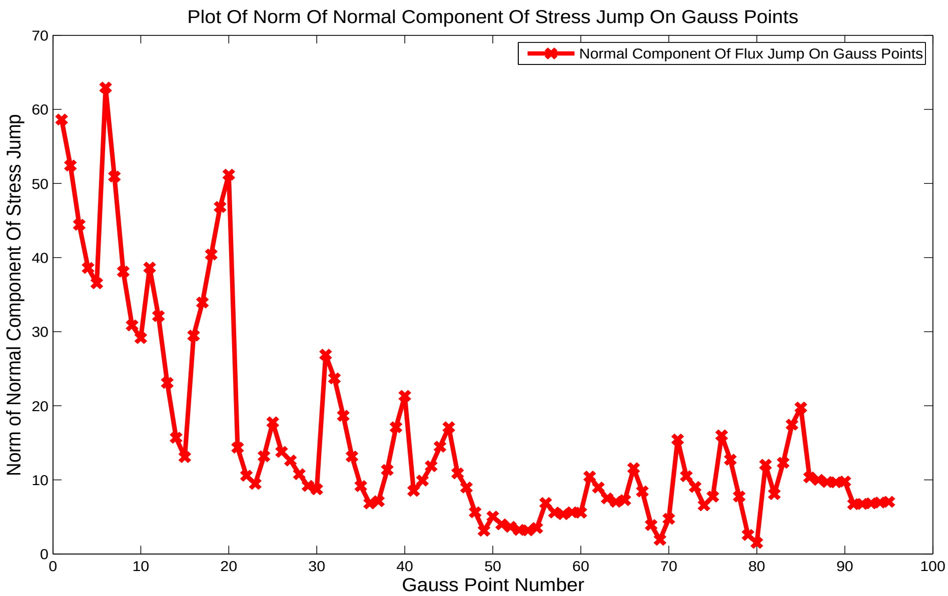

Figure 6.5: Norm Of Normal Component Of Stress Jump On Gauss Points On The Interface When The Continuity Of Stress Is Not Enforced In The Numerical Solution

6.6 is the maximum element of absolute of the weighted continuity of stress condition calculated on each element. The velocity distribution with the enriched elements in

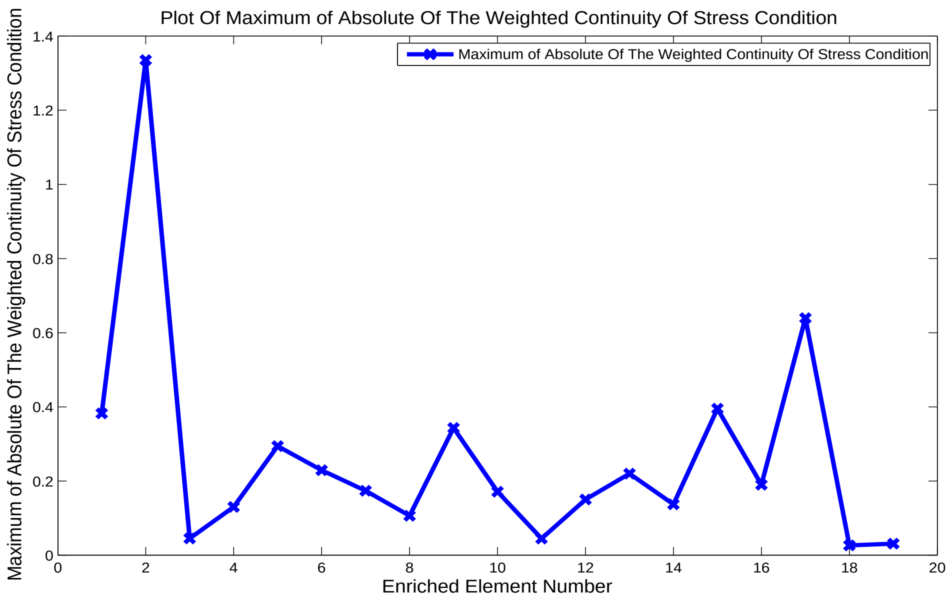

Figure 6.6: Maximum Element Of Absolute Of The Weighted Continuity Of Stress Condition For Each Enriched Element When The Continuity Of Stress Is Not Enforced In The Numerical Solution

the domain when the continuity of normal component of stress across the interface is enforced are given in figure 6.7.

The horizontal axes of the figure 6.5, 6.8, 6.6 and 6.9 are given as Gauss point numbers and vertical axes of the same figures are *Norm Of Normal Component Of Stress Jump On Gauss Points On The Interface* which can be stated as:

$$norm\left(2 \times \left(\nu_1 \nabla^s \overrightarrow{\mathbf{u}} - \nu_2 \nabla^s \overrightarrow{\mathbf{u}}\right) \overrightarrow{\mathbf{n}}\right) \tag{6.2}$$

The horizontal axes of the figure 6.6 and 6.9 are given as enriched element numbers and vertical axes of the same figures are *Maximum Element Of Absolute Of The Weighted Continuity Of Stress Condition For Each Enriched Element* which can be stated as the maximum value of the elements in the result of the integral stated below:

$$\int_{\Gamma^e} \overrightarrow{\mathbf{t_i}} \left(\nu_1 \nabla^s \overrightarrow{\mathbf{u}} - \nu_2 \nabla^s \overrightarrow{\mathbf{u}}\right) \overrightarrow{\mathbf{n}} \tag{6.3}$$

Note that in equation 6.3 the integral is calculated along the interface of the element only.

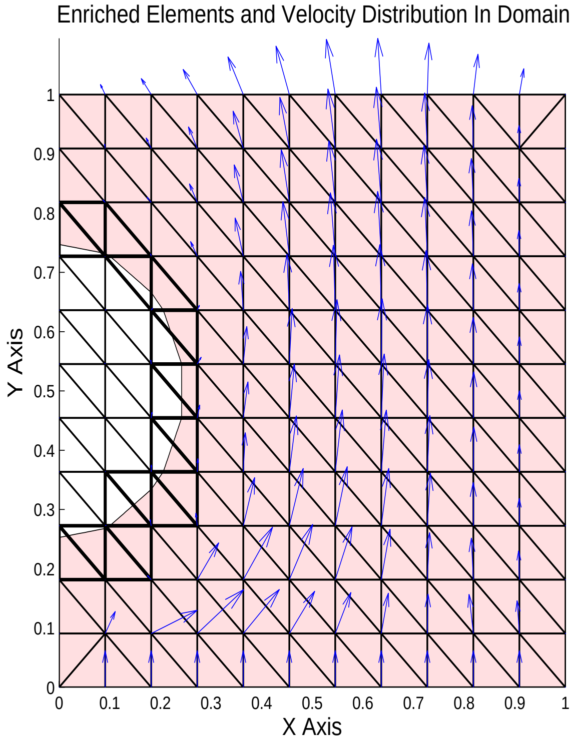

Figure 6.7: Enriched Elements and Velocity Distribution In Problem Domain When Continuity of Normal Component Of Stress Condition Is Enforced

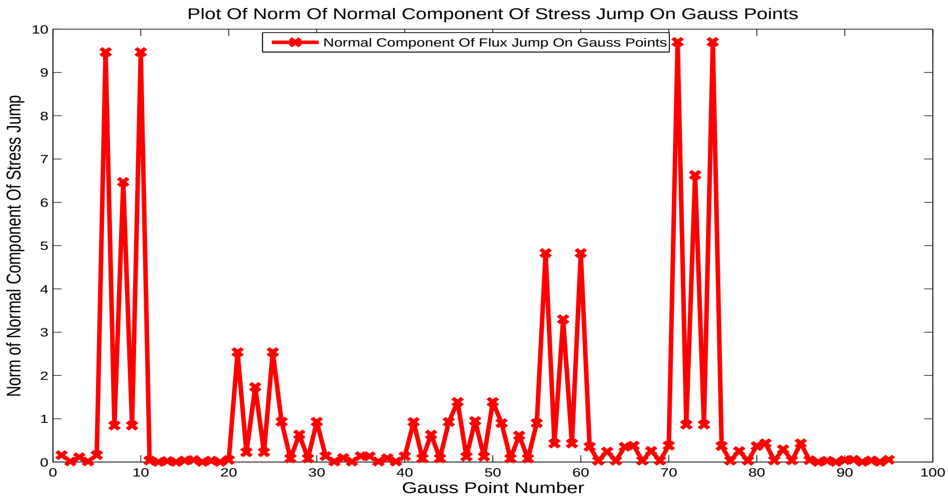

Figure 6.8: Norm Of Normal Component Of Stress Jump On Gauss Points On The Interface When The Continuity Of Stress Is Enforced In The Numerical Solution

According to the results obtained: norm of normal component of stress jump on Gauss points on the interface decreases by a factor of nearly 6 and values in maximum element of absolute of the weighted continuity of stress condition or each

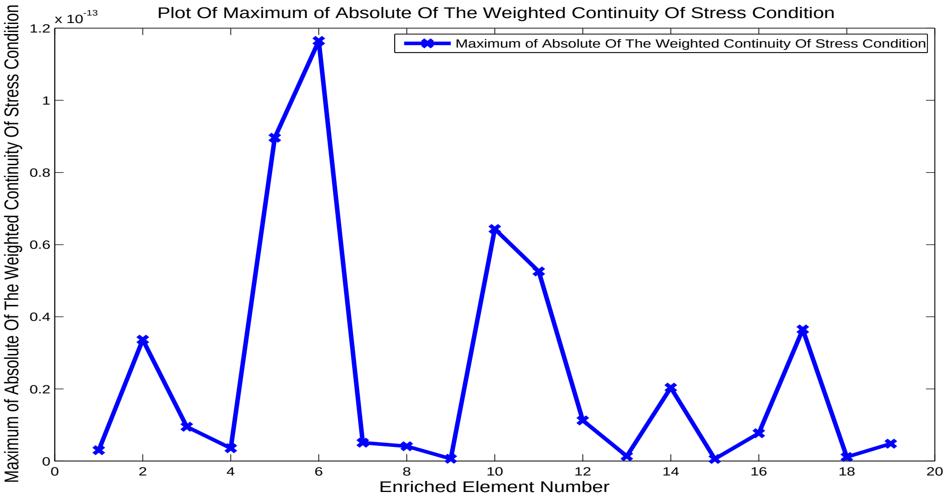

Figure 6.9: Maximum Element Of Absolute Of The Weighted Continuity Of Stress Condition For Each Enriched Element When The Continuity Of Stress Is Enforced In The Numerical Solution

enriched element graph decreases by a factor of 10^{13} and according to the results obtained the continuity of normal component of stresses is satisfied in the solution since it effectively decreases the stress jumps observed along the interface when only Extended Finite Elements Method is used in the solution. The value of the jump in normal component of stress does not become exactly zero since the condition is weakly enforced in the numerical solution. Lastly, the MATLAB function that is used to check if the desired continuity of stress condition is satisfied is given:

```
function plotFlux(X,T,LS,enrElem,stdElem,enrNode,velo,...
    nu1,nu2,interphasePoints)
% Gr = [x y, u_x u_y v_x v_y]
% velo = full velocity (std+enr) in 2 columns (u,v)

global useSym
nGeometryNodes = 3; %Number of geometry nodes
typeOfElement = 2; %Triangular element
ngaus = 7; % Number of gauss points used in the analysis
nNode = size(X,1) + size(T,1);

[pospg,pespg] = quadrature(typeOfElement,ngaus);
%Gauss quadrature points and weights
[N,Nxi,Neta] = shapeFunctions(typeOfElement,4,pospg);
```

```
% Shape functions and derivatives at Gauss points

Gr = [];

for I = 1:length(stdElem)
    Te = T(stdElem(I),:); %local to global vector
    Xe = X(Te(1:3),:); %element coordinates
    Ve = velo(Te,:);  %solution for the element

    if LS(Te(1)) > 0 %selection of viscosity
        %depending on the location of Gauss point
        nu = nu1; % mat 1
    else
        nu = nu2; % mat 2
    end

    for igaus = 1:ngaus %Gauss point loop
        jacob = [Nxi(igaus,1:nGeometryNodes); ...
            Neta(igaus,1:nGeometryNodes)]*Xe;
        %Jacobian matrix
        res = jacob\[Nxi(igaus,:);Neta(igaus,:)];
        %Derivatives of shape functions calculated
        %at Gauss points
        Nx = res(1,:);
        Ny = res(2,:);

        pos = N(igaus,1:nGeometryNodes)*Xe;
        %Gauss points in xy coordinates
        dUdx = Nx*Ve(:,1);
        dVdx = Nx*Ve(:,2);
        dUdy = Ny*Ve(:,1);
        dVdy = Ny*Ve(:,2);

        Gr = [Gr; pos [dUdx dUdy dVdx dVdy]*nu];
    end
end


for I = 1:length(enrElem) %Enriched elements loop
    Te = T(enrElem(I),:); %Local to global vector
```

```
    Re = vectorFind(enrNode, Te(1:nGeometryNodes));
    %Local to global vector for enriched degree of freedoms

    Xe = X(Te(1:3),:); %Element coordinates
    Ve = velo(Te,:); %Solution for the element
    LSe = LS(Te(1:3)); %Level Set values on the element
    Vee = velo(Re+nNode,:);%Local to global vector
    %for enriched degree of freedoms iterated version

    [R,Rxi,Reta] = buildRidge( LSe, ...
        N(:,1:nGeometryNodes), Nxi(:,1:nGeometryNodes),...
        Neta(:,1:nGeometryNodes) );
    %calculation of Ridge function
    for igaus = 1:ngaus %Gauss points loop
        jacob = [Nxi(igaus,1:nGeometryNodes); ...
            Neta(igaus,1:nGeometryNodes)]*Xe;
        res = jacob\[Nxi(igaus,:);Neta(igaus,:)];
        resR = jacob\[Rxi(igaus,:);Reta(igaus,:)];
        Nx = res(1,:);
        Ny = res(2,:);
        Rx = resR(1,:);
        Ry = resR(2,:);
        Mx = Nx(1:nGeometryNodes) * R(igaus) +...
            N(igaus,1:nGeometryNodes) * Rx;
        My = Ny(1:nGeometryNodes) * R(igaus) +...
            N(igaus,1:nGeometryNodes) * Ry;

        pos = N(igaus,1:nGeometryNodes)*Xe;
        dUdx = Nx*Ve(:,1) + Mx*Vee(:,1);
        dVdx = Nx*Ve(:,2) + Mx*Vee(:,2);
        dUdy = Ny*Ve(:,1) + My*Vee(:,1);
        dVdy = Ny*Ve(:,2) + My*Vee(:,2);
        %
        if N(igaus,1:nGeometryNodes)*LSe > 0 %selection
            %of viscosity depending on the location
            %of Gauss point
            nu = nu1; % mat 1
        else
            nu = nu2; % mat 2
        end
```

```
        if useSym
            Gr = [Gr; pos [dUdx 0.5*(dUdy+dVdx)...
                0.5*(dUdy+dVdx) dVdy]*nu];
        else
            Gr = [Gr; pos [dUdx dUdy dVdx dVdy]*nu];
        end
    end
end


%%
figure
plotLShis(X,LS');
hold on
% grad U
quiver( Gr(:,1), Gr(:,2), Gr(:,3), Gr(:,4), 1,...
    'color', 'b' );
% grad V
quiver( Gr(:,1), Gr(:,2), Gr(:,5), Gr(:,6), 1,...
    'color', 'r' );
legend('Interface','grad U','grad V')
%Plot of grad U and grad V




%% compute the stress jump across the interphase
[pg,wg]=quadrature(0,5);
N1d = shapeFunctions(0,2,pg);
icountt=0;
for I = 1:length(enrElem)%enriched elements loop
    pts = [interphasePoints(2*I-1,:);...
        interphasePoints(2*I,:)];
    %positions of points cut by levelset the normal
    dist = pts(1,:)-pts(2,:);
    h = norm(dist);

    Te = T(enrElem(I),:);
    Re = vectorFind(enrNode, Te(1:nGeometryNodes));

```

```
    Xe = X(Te(1:3),:);
    Ve = velo(Te,:);
    LSe = LS(Te(1:3));
    Vee = velo(Re+nNode,:);

    xy = N1d*pts;
    [xi,eta] = invMap(Xe, xy(:,1), xy(:,2));
    [N,Nxi,Neta] = shapeFunctions(typeOfElement,...
        4,[xi,eta]);

    % Ridge evaluated in the positive side
    [Rp,Rxip,Retap] = buildRidge( LSe, ...
        N(:,1:nGeometryNodes), Nxi(:,1:nGeometryNodes),...
        Neta(:,1:nGeometryNodes), 1 );
    % Ridge evaluated in the negative side
    [Rn,Rxin,Retan] = buildRidge( LSe, ...
        N(:,1:nGeometryNodes), Nxi(:,1:nGeometryNodes),...
        Neta(:,1:nGeometryNodes), 2 );

    fprintf('\nElement %d', I);
    int = 0;
    for igaus = 1:length(pg)
        jacob = [Nxi(igaus,1:nGeometryNodes); ...
            Neta(igaus,1:nGeometryNodes)]*Xe;
        res = jacob\[Nxi(igaus,:);Neta(igaus,:)];
        resRp = jacob\[Rxip(igaus,:);Retap(igaus,:)];
        resRn = jacob\[Rxin(igaus,:);Retan(igaus,:)];
        nn=gausspointnfinder(Nxi(igaus,1:nGeometryNodes),...
            Neta(igaus,1:nGeometryNodes),jacob,LSe);
        %Ridge function is converted into xy coordinates here
        %both for negative and positive side of the domain
        Nx = res(1,:);
        Ny = res(2,:);
        Rxp = resRp(1,:);
        Ryp = resRp(2,:);
        Rxn = resRn(1,:);
        Ryn = resRn(2,:);
        Mxp = Nx(1:nGeometryNodes) * Rp(igaus) +...
            N(igaus,1:nGeometryNodes) * Rxp;
        Myp = Ny(1:nGeometryNodes) * Rp(igaus) +...
```

```
            N(igaus,1:nGeometryNodes) * Ryp;
        Mxn = Nx(1:nGeometryNodes) * Rn(igaus) +...
            N(igaus,1:nGeometryNodes) * Rxn;
        Myn = Ny(1:nGeometryNodes) * Rn(igaus) +...
            N(igaus,1:nGeometryNodes) * Ryn;
        %Enrichment functions are calculated for
        %all possibilities
        pos = N(igaus,1:nGeometryNodes)*Xe;
        dUdxp = Nx*Ve(:,1) + Mxp*Vee(:,1);
        dVdxp = Nx*Ve(:,2) + Mxp*Vee(:,2);
        dUdyp = Ny*Ve(:,1) + Myp*Vee(:,1);
        dVdyp = Ny*Ve(:,2) + Myp*Vee(:,2);
        %
        dUdxn = Nx*Ve(:,1) + Mxn*Vee(:,1);
        dVdxn = Nx*Ve(:,2) + Mxn*Vee(:,2);
        dUdyn = Ny*Ve(:,1) + Myn*Vee(:,1);
        dVdyn = Ny*Ve(:,2) + Myn*Vee(:,2);
        %elements of symmetric gradient of
        %velocity is calculated here
        if useSym
            gradSp = [dUdxp 0.5*(dVdxp+dUdyp); ...
                0.5*(dVdxp+dUdyp) dVdyp];
            %symmetric gradient of velocity for positive side
            gradSn = [dUdxn 0.5*(dVdxn+dUdyn); ...
                0.5*(dVdxn+dUdyn) dVdyn];
            %symmetric gradient of velocity for negative side
        else
            gradSp = [dUdxp dUdyp; ...
                dVdxp dVdyp];
            %symmetric gradient of velocity for positive side

            gradSn = [dUdxn dUdyn; ...
                dVdxn dVdyn];
            %symmetric gradient of velocity for negative side
        end

        % jump
        z = 2*(gradSp*nn*nu1 - gradSn*nn*nu2);
         %normal component of stress jump
        fprintf('\n\tz = [%e    %e]', z(1), z(2));
```

```
            icountt=icountt+1;
            znorm(icountt)=norm(z); %norm of normal
            %component of stress jump
            int = int + z * N1d(igaus,:) * wg(igaus) * h/2;
            %continuity of stress condition
        end
        inttrace(I)=max(max(abs(int)));
        fprintf('\n\tint = [%e    %e;   %e   %e]\n',...
            int(1,1), int(1,2), int(2,1), int(2,2));
    end
title('Plot Of Gradients The Components Of Velocity Vector',...
    'fontsize',14)
xlabel('X Axis','fontsize',14)
ylabel('Y Axis','fontsize',14)

figure
plot(1:icountt,znorm,'-xr','linewidth',3,'markersize',9)
title('Plot Of Norm Of Normal Component Of Stress Jump On Gauss ...
    Points','fontsize',13)
xlabel('Gauss Point Number','fontsize',13)
ylabel('Norm of Normal Component Of Stress Jump','fontsize',13)
legend('Normal Component Of Flux Jump On Gauss Points')


figure
plot(1:I,inttrace,'-xb','linewidth',3,'markersize',9)
title('Plot Of Maximum of Absolute Of The Weighted Continuity Of ...
    Stress Condition','fontsize',13)
xlabel('Enriched Element Number','fontsize',13)
ylabel('Maximum of Absolute Of The Weighted Continuity Of Stress ...
    Condition','fontsize',13)
legend('Maximum of Absolute Of The Weighted Continuity Of Stress ...
    Condition')
```

Chapter 7

CONCLUSION

In this work we have proposed a modification to the well-known Extended Finite Elements Method (X-FEM) used in combination with Level Set Method to improve the accuracy of the stresses close to the interface in multiphase flow problems. The proposed scheme is motivated by several observations :

1) Despite X-FEM provides an enhanced solution (with respect to Classical Finite Elements Method) close to the interface, the derivatives of the X-FEM solution are not better than the those provided by FEM. Consequently, the stress jump across the interphase is not zero.

2) In some practical problems the quantity of interest are the fluxes/stresses at the interface. Two examples of these problems are:

i) The update of the interface location based on the fluxes (See Cordero and Díez (2010))

ii) The simulation of cell growth in a flow channel. In this case one of the important factors is measuring the stresses exerted by the flow at the surface of the growing cells. The proposed scheme is based in the explicit solution of the stress continuity equation across the interface. This equation is solved in a weak form and implemented as a restriction of the solution space using Lagrange multipliers. The interpolation space used in the discretization of the stress continuity equation is discontinuous between elements. While this increases the size of the system, it provides a much better approximation of the stress continuity.

Also a MATLAB code which can enforce the continuity of normal component of the stresses in a two–phase flow is developed and submitted with the thesis.

Appendices

Appendix A

Extra Information

A.1 Integration By Parts

Integration by parts is a rule that transforms the integral of products of functions into (generally) simpler integrals. Expanding the differential of a product of two functions f and g:

$$d(fg) = f\ \mathrm{d}g + g\ \mathrm{d}f \tag{A.1}$$

And integrating both sides over the domain where f and g are defined:

$$\int d(fg)\mathrm{d}\mathbf{\Omega} = fg = \int f\ \mathrm{d}g\mathrm{d}\mathbf{\Omega} + \int f\ \mathrm{d}g\mathrm{d}\mathbf{\Omega} \tag{A.2}$$

Equation A.2 can be written as:

$$\int f\ \mathrm{d}g\mathrm{d}\mathbf{\Omega} = fg - \int g\ \mathrm{d}f\mathrm{d}\mathbf{\Omega} \tag{A.3}$$

Equation A.3 is known as *integration by parts rule* in mathematical analysis and it is mainly used to calculate the integrals using simpler integrals. The integral that is going to be calculated can be indefinite or definite. The same rule can be used for the vectorial functions.

A.2 Change Of Variables In Double Integrals

With the aim of calculating the results of integrals that come from the derivation of the finite elements formulations, it is a frequent application to use numerical techniques among which the most popular one is *Gauss Quadrature Integration*. For this purpose the limits of the integrals need to be defined over the reference domain. For example, in 2D applications where triangular elements are used this is a reference triangle which has got unity length sides. From calculus a define integral formula when the main variable is changed from x to u can be expressed as:

$$\int_a^b f(x)\ \mathrm{d}x = \int_c^d f(x(u))\frac{dx}{du}\ \mathrm{d}u \tag{A.4}$$

in equation A.4 it is assumed that x(u) is a continuous function where:

- a and b are the limits of variable x
- c and d are the corresponding limits of variable u

When the same change is done for a double integral in which two variables are defined, namely x and y, the same expression can be expressed as:

$$\iint\limits_{\Omega} f(x,y)\ \mathrm{d}x = \iint\limits_{\Omega^*} f(x(u,v),y(u,v))\left|\frac{\partial(x,y)}{\partial(u,v)}\right|\ \mathrm{d}u\ \mathrm{d}v \tag{A.5}$$

where $\left[\dfrac{\partial(x,y)}{\partial(u,v)}\right]$ is called the Jacobian matrix.

In this case the determinant of the Jacobian matrix can be stated as:

$$|J| = \left|\frac{\partial(x,y)}{\partial(u,v)}\right| = \left|\frac{\partial x}{\partial u}\frac{\partial y}{\partial v} - \frac{\partial x}{\partial v}\frac{\partial y}{\partial u}\right| \tag{A.6}$$

Determinant of Jacobian Matrix is know as a ratio between the area of the element in real domain and the area of the element in reference domain in a two dimension problem.

A.3 Gauss Quadrature Integration

There are many numerical tools that are used to calculate the definite integrals. For example: Rectangular rule, Trapezoidal rule and Simpson's rule... However, Gauss Quadrature Method is the one that is mostly preferred in Finite Element Analysis because of the fact that this method can calculate the results exactly when the integrand is a polynomial as it is the case for most of the Finite Elements Method applications.

In this method the result is expressed as a weighted sum of the integrand at specific points in the domain of integration. If n points are used in the integration the exact solution is obtained up to polynomials which have an order up to 2n-1 in one dimensional case.

Simply writing the integral in 1D assuming that the limits of integral is already converted into the limits in the reference element as stated in section A.2:

$$\int_{-1}^{+1} f(x)\ \mathrm{dx} = \sum_{i=1}^{n} w_i * f(x_i) \tag{A.7}$$

In equation A.7 n is the number of points used in the integration. As n changes the weights and the positions at which the function is calculated changes. The tables that include the Gauss points and corresponding weights used in one dimensional case and two dimensional cases are taken from Liu and Trung (2010) and given in sections A.3.1 and A.3.2. The total number of gauss points used in the numerical integration should change according to the integrand. So, the accuracy order for selection of a total number of gauss points is also given in the same tables.

Since the simulations provided in this thesis is for a two dimensional case, all the positions needed in the reference element and weights are also coded in the MATLAB code submitted in the function quadrature.m.

Find the Gauss Integration Points in Reference Element And Corresponding Weights in the following two sections for a one dimensional and two dimensional case.

A.3.1 One Dimensional Case For One Dimensional Quadrature Domain of $[-1, 1]$

When 2 integration points are used :

Table A.1: List Of Gauss Quadrature Points And Weights For 2 Points For One Dimensional Case, Order Of Accuracy:3

Point	Weight	Position in Reference Element
1	1.0000000000000000	-0.5773502691896257
2	1.0000000000000000	0.5773502691896257

When 3 integration points are used :

Table A.2: List Of Gauss Quadrature Points And Weights For 3 Points For One Dimensional Case, Order Of Accuracy:5

Point	Weight	Position in Reference Element
1	0.8888888888888888	0.0000000000000000
2	0.5555555555555556	-0.7745966692414834
3	0.5555555555555556	0.7745966692414834

When 4 integration points are used :

Table A.3: List Of Gauss Quadrature Points And Weights For 4 Points For One Dimensional Case, Order Of Accuracy:7

Point	Weight	Position in Reference Element
1	0.6521451548625461	-0.3399810435848563
2	0.6521451548625461	0.3399810435848563
3	0.3478548451374538	-0.8611363115940526
4	0.3478548451374538	0.8611363115940526

When 5 integration points are used :

Table A.4: List Of Gauss Quadrature Points And Weights For 5 Points For One Dimensional Case, Order Of Accuracy:9

Point	Weight	Position in Reference Element
1	0.5688888888888889	0.0000000000000000
2	0.4786286704993665	-0.5384693101056831
3	0.4786286704993665	0.5384693101056831
4	0.2369268850561891	-0.9061798459386640
5	0.2369268850561891	0.9061798459386640

A.3.2 Two Dimensional Case for a Isosceles Right Triangular Quadrature Domain

When 3 integration points are used:

Table A.5: List Of Gauss Quadrature Points And Weights For 3 Points For Two Dimensional Case, Order Of Accuracy:2

Point	Weight	ξ	η
1	1/6	1/6	1/6
2	4/6	1/6	1/6
3	1/6	4/6	4/6

When 4 integration points are used:

Table A.6: List Of Gauss Quadrature Points And Weights For 4 Points For Two Dimensional Case, Order Of Accuracy:3

Point	Weight	ξ	η
1	25/96	1/5	1/5
2	25/96	3/5	1/5
3	25/96	1/5	3/5
4	-9/32	1/3	1/3

When 6 integration points are used:

Table A.7: List Of Gauss Quadrature Points And Weights For 6 Points For Two Dimensional Case, Order Of Accuracy:4

Point	Weight	ξ	η
1	0.0549758718	0.0915762135	0.0915762135
2	0.0549758718	0.8168475729	0.0915762135
3	0.0549758718	0.0915762135	0.8168475729
4	0.1116907948	0.4459484909	0.4459484909
5	0.1116907948	0.1081030181	0.4459484909
6	0.1116907948	0.4459484909	0.1081030181

When 7 integration points are used:

Table A.8: List Of Gauss Quadrature Points And Weights For 7 Points For Two Dimensional Case, Order Of Accuracy:5

Point	Weight	ξ	η
1	0.0629695902	0.1012865073	0.1012865073
2	0.0629695902	0.7974269853	0.1012865073
3	0.0629695902	0.10128650732	0.7974269853
4	0.0661970763	0.47014206410	0.05971587178
5	0.0661970763	0.47014206410	0.47014206410
6	0.0661970763	0.05971587178	0.47014206410
7	0.1125000000	0.33333333333	0.33333333333

A.4 Lagrangian , Eulerian And ALE Descriptions Of Motion

For the mathematical description of flow problems it is certain that a kinematical description of the flow field is required. In continuum mechanics, there are mainly three descriptions of motion. They are:

1. Lagrangian description of motion

2. Eulerian description of motion

3. ALE description of motion

In Lagrangian description, each node of the mesh follows a specific particle throughout the motion. This approach is mainly used in solid mechanics applications. The Lagrangian description lets tracking interfaces and the free surfaces easily. The bad side of this approach is that it is unable to follow large distortions in the domain unless a frequent remeshing is used. Figure A.1 taken from Donea and Huerta (2002), shows the Lagrangian description in reference and last configurations. In the figure given ϕ is a point to point mapping function which relates the material coordinates to the spatial coordinates in such a way that :

$$(\overrightarrow{\mathbf{X}}, t) \rightarrow \phi(\overrightarrow{\mathbf{X}}, t) = (\overrightarrow{\mathbf{x}}, t) \tag{A.8}$$

where:

- $\overrightarrow{\mathbf{x}}$ is the spatial coordinates
- $\overrightarrow{\mathbf{X}}$ is the material coordinates
- t is time

Using mapping function ϕ the material coordinates are related to the spatial coordinates which makes it possible to write the spatial coordinates as a function of material coordinates and time directly :

$$\overrightarrow{\mathbf{x}} = \overrightarrow{\mathbf{x}}(\overrightarrow{\mathbf{X}}, t) \tag{A.9}$$

Eulerian description of motion uses a fixed computational mesh and the fluid moves with respect to the fixed mesh. In this case, large deformations is not a problem and it is very appropriate for turbulent flow simulation. The bad side of this approach is that it is difficult to track free surfaces and interfaces between different types of materials.

ALE description includes the introduction of a mesh which can move with a velocity independent of the velocity of the particles in the problem. This approach is pretty helpful in flow problems which include a large amount of distortion and in presence of moving boundaries in the problems. Mentioning the interaction between a flexible structure and a fluid would be a good example.

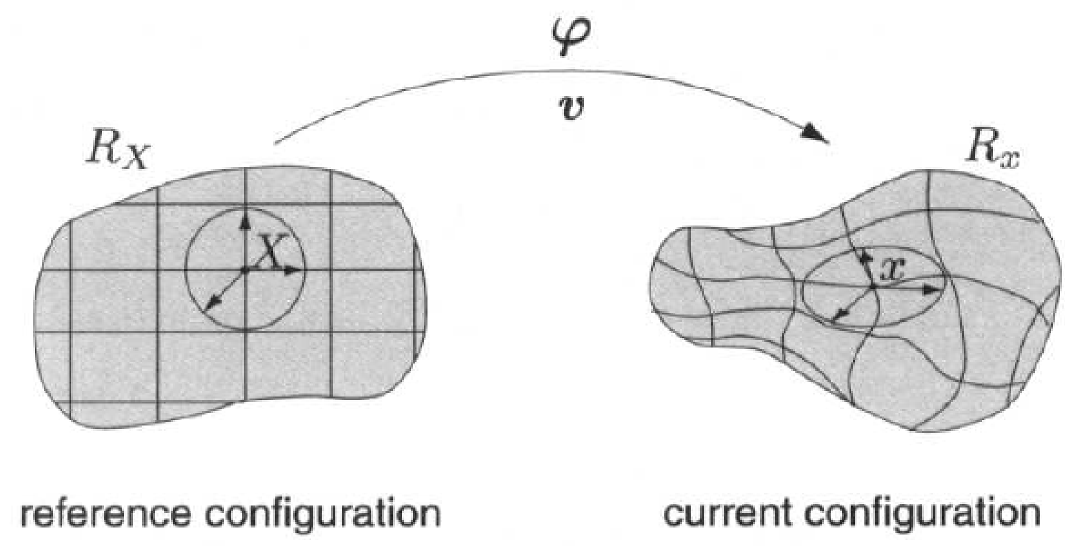

Figure A.1: Lagrangian Description Of Motion

In all the calculations throughout this thesis an *Eulerian Framework* is used which means that the problem includes a fixed mesh and physical quantities associated with the fluid flow is passing through a fixed region in space. Accordingly, in all the computations spatial coordinates are used.

Last information to be given under this headline is the expression of the relation between the time derivative of a scalar quantity f in spatial and material coordinates. The relation can be expresses as in the equation A.10

$$\frac{Df}{dt} = \frac{\partial f}{\partial t} + \overrightarrow{\mathbf{v}} \cdot \nabla f \tag{A.10}$$

A.5 Integral Theorems

A.5.1 Reynolds Transport Theorem

To get the integral form of the basic equations, such as conservation of mass momentum and energy, it is required to know the rate of change of integrals which are defined on non-stationary volumes. Imagine a material volume V_m and this volume is bounded by a closed surface S_m. The points on this surface move with a material velocity defined as $\overrightarrow{\mathbf{v}} = \overrightarrow{\mathbf{v}}(\overrightarrow{\mathbf{x}}, t)$. The material time derivative (sometimes referred as total time derivative) of a smooth enough scalar function $f(\overrightarrow{\mathbf{x}}, t)$ over the mentioned non-stationary material volume is expressed by *Reynolds Transport Theorem:*

$$\frac{d}{dt}\int_{V_m} f(\overrightarrow{\mathbf{x}},t)\ \mathrm{d}V = \underbrace{\int_{V_m\equiv V_t} \frac{\partial f(\mathbf{x},t)}{\partial t}\ \mathrm{d}V}_{\text{variation of f inside } V_t} + \underbrace{\int_{S_m\equiv S_t} f(\overrightarrow{\mathbf{x}},t)\overrightarrow{\mathbf{v}}\cdot\overrightarrow{\mathbf{n}}\ \mathrm{d}S}_{\text{flux across } S_t} \tag{A.11}$$

Here:

- The first integral on the right hand side is defined over a fixed volume in space and it is the same volume of the moving material volume V_m
- S_t is the surface that bounds the volume S_t at the considered time instant
- $\overrightarrow{\mathbf{n}}$ is the unit normal vector to the surface S_t at the considered time instant
- $\overrightarrow{\mathbf{v}}$ is the velocity in S_t

In equation A.11, the first term on the right-hand side is the local time derivative of the scalar function f and the second term represent the flux across the fixed surface. This equation can be considered as taking a snapshot of a control volume at time instant t since the first term on right-hand side of equation A.11 represents the total change at a specific location in space and the second term on the right-hand side represents the change due to the movement of the control volume. The integrals on the right-hand side of the equation A.11 are calculated in a control volume which coincides with the moving volume V_t

A.5.2 Divergence Theorem

If $\overrightarrow{\mathbf{F}}$ is a vector function of position and V is a volume surrounded by a closed surface S then,

$$\int_V \nabla\cdot\overrightarrow{\mathbf{F}}\ \mathrm{dV} = \int_S \overrightarrow{\mathbf{F}}\cdot\overrightarrow{\mathbf{n}}\ \mathrm{dS} \tag{A.12}$$

where $\overrightarrow{\mathbf{n}}$ is the unit outward normal vector to the closed surface S.

A.6 Main Equations Used For The Solution Of Fluid Flow Problems

A.6.1 Conservation Of Mass (Continuity Equation)

In non-relativistic mechanics, a basic law is the conservation of mass in a material volume. Writing the rate of change of mass in a material volume:

$$Q = \frac{dM}{dt} \tag{A.13}$$

where:

- M is the mass in the material volume
- Q is the rate of injection of material into the material volume.

Assuming that there is no injection of material and writing M in integral form defined over a moving volume the formula becomes:

$$0 = \frac{dM}{dt} = \frac{d}{dt}\int_{V_m} \rho \;\; \mathrm{d}V \tag{A.14}$$

In equation A.14, ρ is the density of the material. Using Reynolds Transport Theorem in equation A.14:

$$0 = \frac{dM}{dt} = \int_{V_t} \frac{\partial \rho}{\partial t}\, \mathrm{d}V + \int_{S_t} \rho \overrightarrow{\mathbf{v}} \cdot \overrightarrow{\mathbf{n}} \;\; \mathrm{d}S \tag{A.15}$$

Applying the divergence theorem to the second term on the right-hand side lastly:

$$0 = \frac{dM}{dt} = \int_{V_t} \left(\frac{\partial \rho}{\partial t} + \nabla \cdot (\rho \overrightarrow{\mathbf{v}}) \right) \;\; \mathrm{d}V \tag{A.16}$$

Because of the fact that equation A.16 is valid for all choices of V_t the expression in the integral must be zero. So, writing the final expression, the mass conservation equation is obtained as:

$$\frac{\partial \rho}{\partial t} + \nabla \cdot (\rho \overrightarrow{\mathbf{v}}) = 0 \tag{A.17}$$

At this point, it is useful to note that in cases where the density is constant equation A.17 reduces to the simple form:

$$\nabla \cdot (\overrightarrow{\mathbf{v}}) = 0 \tag{A.18}$$

Equation A.18 gives the information which gives the information that velocity field of an incompressible fluid is divergence free.

A.6.2 Conservation Of Momentum (Cauchy Equation)

Momentum equation, known as equation of motion, is the equation that relates the forces acting on a selected part of fluid and the rate of change of momentum in that part of the fluid using Newton's second law. According to this law, mass multiplied by the acceleration is equal to the vectorial sum of all the forces acting on that portion of mass.

In general, it is possible to mention about two different types of forces acting on fluids. They are body (or volume) and surface forces. Body forces act on the whole material under consideration whereas surface forces act on the surface of the fluid portion. In general, in analyses gravity is selected as the only body force that exist in engineering problems unless otherwise stated.

The derivation of momentum equation is also clearly stated in Batchelor (1967), Ranalli (1995) , Dobretsov and Kirdyashkin (1998), Donea and Huerta (2002) and Schubert et al. (2001)

According to Newton's second law the change of momentum in a control volume is equal to the net forces acting on it. The variation of momentum for a control volume V_t can be expressed as:

$$\frac{D}{Dt}\int_{V_t} \rho \overrightarrow{\mathbf{v}} \, \mathrm{d}V \tag{A.19}$$

Here, using the Reynolds transport theorem and divergence theorems, the rate of change of momentum can be expressed as:

$$\begin{aligned} \frac{D}{Dt}\int_{V_t} \rho \overrightarrow{\mathbf{v}} \, \mathrm{d}V &= \int_{V_t} \frac{\partial \rho \overrightarrow{\mathbf{v}}}{\partial t} \, \mathrm{d}V + \int_{S_t} (\rho \overrightarrow{\mathbf{v}} \otimes \overrightarrow{\mathbf{v}}) \cdot \overrightarrow{\mathbf{n}} \, \mathrm{d}S \\ &= \int_{V_t} \left(\frac{\partial \rho \overrightarrow{\mathbf{v}}}{\partial t} + \nabla \cdot (\rho \overrightarrow{\mathbf{v}} \otimes \overrightarrow{\mathbf{v}}) \right) \mathrm{d}V \end{aligned} \tag{A.20}$$

where the tensor product operator is defined as:

$$\left[\overrightarrow{\mathbf{v}} \otimes \overrightarrow{\mathbf{v}}\right]_{ij} = \mathrm{v}_i \ \mathrm{v}_j \tag{A.21}$$

Using the continuity equation and the definition of the material derivative at this point :

$$\frac{D}{Dt}\int_{V_t} \rho \overrightarrow{\mathbf{v}} \ \mathrm{d}V = \int_{V_t} \rho \frac{D\overrightarrow{\mathbf{v}}}{Dt} \ \mathrm{d}V \tag{A.22}$$

Forces acting on the control volume can be either body forces or surface forces and they are expressed in equations A.23 and A.24:

$$\text{Body force} = \int_{V_t} \rho \overrightarrow{\mathbf{b}} \ \mathrm{d}V \tag{A.23}$$

$$\text{Surface force} = \int_{S_t} \underline{\underline{\boldsymbol{\sigma}}} \cdot \overrightarrow{\mathbf{n}} \ \mathrm{d}S = \int_{V_t} \nabla \cdot \underline{\underline{\boldsymbol{\sigma}}} \ \mathrm{d}V \tag{A.24}$$

where:

- $\overrightarrow{\mathbf{b}}$ is the body force acting on unit mass of fluid
- $\underline{\underline{\boldsymbol{\sigma}}}$ is the Cauchy stress tensor

Writing the equilibrium for a control volume:

$$\int_{V_t} \rho \frac{D\overrightarrow{\mathbf{v}}}{Dt} \ \mathrm{d}V = \int_{V_t} \rho \overrightarrow{\mathbf{b}} \ \mathrm{d}V + \int_{V_t} \nabla \cdot \underline{\underline{\boldsymbol{\sigma}}} \ \mathrm{d}V \tag{A.25}$$

Since equation A.25 is valid for any control volume it can be written in the form:

$$\rho \frac{D\overrightarrow{\mathbf{v}}}{Dt} = \rho \overrightarrow{\mathbf{b}} + \nabla \cdot \underline{\underline{\boldsymbol{\sigma}}} \tag{A.26}$$

Expanding the material derivative on the left-hand side of equation A.26 the following form of the momentum conservation equation can be obtained :

$$\rho \frac{\partial \overrightarrow{\mathbf{v}}}{\partial t} + \rho \left(\overrightarrow{\mathbf{v}} \cdot \nabla\right) \overrightarrow{\mathbf{v}} = \nabla \cdot \underline{\underline{\boldsymbol{\sigma}}} + \rho \overrightarrow{\mathbf{b}} \tag{A.27}$$

where :

- $\overrightarrow{\mathbf{v}}$ is velocity field
- ρ is density of fluid
- t is time
- $\overrightarrow{\mathbf{b}}$ is the body force acting on unit mass of fluid
- $\underline{\underline{\boldsymbol{\sigma}}}$ is stress tensor

The left hand side of equation A.27 is the product of the mass and the acceleration per unit volume in an elementary parcel. The first term of the right hand side is the divergence of the net surface forces per unit volume of the elemental parcel and the last term is the net body force acting unit volume of the elementary parcel .

A.6.3 Energy Conservation

For incompressible fluids, flow motion can be directly determined by only solving the continuity equation and the conservation of momentum equation. However, if the flow is compressible then the energy equation (and also an equation of state) has to be added to the system of equations to close the equation system and to determine the flow motion.

Since throughout the thesis flow is assumed to be incompressible, energy conservation equation is not needed. For this reason, final form is directly written rather then doing the derivation. A detailed derivation can be found in Lewis et al. (2004)

$$\rho\frac{De}{Dt} = \underline{\underline{\boldsymbol{\sigma}}} : \nabla\overrightarrow{\mathbf{v}} - \nabla\cdot\overrightarrow{\mathbf{q}} \tag{A.28}$$

where :

- e is internal energy
- $\overrightarrow{\mathbf{q}}$ is flux of energy

Expanding the material derivative in equation A.28 it can be expressed in the local form :

$$\underbrace{\rho\frac{\partial e}{\partial t} + \rho\overrightarrow{\mathbf{v}} \cdot \nabla e}_{1} = \underbrace{\underline{\underline{\boldsymbol{\sigma}}} : \nabla\overrightarrow{\mathbf{v}}}_{2} - \underbrace{\nabla \cdot \overrightarrow{\mathbf{q}}}_{3} \tag{A.29}$$

In equation A.29 the terms can be explained as:

1. Rate of change of internal energy (Sum of temporal change and local convective change)

2. Conversion of mechanical energy into thermal energy due to surface stresses

3. Rate at which the heat added externally

A.7 Lagrange Multipliers Method To Impose Dirichlet Boundary Conditions

To impose *Dirichlet boundary conditions* in another words *Essential boundary conditions* a popular technique used is called Lagrange Multipliers Method. In case Lagrange Multipliers Method is used the known values of the Dirichlet part of the boundary are imposed adding linear constraints to the original system which is generally singular. Let's say totally n_λ unknowns and lines are added to the system (n_λ Lagrange multipliers λ.) . What Finite Elements Method in the end gives us is a linear system of equations which can be expressed in the general form :

$$\mathbf{K}\overrightarrow{\mathbf{u}} = \overrightarrow{\mathbf{f}} \tag{A.30}$$

where:

- $\mathbf{K}$ is the stiffness matrix of the global system
- $\overrightarrow{\mathbf{u}}$ is the vector of unknowns of the global system
- $\overrightarrow{\mathbf{f}}$ is the forcing vector of the global system

Assuming that there are n_t lines in this system and some of the elements in the vector of unknowns are known as essential boundary conditions. After adding the mentioned Lagrange multipliers system system can be expressed as:

$$\mathbf{K}\overrightarrow{\mathbf{u}} + \mathbf{A}^T\overrightarrow{\boldsymbol{\lambda}} = \overrightarrow{\mathbf{f}} \tag{A.31}$$

$$\mathbf{A}\overrightarrow{\mathbf{u}} = \overrightarrow{\mathbf{g}} \tag{A.32}$$

where:

- $\overrightarrow{\mathbf{g}}$ is the given values of the relation of unknowns
- $\mathbf{A}$ is a rectangular matrix which contains the coefficients of the relation between unknowns of the problem (size is $n_\lambda \times n_t$)
- $\overrightarrow{\boldsymbol{\lambda}}$ is the vector containing added Lagrange multipliers to the problem

So the the global system defined in equation A.30 imposing the essential boundary conditions can be expressed as :

$$\begin{bmatrix} \mathbf{K} & \mathbf{A}^T \\ \mathbf{A} & \mathbf{0} \end{bmatrix} \begin{bmatrix} \overrightarrow{\mathbf{u}} \\ \overrightarrow{\boldsymbol{\lambda}} \end{bmatrix} = \begin{bmatrix} \overrightarrow{\mathbf{f}} \\ \overrightarrow{\mathbf{g}} \end{bmatrix} \tag{A.33}$$

defining $\mathbf{0}$ a zero matrix that will make the system a square.

By usage of Lagrange Multipliers technique it is not only possible to impose the values of essential boundary conditions given in the problem but also it is possible to impose the linear relations between unknowns of the problem in consideration.

Appendix B

List of Publications Related To X-FEM

B.1 Oil and Gas Industry Related Publications

- Elguedj et al. (2005), Appropriate Extended Functions For X-Fem Simulation Of Plastic Fatigue Crack Growth
- Khoei et al. (2011), Modeling Of Crack Propagation And Fluid Flow In Multi-Phase Porous Mediausing A Modified X-FEM Technique
- Meschke and Leonhart (2011), Recent Advances In X-FEM Based Crack Modeling In The Context Of Poromechanics
- Kim et al. (2007), A Mortared Finite Element Method For Frictional Contact On Arbitrary Interfaces
- Korsawe et al. (2006), Finite Element Analysis Of Poro-Elastic Consolidation In Porous Media
- Keshavarzi and Mohammadi (2011), Fully Coupled Modeling Of Interaction Between Hydraulic And Natural Fractures In Naturally Fractured Reservoirs By XFEM: The Effect Of Pore Pressure Change
- Sukumar et al. (2003), Extended Finite Element Method And Fast Marching Method For Three-Dimensional Fatigue Crack Propagation

- Stolarska and Chopp (2003), Modeling Thermal Fatigue Cracking In Integrated Circuits By Level Sets And The Extended Finite Element Method
- Fumagalli and Scotti (2011), Numerical Modelling Of Multiphase Subsurface Flow In The Presence Of Fractures
- Xiao and Karihaloo (2003), Direct Evaluation Of Accurate Coefficients Of The Linear Elastic Crack Tip Asymptotic Field
- Chopp and Sukumar (2003), Fatigue Crack Propagation Of Multiple Coplanar Cracks With The Coupled Extended Finite Element/Fast Marching Method
- Li et al. (2012), Analysis of Fretting Crack Propagation Behavior with X-FEM Method
- Watanabe and Kolditz (2011), Mechanically Enriched Fracture Elements For A Hydromechanical Problem In Fractured Rocks
- Lin et al. (2010), Simulation On Crack Growth Of Drill Pipe With XFEM
- Lamb et al. (2010), Coupled Deformation And Fluid Flow In Fractured Porous Media Using Dual Permeability And Explicitly Defined Fracture Geometry
- Anciaux and Molinari (2009), Contact Mechanics At The Nanoscale, A 3D Multiscale Approach

B.2 Aviation Related Publications

B.2.1 Structural Mechanics And Crack Propagation Related Publications

- Yang et al. (2008), Infinite Sequence Of Parallel Cracks In An Anisotropic Piezoelectric Solid
- Xiao and Karihaloo (2007), Implementation Of Hybrid Crack Element On A General Finite Element Mesh And In Combination With XFEM
- Wyart et al. (2007), A Substructured FE-shell/XFE 3D Method For Crack Analysis in Thin Walled Structures

- Unger et al. (2007), Modelling Of Cohesive Crack Growth In Concrete Structures With The Extended Finite Element Method
- Sukumar and Prévost (2003), Modeling Quasi-Static Crack Growth With The Extended Finite Element Method, Part I: Computer Implementation
- Sukumar et al. (2001), Modeling Holes And Inclusions By Level Sets In The Extended Finite Element Method
- Sukumar et al. (2008), Three-Dimensional Non-Planar Crack Growth By A Coupled Extended Finite Element And Fast Marching Method
- Sukumar et al. (2000), Extended Finite Element Method For Three-Dimensional Crack Modelling
- Xiao and Karihaloo (2006), Improving The Accuracy Of XFEM Crack Tip Fields Using Higher Order Quadrature And Statically Admissible Stress Recovery
- Huynh and Belytschko (2009), The Extended Finite Element Method For Fracture In Composite Materials
- Stolarska et al. (2001), The Extended Finite Element Method For Fracture In Composite Materials
- Mariano and Stazi (2004), Strain Localization Due To Crack-Microcrack Interactions: X-FEM For A Multifield Approach
- Stazi et al. (2003), An Extended Finite Element Method With Higher-order Elements For Curved Cracks
- Simone et al. (2003), From Continuous To Discontinuous Failure In A Gradient-Enhanced Continuum Damage Model
- Wyart et al. (2008), Substructuring FE-XFE Approaches Applied To Three-Dimensional Crack Propagation
- Réthoré et al. (2005a), An Energy-Conserving Scheme For Dynamic Crack Growth Using The Extended Finite Element Method

- Nistor et al. (2008), Numerical Implementation Of The Extended Finite Element Method For Dynamic Crack Analysis
- Peirce and Detournay (2008), An Implicit Level Set Method For Modeling Hydraulically Driven Fractures
- Hettich and Ramm (2006), Interface Material Failure Modeled By The Extended Finite Element Method And Level Sets
- Laborde et al. (2005), High-Order Extended Finite Element Method For Cracked Domains
- Zi and Belytschko (2003), New Crack-Tip Elements For XFEM And Applications To Cohesive Cracks
- Larsson and Fagerström (2005), A Framework For Fracture Modelling Based On The Material Forces Concept With XFEM Kinematics
- Menouillard et al. (2008), Mass Lumping Strategies For X-FEM Explicit Dynamics: Application To Crack Propagation
- Möes et al. (1999), A Finite Element Method For Crack Growth Without Remeshing
- Legrain et al. (2005), Stress Analysis Around Crack Tips In Finite Strain Problems Using The Extended Finite Element Method
- Huang et al. (2003a), Channel-Cracking Of Thin Films With The Extended Finite Element Method
- Meschke and Dumstorff (2007), Energy-Based Modeling Of Cohesive And Cohesionless Cracks Via X-FEM
- Nakasumi et al. (2008), Crack Growth Analysis Using Mesh Superposition Technique And X-FEM
- Moës et al. (2002), Non-Planar 3D Crack Growth By The Extended Finite Element And Level Sets, Part I: Mechanical Model

- Rabinovich et al. (2007), XFEM-Based Crack Detection Scheme Using A Genetic Algorithm

- Belytschko and Gracie (2007), On XFEM Applications To Dislocations And Interfaces

- Béchet et al. (2005), Improved Implementation And Robustness Study Of The X-FEM For Stress Analysis Around Cracks

- Hettich et al. (2008), Modeling Of Failure In Composites By X-FEM And Level Sets Within A Multiscale Framework

- Gürses and Miehe (2009), A Computational Framework Of Three-Dimensional Configurational-Force-Driven Brittle Crack Propagation

- Areias and Belytschko (2005a), Analysis Of Three-Dimensional Crack Initiation And Propagation Using The Extended Finite Element Method

- Duarte et al. (2007), A High-Order Generalized FEM For Through-The-Thickness Branched Cracks

- Comi and Mariani (2007), Extended Finite Element Simulation Of Quasi-Brittle Fracture In Functionally Graded Materials

- Lee et al. (2004), Combined Extended And Superimposed Finite Element Method For Cracks

- Prabel et al. (2007), Level Set X-FEM Non-Matching Meshes: Application To Dynamic Crack Propagation In Elastic-Plastic Media

- de Borst et al. (2004), Cohesive-Zone Models, Higher-Order Continuum Theories And Reliability Methods For Computational Failure Analysis

- Fagerström and Larsson (2006), Theory And Numerics For Finite Deformation Fracture Modelling Using Strong Discontinuities

- Liu and Borja (2008), A Contact Algorithm For Frictional Crack Propagation With The Extended Finite Element Method

- Chahine et al. (2008), Crack Tip Enrichment In The XFEM Using A Cutoff Function
- Hansbo and Hansbo (2004), A Finite Element Method For The Simulation Of Strong And Weak Discontinuities In Solid Mechanics
- Moës and Belytschko (2002), Extended Finite Element Method for Cohesive Crack Growth
- Guidault et al. (2007), A Two-Scale Approach With Homogenization For The Computation Of Cracked Structures
- Pannachet et al. (2009), Error Estimation And Adaptivity For Discontinuous Failure
- Elguedj et al. (2006), Appropriate Extended Functions For X-FEM Simulation Of Plastic Fracture Mechanics
- Ayhan and Nied (2002), Stress Intensity Factors For Three-Dimensional Surface Cracks Using Enriched Finite Elements
- Areias and Belytschko (2005b), Non-Linear Analysis Of Shells With Arbitrary Evolving Cracks Using XFEM
- Hazard and Bouillard (2007), Structural Dynamics Of Viscoelastic Sandwich Plates By The Partition Of Unity Finite Element Method
- Li and Ghosh (2006), Extended Voronoi Cell Finite Element Model For Multiple Cohesive Crack Propagation In Brittle Materials
- Budyn et al. (2004), A Method For Multiple Crack Growth In Brittle Materials Without Remeshing
- Bordas and Moran (2006), Enriched Finite Elements And Level Sets For Damage Tolerance Assessment Of Complex Structures
- Asferg et al. (2007), A Consistent Partly Cracked XFEM Element For Cohesive Crack Growth

- Heyliger and Kriz (1989), Stress Intensity Factors by Enriched Mixed Finite Elements
- Benvenuti et al. (2008), A Regularized XFEM Model For The Transition From Continuous To Discontinuous Displacements
- Karihaloo and Xiao (2003), Modelling Of Stationary And Growing Cracks In FE Framework Without Remeshing: A State-Of-The-Art Review
- Ishii et al. (2006), Failure Analysis Of Quasi-Brittle Materials Involving Multiple Mechanisms On Fractured Surfaces
- Duarte et al. (2000), Generalized Finite Element Methods For Three-Dimensional Structural Mechanics Problems
- Mohammadi (2012), XFEM Fracture Analysis of Composites
- Huang et al. (2003b), Modeling Quasi-Static Crack Growth With The Extended Finite Element Method, Part II: Numerical Applications
- Gracie and Belytschko (2009), Concurrently Coupled Atomistic And XFEM Models For Dislocations And Cracks
- Benvenuti (2008), A Regularized XFEM Framework For Embedded Cohesive Interfaces
- Gravouil et al. (2002), Non-Planar 3D Crack Growth By The Extended Finite Element And Level Sets, Part II: Level Set Update
- Belytschko et al. (2003), Structured Extended Finite Element Methods Of Solids Defined By Implicit Surfaces
- Guidault et al. (2008), A Multiscale Extended Finite Element Method For Crack Propagation

B.2.2 Flow Theory Related Publications

- Fries (2009), The Intrinsic XFEM For Two-Fluid Flows

- Sussman and Fatemi (1999), An Efficient Interface-Preserving Level Set Redistancing Algorithm And Its Application To Interfacial Incompressible Fluid Flow
- Wagner et al. (2003), Particulate Flow Simulations Using Lubrication Theory Solution Enrichment
- Wagner et al. (2001), The Extended Finite Element Method For Rigid Particles In Stokes Flow
- Ramanan and Engelman (1996), An Algorithm For Simulation Of Steady Free Surface Flows
- Tezaur et al. (2008), A Discontinuous Enrichment Method For Capturing Evanescent Waves In Multiscale Fluid And Fluid/Solid Problems
- Groß and Reusken (2007), An Extended Pressure Finite Element Space For Two-Phase Incompressible Flows With Surface Tension
- Chessa and Belytschko (2003b), An Enriched Finite Element Method And Level Sets For Axisymmetric Two-Phase Flow With Surface Tension
- Chessa and Belytschko (2003a), An Extended Finite Element Method for Two-Phase Fluids

Fluid Structure Interaction Related Publications

- Legay et al. (2006), An Eulerian-Lagrangian Method For Fluid-Structure Interaction Based On Level Sets
- Sawada and Tezuka (2011), LLM And X-FEM Based Interface Modeling Of Fluid-Thin Structure Interactions On A Non-Interface-Fitted Mesh
- Gerstenberger and Wall (2008a), Enhancement Of Fixed-Grid Methods Towards Complex Fluid-Structure Interaction Applications
- Cirak et al. (2007), Large-Scale Fluid-Structure Interaction Simulation Of Viscoplastic And Fracturing Thin-Shells Subjected To Shocks And Detonations

- Mayer et al. (2010), 3D FluidStructure-Contact Interaction Based On A Combined XFEM FSI And Dual Mortar Contact Approach
- Gerstenberger and Wall (2008b), An Extended Finite Element Method/Lagrange Multiplier Based Approach For Fluid-Structure Interaction

B.3 Mining Industry Related Publications

- Shamloo et al. (2005), Modeling Of Pressure-Sensitive Materials Using A Cap Plasticity Theory In Extended Finite Element Method
- Debasis and Dash (2009), Extended Finite Element Method (XFEM) For Analysis Of Cohesive Rock Joint
- Anahid and Khoei (2008), New Development In Extended Finite Element Modeling Of Large Elasto-Plastic Deformations
- Elguedj et al. (2006), Appropriate Extended Functions For X-FEM Simulation Of Plastic Fracture Mechanics
- Khoei et al. (2008), Extended Finite Element Method For Three-Dimensional Large Plasticity Deformations On Arbitrary Interfaces
- Prabel et al. (2007), Level Set X-FEM Non-Matching Meshes: Application To Dynamic Crack Propagation In Elastic-Plastic Media
- Deb and Das (2010), Extended Finite Element Method for the Analysis of Discontinuities in Rock Masses
- Zhang et al. (2011), Gpu Accelerated Xfem And Its Applications In The Simulation Of Underground Excavation
- Zlotnik et al. (2007), Numerical Modelling Of Tectonic Plates Subduction Using X-FEM

B.4 Biomechanics Related Publications

- Duddu et al. (2008), A Combined Extended Finite Element And Level Set Method For Biofilm Growth

- Smith et al. (2007), The Extended Finite Element Method For Boundary Layer Problems In Biofilm Growth
- Zilian (2011), Modeling And Enriched Approximations For Multi-Field Problems In Engineering Applications
- Cotin et al. (2000), A Hybrid Elastic Model Allowing Real-Time Cutting, Deformations And Force-Feedback For Surgery Training And Simulation
- Vigneron et al. (2011), Serial FEM/XFEM-Based Update Of Preoperative Brain Images Using Intraoperative MRI
- Vigneron et al. (2008), Fem And Xfem Based Biomechanical Models For Advanced Image-Guided Neurosurgery
- Vernerey and Farsad (2011), An Eulerian/XFEM Formulation For The Large Deformation Of Cortical Cell Membrane

B.5 Other Publications

B.5.1 Heat Transfer Related Publications

- Ji et al. (2002), A Hybrid Extended Finite Element/Level Set Method For Modeling Phase Transformations
- Duflot (2008), The Extended Finite Element Method In Thermoelastic Fracture Mechanics
- Merle and Dolbow (2002), Solving Thermal And Phase Change Problems With The Extended Finite Element Method
- Areias and Belytschko (2007), Two-Scale Method For Shear Bands: Thermal Effects And Variable Bandwidth
- Duarte et al. (2009), Generalized Finite Element Analysis Of Three-Dimensional Heat Transfer Problems Exhibiting Sharp Thermal Gradients
- Chessa et al. (2002), The Extended Finite Element Method (XFEM) For Solidification Problems

B.5.2 Publications That Include Basics Information And Analysis Of The Method With Comparison And Contrast With Other Methods

- Legrain et al. (2008), Stability Of Incompressible Formulations Enriched With X-FEM
- Bordas and Duflot (2007), Derivative Recovery And A Posteriori Error Estimate For Extended Finite Elements
- Strouboulis et al. (2007), Assessment Of The Cost And Accuracy Of The Generalized FEM
- Chessa and Belytschko (2006), A Local Space-Time Discontinuous Finite Element Method
- Ródenas et al. (2008), A Recovery-Type Error Estimator For The Extended Finite Element Method Based On Singular+Smooth Stress Field Splitting
- Ji and Dolbow (2004), On Strategies For Enforcing Interfacial Constraints And Evaluating Jump Conditions With The Extended Finite Element Method
- Moës et al. (2006), Imposing Dirichlet Boundary Conditions In The Extended Finite Element Method
- Asadpoure and Mohammadi (2007), Developing New Enrichment Functions For Crack Simulation In Orthotropic Media By The Extended Finite Element Method
- Belytschko and Black (1999), Elastic Crack Growth in Finite Elements With Minimal Remeshing
- Vaughan et al. (2006), A Comparison Of The Extended Finite Element Method With The Immersed Interface Method For Elliptic Equations With Discontinuous Coefficients And Singular Sources
- Park et al. (2009), Integration Of Singular Enrichment Functions In The Generalized/Extended Finite Element Method For Three-Dimensional Problems

- Melenk and Babuka (1996), The Partition Of Unity Finite Element Method: Basic Theory And Applications
- Duflot and Bordas (2008), A Posteriori Error Estimation For Extended Finite Elements By An Extended Global Recovery
- Strouboulis et al. (2006), A Posteriori Error Estimation For Generalized Finite Element Methods
- Menouillard et al. (2006), Efficient Explicit Time Stepping For The Extended Finite Element Method (X-FEM)
- Dolbow and Harari (2009), An Efficient Finite Element Method For Embedded Interface Problems
- Fleming et al. (1997), Enriched Element-Free Galerkin Methods For Crack Tip Fields
- Chessa and Belytschko (2004), Arbitrary Discontinuities In Space-Time Finite Elements By Level-Sets And X-FEM
- Réthoré et al. (2005b), A Combined Space-Time Extended Finite Element Method
- Dolbow et al. (2000), Modeling Fracture In Mindlin-Reissner Plates With The Extended Finite Element Method
- Hysing (2005), A New Implicit Surface Tension Implementation For Interfacial Flows
- Dolbow et al. (2001), An Extended Finite Element Method For Modeling Crack Growth With Frictional Contact
- Duarte and Kim (2008), Analysis And Applications Of A Generalized Finite Element Method With Global-Local Enrichment Functions
- Oliver et al. (2006), A Comparative Study On Finite Elements For Capturing Strong Discontinuities: E-FEM Vs X-FEM
- Bordas et al. (2007), A Simple Error Estimator For Extended Finite Elements

- Fries and Zilian (2009), On Time Integration In The XFEM
- Duarte et al. (2001), A Generalized Finite Element Method For The Simulation Of Three-Dimensional Dynamic Crack Propagation
- Cox (2009), An Extended Finite Element Method With Analytical Enrichment For Cohesive Crack Modeling
- Barros et al. (2004), On Error Estimator And P-Adaptivity In The Generalized Finite Element Method
- Fries and Belytschko (2007), The Intrinsic Partition Of Unity Method
- Daux et al. (2000), Arbitrary Branched And Intersecting Cracks With The Extended Finite Element Method

B.5.3 Micromechanics Related X-FEM Publications

- Pierres et al. (2010), 3D Two Scale X-FEM Crack Model With Interfacial Frictional Contact: Application To Fretting Fatigue
- Souza and Allen (2011), Modeling The Transition Of Microcracks Into Macrocracks In Heterogeneous Viscoelastic Media Using A Two-Way Coupled Multiscale Model
- Loehnert and Belytschko (2007), A Multiscale Projection Method For Macro/Microcrack Simulations
- Moës et al. (2003), A Computational Approach To Handle Complex Microstructure Geometries
- Vajragupta et al. (2012), A Micromechanical Damage Simulation Of Dual Phase Steels Using XFEM
- Dai et al. (2011), Micromechanics Models And Innovative Sensor Technologies To Evaluate Internal-Frost Damage Of Concrete
- Khoei and Nikbakht (2006), Contact Friction Modeling With The Extended Finite Element Method (X-FEM)

- Jafar et al. (2011), Modeling Large Sliding Frictional Contact Along Non-Smooth Discontinuities In X-FEM

B.5.4 Level Set Method Related Publications

- Sethian (2001), Evolution, Implementation And Application Of Level Set And Fast Marching Methods For Advancing
- Olsson et al. (2007), A Conservative Level Set Method For Two Phase Flow II
- Russo and Smereka (2000), A Remark on Computing Distance Functions
- Osher and Fedkiw (2001), Level Set Methods: An Overview And Some Recent Results
- Sethian (1996), A Fast Marching Level Set Method for Monotonically Advancing Fronts
- Zhao et al. (1996), A Variational Level Set Approach To Multiphase Motion
- Van der Pijl et al. (2005), A Mass-Conserving Level-Set Method For Modelling Of Multi-Phase Flows
- Di Pietro et al. (2006), Mass Preserving Finite Element Implementations Of The Level Set Method
- Ventura et al. (2003), Vector Level Sets For Description Of Propagating Cracks In Finite Elements
- Sethian (1999), Level Set Methods and Fast Marching Methods: Evolving Interfaces in Computational Geometry, Fluid Mechanics, Computer Vision, and Materials Science
- Marchandisea et al. (2006), A Quadrature-Free Discontinuous Galerkin Method For The Levelset Equation
- Duflot (2007), A Study Of The Representation Of Cracks With Level-Sets

- Burger and Osher (2005), A Survey Of Level Set Methods For Inverse Problems And Optimal Design
- Sussmann et al. (1998), An Improved Level Set Method for Incompressible Two-Phase Flows
- Peng et al. (1999), A PDE-Based Fast Local Level Set Method
- Losassoa et al. (2005), Spatially Adaptive Techniques For Level Set Methods And Incompressible Flow

Bibliography

M. Anahid and A.R. Khoei. New development in extended finite element modeling of large elasto-plastic deformations. *International Journal for Numerical Methods in Engineerin*, 75:1133–1171, 2008.

G. Anciaux and J.F. Molinari. Contact mechanics at the nanoscale, a 3d multiscale approach. *International Journal for Numerical Methods in Engineering*, 79:1041–1067, 2009. doi: 10.1002/nme.2590.

P.M.A. Areias and T. Belytschko. Analysis of three-dimensional crack initiation and propagation using the extended finite element method. *International Journal for Numerical Methods in Engineering*, 63:760–788, 2005a.

P.M.A. Areias and T. Belytschko. Non-linear analysis of shells with arbitrary evolving cracks using xfem. *International Journal for Numerical Methods in Engineering*, 62:384–415, 2005b.

P.M.A. Areias and T. Belytschko. Two-scale method for shear bands: Thermal effects and variable bandwidth. *International Journal for Numerical Methods in Engineering*, 72:658–696, 2007.

A. Asadpoure and S. Mohammadi. Developing new enrichment functions for crack simulation in orthotropic media by the extended finite element method. *International Journal for Numerical Methods in Engineering*, 69:2150–2172, 2007.

J.L. Asferg, P.N. Poulsen, and L.O. Nielsen. A consistent partly cracked xfem element for cohesive crack growth. *International Journal for Numerical Methods in Engineering*, 72:464–485, 2007.

A.O. Ayhan and H.F. Nied. Stress intensity factors for three-dimensional surface cracks using enriched finite elements. *International Journal for Numerical Methods in Engineering*, 54:899–921, 2002.

Ivo Babuka. Error-bounds for finite element method. *Numerische Mathematik*, 16: 322–333, 1971. ISSN 0029-599X. doi: 10.1007/BF02165003.

F.B. Barros, S.P.B. Proença, and C.S. Barcellos. On error estimator and p-adaptivity in the generalized finite element method. *International Journal For Numerical Methods In Engineering*, 60:2373–2398, 2004.

G. K. Batchelor. *Fluid Dynamics*. Cambridge University Press, 1967.

T. Belytschko and T. Black. Elastic crack growth in finite elements with minimal remeshing. *International Journal for Numerical Methods in Engineering*, 45:601–620, 1999.

T. Belytschko and R. Gracie. On xfem applications to dislocations and interfaces. *International Journal of Plasticity*, 23:1721–1738, 2007. doi: 10.1016/j.ijplas.2007.03.003.

T. Belytschko, C. Parimi, N. Moës, N. Sukumar, and S. Usui. Structured extended finite element methods of solids defined by implicit surfaces. *International Journal for Numerical Methods in Engineering*, 56:609–635, 2003. doi: 10.1002/nme.686.

E. Benvenuti. A regularized xfem framework for embedded cohesive interfaces. *Computer Methods in Applied Mechanics and Engineering*, 197:4367–4378, 2008.

E. Benvenuti, A. Tralli, and G. Ventura. A regularized xfem model for the transition from continuous to discontinuous displacements. *International Journal for Numerical Methods in Engineering*, 74:911–944, 2008.

S. Bordas and M. Duflot. Derivative recovery and a posteriori error estimate for extended finite elements. *Computer Methods in Applied Mechanics and Engineering*, 196:3381–3399, 2007.

S. Bordas and B. Moran. Enriched finite elements and level sets for damage tolerance assessment of complex structures. *Engineering Fracture Mechanics*, 73:1176–1201, 2006.

S. Bordas, M. Duflot, and P. Le. A simple error estimator for extended finite elements. *Communications in Numerical Methods in Engineering*, 24:961–971, 2007.

F. Brezzi. On the existence, uniqueness and approximation of saddle-point problems arising from lagrangian multipliers. *ESAIM: Mathematical Modelling and Numerical Analysis - Modélisation Mathématique et Analyse Numérique*, 8: 129–151, 1974.

É. Budyn, G. Zi, N. Moës, and T. Belytschko. A method for multiple crack growth in brittle materials without remeshing. *International Journal for Numerical Methods in Engineering*, 61:1741–1770, 2004.

M. Burger and S.J. Osher. A survey of level set methods for inverse problems and optimal design. *European Journal of Applied Mathematics*, 16:263–301, 2005. doi: 10.1017/s0956792505006182.

E. Béchet, H. Minnebo, N. Moës, and B. Burgardt. Improved implementation and robustness study of the x-fem for stress analysis around cracks. *International Journal for Numerical Methods in Engineering*, 64:1033–1056, 2005.

E. Chahine, P. Laborde, and Y. Renard. Crack tip enrichment in the xfem using a cutoff function. *International Journal for Numerical Methods in Engineering*, 75: 629–646, 2008.

J. Chessa and T. Belytschko. An extended finite element method for two-phase fluids. *Journal of Applied Mechanics*, 70:10–17, 2003a. doi: 10.1115/1.1526599.

J. Chessa and T. Belytschko. An enriched finite element method and level sets for axisymmetric two-phase flow with surface tension. *International Journal for Numerical Methods in Engineering*, 58:2041–2064, 2003b.

J. Chessa and T. Belytschko. Arbitrary discontinuities in space-time finite elements by level-sets and x-fem. *International Journal for Numerical Methods in Engineering*, 16:2595–2614, 2004. doi: 10.1002/nme.1155.

J. Chessa and T. Belytschko. A local space-time discontinuous finite element method. *Computer Methods in Applied Mechanics and Engineering*, 195:1325–1343, 2006.

J. Chessa, P. Smolinski, and T. Belytschko. The extended finite element method (xfem) for solidification problems. *International Journal for Numerical Methods in Engineering*, 53:1959–1977, 2002.

D.L. Chopp and N. Sukumar. Fatigue crack propagation of multiple coplanar cracks with the coupled extended finite element/fast marching method. *International Journal of Engineering Science*, 41:845–869, 2003.

F. Cirak, R. Deiterding, and S.P. Mauch. Large-scale fluid-structure interaction simulation of viscoplastic and fracturing thin-shells subjected to shocks and detonations. *Computers and Structures*, 85:1049–1065, 2007.

C. Comi and S. Mariani. Extended finite element simulation of quasi-brittle fracture in functionally graded materials. *Computer Methods In Applied Mechanics And Engineering*, 196:4013–4026, 2007.

F. Cordero and P. Díez. XFEM+: una modificación de XFEM para mejorar la precisión de los flujos locales en problemas de difusión con conductividades muy distintas. *Revista Internacional Métodos Numéricos para Cálculo y Diseño en Ingeniería*, 26:121–133, 2010.

S. Cotin, H. Delingette, and N. Ayache. A hybrid elastic model allowing real-time cutting, deformations and force-feedback for surgery training and simulation. *The Visual Computer*, 16:437–452, 2000.

R. Cottereau, P. Diez, and A. Huerta. Modeling, with a unified level-set representation, of the expansion of a hollow in the ground under different physical phenomena. *Computational Mechanics*, 46:315–327, 2010. doi: 10.1007/s00466-009-0443-y.

J.V. Cox. An extended finite element method with analytical enrichment for cohesive crack modeling. *International Journal for Numerical Methods in Engineering*, 78:48–83, 2009. doi: 10.1002/nme.2475.

Q. Dai, K. Ng, and J. Zhou. Micromechanics models and innovative sensor technologies to evaluate internal-frost damage of concrete. *Nondestructive Characterization for Composite Materials, Aerospace Engineering, Civil Infrastructure, and Homeland Security*, 7983, 2011. doi: 10.3141/2240-08.

C. Daux, N. Moës, J. Dolbow, N. Sukumar, and T. Belytschko. Arbitrary branched and intersecting cracks with the extended finite element method. *International Journal for Numerical Methods in Engineering*, 48:1741–1760, 2000.

R. de Borst, M.A. Gutiérrez, G.N. Wells, J.J.C. Remmers, and H. Askes. Cohesive-zone models, higher-order continuum theories and reliability methods for computational failure analysis. *International Journal for Numerical Methods in Engineering*, 60:289–315, 2004.

J. M. Dealy and K. F. Wissbrun. *Melt Rheology and Its Role in Plastics Processing Theory and Applications*. Kluwer Academics Publishers, 1990.

D. Deb and K.C. Das. Extended finite element method for the analysis of discontinuities in rock masses. *Geotechnical and Geological Engineering*, 28:643–659, 2010.

D. Debasis and K. Dash. Extended finite element method (xfem) for analysis of cohesive rock joint. *Journal of Scientific and Industrial Research*, 68:575–583, 2009.

D.A. Di Pietro, S. Lo Forte, and N. Parolini. Mass preserving finite element implementations of the level set method. *Applied Numerical Mathematics*, 56: 1179–1195, 2006.

P. Diez, S. Zlotnik, and R. Cottereau. A stable xfem formulation for multi-phase problems enforcing the accuracy of the fluxes through lagrange multipliers. *INTERNATIONAL JOURNAL FOR NUMERICAL METHODS IN ENGINEERING*, 00:1–21, 2011.

N. L. Dobretsov and A. G. Kirdyashkin. *Deep Level Geodynamics*. BALKEMA,A.A., 1998.

J. Dolbow and I. Harari. An efficient finite element method for embedded interface problems. *International Journal for Numerical Methods in Engineering*, 78:229–252, 2009. doi: 10.1002/nme.2486.

J. Dolbow, N. Moës, and T. Belytschko. Modeling fracture in mindlin-reissner plates with the extended finite element method. *International Journal of Solids and Structures*, 37:7161–7183, 2000.

J. Dolbow, N. Moës, and T. Belytschko. An extended finite element method for modeling crack growth with frictional contact. *Computer Methods in Applied Mechanics and Engineering*, 190:6825–6846, 2001.

J. Dolbow, E. Fried, and H. Ji. A numerical strategy for investigating the kinetic response of stimulus-responsive hydrogels. *Computer Methods in Applied Mechanics and Engineering*, 194:4447–4480, 2005. doi: 10.1016/j.cma.2004.12.004.

J. Donea and A. Huerta. *Finite Element Methods for Flow Problems*. Wiley, 2002.

C.A. Duarte and D.J. Kim. Analysis and applications of a generalized finite element method with global-local enrichment functions. *Computer Methods in Applied Mechanics and Engineering*, 197:487–504, 2008.

C.A. Duarte, I. Babuka, and J.T. Oden. Generalized finite element methods for three-dimensional structural mechanics problems. *Computers and Structures*, 77: 215–232, 2000.

C.A. Duarte, O.N. Hamzeh, T.J. Liszka, and W.W. Tworzydlo. A generalized finite element method for the simulation of three-dimensional dynamic crack propagation. *Computer Methods in Applied Mechanics and Engineering*, 190: 2227–2262, 2001.

C.A. Duarte, L.G. Reno, and A. Simone. A high-order generalized fem for through-the-thickness branched cracks. *International Journal for Numerical Methods in Engineering*, 72:325–351, 2007.

C.A. Duarte, P. O'Hara, and T. Eason. Generalized finite element analysis of three-dimensional heat transfer problems exhibiting sharp thermal gradients. *Computer Methods in Applied Mechanics and Engineering*, 198:1857–1871, 2009. doi: 10.1016/j.cma.2008.12.024.

R. Duddu, S. Bordas, D. Chopp, and B. Moran. A combined extended finite element and level set method for biofilm growth. *International Journal for Numerical Methods in Engineering*, 74:848–870, 2008.

M. Duflot. A study of the representation of cracks with level-sets. *International Journal for Numerical Methods in Engineering*, 70:1261–1302, 2007.

M. Duflot. The extended finite element method in thermoelastic fracture mechanics. *International Journal for Numerical Methods in Engineering*, 74:827–847, 2008.

M. Duflot and S. Bordas. A posteriori error estimation for extended finite elements by an extended global recovery. *International Journal for Numerical Methods in Engineering*, 76:1123–1138, 2008.

T. Elguedj, A. Gravouil, and A. Combescure. Appropriate extended functions for x-fem simulation of plastic fatigue crack growth. In *International Conference on Fracture Italy, 2005*, 2005.

T. Elguedj, A. Gravouil, and A. Combescure. Appropriate extended functions for x-fem simulation of plastic fracture mechanics. *Computer Methods in Applied Mechanics and Engineering*, 195:501515, 2006.

M. Fagerström and R. Larsson. Theory and numerics for finite deformation fracture modelling using strong discontinuities. *International Journal for Numerical Methods in Engineering*, 66:911–948, 2006.

M. Fleming, Y.A. Chu, B. Moran, and T. Belytschko. Enriched element-free galerkin methods for crack tip fields. *International Journal for Numerical Methods in Engineering*, 40:1483–1504, 1997.

T.P. Fries. The intrinsic xfem for two-fluid flows. *International Journal for Numerical Methods in Fluids*, 60:437–471, 2009. doi: DOI:10.1002/fld.1901,2008.

T.P. Fries and T. Belytschko. The intrinsic partition of unity method. *Computational Mechanics*, 40:803–814, 2007.

T.P. Fries and A. Zilian. On time integration in the xfem. *International Journal for Numerical Methods in Engineering*, 79:69–93, 2009. doi: 10.1002/nme.2558.

A. Fumagalli and A. Scotti. Numerical modelling of multiphase subsurface flow in the presence of fractures. Technical report, Modellistica e Calcolo Scientifico OX, 2011.

A. Gerstenberger and W.A. Wall. Enhancement of fixed-grid methods towards complex fluid-structure interaction applications. *International Journal for Numerical Methods in Fluids*, 57:1227–1248, 2008a.

A. Gerstenberger and W.A. Wall. An extended finite element method/lagrange multiplier based approach for fluid-structure interaction. *Computer Methods in Applied Mechanics and Engineering*, 197:1699–1714, 2008b.

R. Gracie and T. Belytschko. Concurrently coupled atomistic and xfem models for dislocations and cracks. *International Journal for Numerical Methods in Engineering*, 78:354–378, 2009.

A. Gravouil, N. Moës, and T. Belytschko. Non-planar 3d crack growth by the extended finite element and level sets, part ii: Level set update. *International Journal for Numerical Methods in Engineering*, 53:2569–2586, 2002.

S. Groß and A. Reusken. An extended pressure finite element space for two-phase incompressible flows with surface tension. *Journal of Computational Physics*, 224: 40–58, 2007.

P.A. Guidault, O. Allix, L. Champaney, and J.P. Navarro. A two-scale approach with homogenization for the computation of cracked structures. *Computers and Structures*, 85:1360–1371, 2007.

P.A. Guidault, O. Allix, L. Champaney, and C. Cornuault. A multiscale extended finite element method for crack propagation. *Computer Methods in Applied Mechanics and Engineering*, 197:381–399, 2008.

L.F. Gutiérrez and F. Ramos. Xfem framework for cutting soft tissue - including topological changes in a surgery simulation. In *GRAPP*, pages 275–283, 2010.

E. Gürses and C. Miehe. A computational framework of three-dimensional configurational-force-driven brittle crack propagation. *Computer Methods in Applied Mechanics and Engineering*, 198:1413–1428, 2009.

A. Hansbo and P. Hansbo. A finite element method for the simulation of strong and weak discontinuities in solid mechanics. *Computer Methods in Applied Mechanics and Engineering*, 193:3523–3540, 2004.

L. Hazard and P. Bouillard. Structural dynamics of viscoelastic sandwich plates by the partition of unity finite element method. *Computer Methods in Applied Mechanics and Engineering*, 196:4101–4116, 2007.

T. Hettich and E. Ramm. Interface material failure modeled by the extended finite-element method and level sets. *Computer Methods in Applied Mechanics and Engineering*, 195:4753–4767, 2006.

T. Hettich, A. Hund, and E. Ramm. Modeling of failure in composites by x-fem and level sets within a multiscale framework. *Computer Methods in Applied Mechanics and Engineering*, 197:414–424, 2008.

P.R. Heyliger and R.D. Kriz. Stress intensity factors by enriched mixed finite elements. *International Journal for Numerical Methods in Engineering*, 28:1461–1473, 1989.

R. Huang, J.H. Prévost, Z.Y. Huang, and Z. Suo. Channel-cracking of thin films with the extended finite element method. *Engineering Fracture Mechanics*, 70: 2513–2526, 2003a.

R. Huang, N. Sukumar, and J.H. Prévost. Modeling quasi-static crack growth with the extended finite element method, part ii: Numerical applications. *International Journal of Solids and Structures*, 40:7539–7552, 2003b.

A. Huerta and W. K. Liu. Viscous flow with large free surface motion. *Computer Methods In Applied Mechanics And Engineering*, 69:277–324, 1988.

T.J.R. Hughes. *The Finite Element Method Linear Static and Dynamics Finite Element Analysis*. Prentice Hall, 2000.

D.B.P. Huynh and T. Belytschko. The extended finite element method for fracture in composite materials. *International Journal for Numerical Methods in Engineering*, 77:214–239, 2009.

S. Hysing. A new implicit surface tension implementation for interfacial flows. *International Journal for Numerical Methods in Fluids*, 51:659–672, 2005.

T. Ishii, K. Terada, and T. Kyoya. Failure analysis of quasi-brittle materials involving multiple mechanisms on fractured surfaces. *International Journal for Numerical Methods in Engineering*, 67:960–988, 2006.

S.M. Jafar, T. Mousavi, and S. Mohadeseh. Modeling large sliding frictional contact along non-smooth discontinuities in x-fem. *International Journal of Modeling and Optimization*, 1:169–173, 2011.

H. Ji and J.E. Dolbow. On strategies for enforcing interfacial constraints and evaluating jump conditions with the extended finite element method. *International Journal for Numerical Methods in Engineering*, 61:2508–2535, 2004.

H. Ji, D. Chopp, and J.E. Dolbow. A hybrid extended finite element/level set method for modeling phase transformations. *International Journal for Numerical Methods in Engineering*, 54:1209–1233, 2002.

B.L. Karihaloo and Q.Z. Xiao. Modelling of stationary and growing cracks in fe framework without remeshing: A state-of-the-art review. *Computers and Structures*, 81:119–129, 2003.

K.H. Karlsen, K.A. Lie, and N.H. Risebro. A fast marching method for reservoir simulation. *Computational Geosciences*, 4:185–206, 2000. doi: 10.1023/a:1011564017218.

R. Keshavarzi and S. Mohammadi. Fully coupled modeling of interaction between hydraulic and natural fractures in naturally fractured reservoirs by xfem: The effect of pore pressure change. In *The 2nd International Conference on the Extended Finite Element Method (XFEM2011), Cardiff, UK,*, 2011.

A.R. Khoei and M. Nikbakht. Contact friction modeling with the extended finite element method (x-fem). *Journal of Materials Processing Technology*, 177:58–62, 2006.

A.R. Khoei, S.O.R. Biabanaki, and M. Anahid. Extended finite element method for three-dimensional large plasticity deformations on arbitrary interfaces. *Computer Methods in Applied Mechanics and Engineering*, 197:1100–1114, 2008.

A.R. Khoei, T. Mohammadnejad, and E. Haghighat. Modeling of crack propagation and fluid flow in multi-phase porous mediausing a modified x-fem technique. In *International Conference on Extended Finite Element Methods - XFEM 2011 June 29 July 1, Cardiff, United Kingdom*, 2011.

T.Y. Kim, J. Dolbow, and T. Laursen. A mortared finite element method for frictional contact on arbitrary interfaces. *Computational Mechanics*, 39:223–235, 2007.

A. Knapen, J. Poesen, G. Govers, G. Gyssels, and J. Nachtergaele. Resistance of soils to concentrated flow erosion: A review. *Earth-Science Reviews*, 80:75109, 2007. doi: 10.1016/j.earscirev.2006.08.001.

J. Korsawe, G. Starke, G. Wang, and O. Kolditz. Finite element analysis of poro-elastic consolidation in porous media. *Computer Methods in Applied Mechanics and Engineering*, 195:1096–1115, 2006.

P. Laborde, J. Pommier, Y. Renard, and M. Salaün. High-order extended finite element method for cracked domains. *International Journal For Numerical Methods In Engineering*, 64:354–381, 2005.

O. A. Ladyzhenskaya. *The Mathematical Theory of Viscous Incompressible Flow.* Gordon and Breach Science Publishers, 1969.

A. Lamb, G. Gorman, O. Gosselin, and A. Onaisi. Coupled deformation and fluid flow in fractured porous media using dual permeability and explicitly defined fracture geometry. *EAGE*, pages 14 – 17, 2010.

R. Larsson and M. Fagerström. A framework for fracture modelling based on the material forces concept with xfem kinematics. *International Journal for Numerical Methods in Engineering*, 62:1763–1788, 2005.

S.H. Lee, J.H. Song, Y.C. Yoon, G. Zi, and T. Belytschko. Combined extended and superimposed finite element method for cracks. *International Journal for Numerical Methods in Engineering*, 59:1119–1136, 2004.

A. Legay, J. Chessa, and T. Belytschko. An eulerian-lagrangian method for fluid-structure interaction based on level sets. *Computer Methods in Applied Mechanics and Engineering*, 195:2070–2087, 2006.

G. Legrain, N. Moës, and E. Verron. Stress analysis around crack tips in finite strain problems using the extended finite element method. *International Journal for Numerical Methods in Engineering*, 63:290–314, 2005.

G. Legrain, N. Moës, and A. Huerta. Stability of incompressible formulations enriched with x-fem. *Computer Methods in Applied Mechanics and Engineering*, 97:1835–1849, 2008.

R.W. Lewis, P. Nithiarasu, and K.N. Seetharamu. *Fundamentals of the Finite Element Method for Heat and Fluid Flow.* John Wiley and Sons, 2004.

S. Li and S. Ghosh. Extended voronoi cell finite element model for multiple cohesive crack propagation in brittle materials. *International Journal for Numerical Methods in Engineer*, 65:10281067, 2006.

W. Li, R.D. Liao, L.T. Liu, and X. Z. Zheng. Analysis of fretting crack propagation behavior with x-fem method. *Applied Mechanics and Materials*, 157-158:1162–1166, 2012.

T. Lin, Z. Lian, X. Zeng, Y. Cheng, and X. Liu. Simulation on crack growth of drill pipe with xfem. *Journal of Chongqing University*, 4:634, 2010.

F. Liu and R.I. Borja. A contact algorithm for frictional crack propagation with the extended finite element method. *International Journal for Numerical Methods in Engineering*, 76:1489–1512, 2008.

G.R. Liu and N.T. Trung. *Smoothed Finite Element Methods.* CRC Press, 2010.

X. Liu and S. Li. A variational multiscale stabilized finite element method for the stokes flow problem. *Finite Elements in Analysis and Design*, 42:580–291, 2006.

S. Loehnert and T. Belytschko. A multiscale projection method for macro/micro-crack simulations. *International Journal for Numerical Methods in Engineering*, 71:1466–1482, 2007.

F. Losassoa, R. Fedkiwa, and S. Osher. Spatially adaptive techniques for level set methods and incompressible flow. *Computers and Fluids*, 35:995–1010, 2005. doi: 10.1016/j.compfluid.2005.01.006.

E. Marchandisea, R. Jean-François, and N. Chevaugeon. A quadrature-free discontinuous galerkin method for the levelset equation. *Journal of Computational Physics*, 212:338–357, 2006. doi: 10.1016/j.jcp.2005.07.006.

P.M. Mariano and F.L. Stazi. Strain localization due to crack-microcrack interactions: X-fem for a multifield approach. *Computer Methods in Applied Mechanics and Engineering*, 193:5035–5062, 2004.

U.M. Mayer, A. Popp, A. Gerstenberger, and W.A. Wall. 3d fluidstructure-contact interaction based on a combined xfem fsi and dual mortar contact approach. *Computational Mechanics*, 46:53–67, 2010.

J.M. Melenk and I. Babuka. The partition of unity finite element method: Basic theory and applications. *Computer Methods In Applied Mechanics And Engineering*, 139:289–314, 1996.

T. Menouillard, J. Réthoré, A. Combescure, and H. Bung. Efficient explicit time stepping for the extended finite element method (x-fem). *International Journal for Numerical Methods in Engineering*, 68:911–939, 2006.

T. Menouillard, J. Réthoré, N. Moës, A. Combescure, and H. Bung. Mass lumping strategies for x-fem explicit dynamics: Application to crack propagation. *International Journal for Numerical Methods in Engineering*, 74:447–474, 2008.

R. Merle and J. Dolbow. Solving thermal and phase change problems with the extended finite element method. *Computational Mechanics*, 28:339–350, 2002.

G. Meschke and P. Dumstorff. Energy-based modeling of cohesive and cohesionless cracks via x-fem. *Computer Methods in Applied Mechanics and Engineering*, 196: 2338–2357, 2007.

G. Meschke and D. Leonhart. Recent advances in x-fem based crack modeling in the context of poromechanics. In *The 2nd International Conference on the Extended Finite Element Method (XFEM2011), Cardiff, UK*, 2011.

N. Moës, M. Cloirec, P. Cartaud, and J. F. Remacle. A computational approach to handle complex microstructure geometries. *Computer Methods in Applied Mechanics*, 192:3163–3177, 2003.

S Mohammadi. *XFEM Fracture Analysis of Composites*. Wiley-Blackwell, 2012.

N. Moës and T. Belytschko. Extended finite element method for cohesive crack growth. *Eng. Fract. Mech.*, 69:813–833, 2002. doi: 10.1002/nme.1675.

N. Moës, A. Gravouil, and T. Belytschko. Non-planar 3d crack growth by the extended finite element and level sets, part i: Mechanical model. *International Journal for Numerical Methods in Engineering*, 53:2549–2568, 2002.

N. Moës, E. Béchet, and M. Tourbier. Imposing dirichlet boundary conditions in the extended finite element method. *International Journal for Numerical Methods in Engineering*, 67:1641–1669, 2006.

W. Mulder, S. Osher, and J.A. Sethian. Computing interface motion in compressible gas dynamics. *Journal of Computational Physics*, 100:209–228, 1992. doi: 10.1016/0021-9991(92)90229-R.

N. Möes, J. Dolbowz, and T. Belytschko. A finite element method for crack growth without remeshing. *International Journal for Numerical Methods in Engineering*, 46:131–150, 1999.

S. Nakasumi, K. Suzuki, and H. Ohtsubo. Crack growth analysis using mesh superposition technique and x-fem. *International Journal for Numerical Methods in Engineering*, 75:291–304, 2008.

L.K. Nielsen, H. Li, X.C. Tai, S.I. Aanonsen, and M. Espedal. Reservoir description using a binary level set model. *Computing And Visualization In Science*, 13:41–58, 2008. doi: 10.1007/s00791-008-0121-1.

I. Nistor, O. Pantalé, and S. Caperaa. Numerical implementation of the extended finite element method for dynamic crack analysis. *Advances in Engineering Software*, 39:573–587, 2008.

J. Oliver, A.E. Huespe, and P.J. Sánchez. A comparative study on finite elements for capturing strong discontinuities: E-fem vs x-fem. *Computer Methods in Applied Mechanics and Engineering*, 195:4732–4752, 2006.

E. Olsson, G. Kreiss, and S. Zahedi. A conservative level set method for two phase flow ii. *Journal of Computational Physics*, 225:785–807, 2007.

S. Osher and R. Fedkiw. Level set methods: An overview and some recent results. *Journal of Computational Physics*, 169:463–502, 2001.

S. Osher and J.A. Sethian. Fronts propagating with curvature-dependent speed: Algorithms based on hamilton-jacobi formulations. *Journal Of Computational Physics*, 79:1249, 1988. doi: 10.1016/0021-9991(88)90002-2.

M. Pais, N.H. Kim, and T. Davis. Reanalysis of the extended finite element method for crack initiation and propagation. In *51st AIAA/ASME/ASCE/AHS/ASC Structures, Structural Dynamics, and Materials Conference, Orlando, Florida*, 2010.

T. Pannachet, L.J. Sluys, and H. Askes. Error estimation and adaptivity for discontinuous failure. *International Journal for Numerical Methods in Engineering*, 78:528–563, 2009. doi: DOI:10.1002/nme.2495,2009.

K. Park, J.P. Pereira, C.A. Duarte, and G.H. Paulino. Integration of singular enrichment functions in the generalized/extended finite element method for three-dimensional problems. *International Journal For Numerical Methods In Engineering*, 78:1220–1257, 2009. doi: 10.1002/nme.2530.

A. Peirce and E. Detournay. An implicit level set method for modeling hydraulically driven fractures. *Computer Methods in Applied Mechanics and Engineering*, 197: 2858–2885, 2008.

D. Peng, B. Merriman, S. Osher, H. Zhao, and M. Kang. A pde-based fast local level set method. *Journal of Computational Physics*, 155:410–438, 1999.

E. Pierres, M.C. Baietto, A. Gravouil, and G. Morales-Espejel. 3d two scale x-fem crack model with interfacial frictional contact: Application to fretting fatigue. *Tribology International*, 43:1831–1841, 2010. ISSN 0301-679X. doi: 10.1016/j.triboint.2010.05.004.

B. Prabel, A. Combescure, A. Gravouil, and S. Marie. Level set x-fem non-matching meshes: Application to dynamic crack propagation in elastic-plastic media. *International Journal for Numerical Methods in Engineering*, 69:1553–1569, 2007.

D. Rabinovich, D. Givoli, and S. Vigdergauz. Xfem-based crack detection scheme using a genetic algorithm. *International Journal for Numerical Methods in Fluids*, 71:1051–1080, 2007.

N. Ramanan and M.S. Engelman. An algorithm for simulation of steady free surface flows. *International Journal For Numerical Methods In Fluids*, 22:103–120, 1996.

G. Ranalli. *Rheology of the Earth*. Chapman and Hall, 1995.

G. Russo and P. Smereka. A remark on computing distance functions. *Journal of Computational Physics*, 163:51–67, 2000.

J. Réthoré, A. Gravouil, and A. Combescure. An energy-conserving scheme for dynamic crack growth using the extended finite element method. *International Journal for Numerical Methods in Engineering*, 63:631–659, 2005a.

J. Réthoré, A. Gravouil, and A. Combescure. A combined space-time extended finite element method. *International Journal for Numerical Methods in Engineering*, 64: 260–284, 2005b.

J.J. Ródenas, O.A. González-Estrada, J.E. Tarancón, and F.J. Fuenmayor. A recovery-type error estimator for the extended finite element method based on singular+smooth stress field splitting. *International Journal for Numerical Methods in Engineering*, 76:545–571, 2008.

T. Sawada and A. Tezuka. Llm and x-fem based interface modeling of fluid—thin structure interactions on a non-interface-fitted mesh. *Computational Mechanics Archive*, 48:319–332, 2011. doi: 10.1007/s00466-011-0600-y.

G. Schubert, D. L. Turcotte, and P. Olson. *Mantle Convection in Earth and Planets*. Cambridge University Press, 2001.

J. A. Sethian and P. Smereka. Level set methods for fluid interfaces. *Annual Review of Fluid Mechanics*, 35:341–372, 2003.

J.A. Sethian. A fast marching level set method for monotonically advancing fronts. *Proceedings of the National Academy of Sciences*, 93:1591–1595, 1996.

J.A. Sethian. *Level Set Methods and Fast Marching Methods: Evolving Interfaces in Computational Geometry, Fluid Mechanics, Computer Vision, and Materials Science*. Cambridge University Press, 1999.

J.A. Sethian. Evolution, implementation and application of level set and fast marching methods for advancing fronts. *Journal of Computational Physics*, 169: 503–555, 2001.

A. Shamloo, A. R. Azami, and A.R. Khoei. Modeling of pressure-sensitive materials using a cap plasticity theory in extended finite element method. *Journal of Materials Processing Technology*, 164–165:1248–1257, 2005.

A. Simone. Partition of unity-based discontinuous finite elements: GFEM, PUFEM, XFEM. *Revue Européenne de Génie Civil*, 11:1045–1068, 2007. doi: 10.3166/regc.11.1045-1068.

A. Simone, G.N. Wells, and L.J. Sluys. From continuous to discontinuous failure in a gradient-enhanced continuum damage model. *Computer Methods in Applied Mechanics and Engineering*, 192:4581–4607, 2003.

B.G. Smith, B.L. Vaughan, and D.L. Chopp. The extended finite element method for boundary layer problems in biofilm growth. *Communications in Applied Mathematics and Computational Science*, 2:35–56, 2007.

F.V. Souza and D.H. Allen. Modeling the transition of microcracks into macrocracks in heterogeneous viscoelastic media using a two-way coupled multiscale model. *International Journal of Solids and Structures*, 48:3160–3175, 2011. ISSN 0020-7683. doi: 10.1016/j.ijsolstr.2011.07.010.

F.L. Stazi, E. Budyn, J. Chessa, and T. Belytschko. An extended finite element method with higher-order elements for curved cracks. *Computational Mechanics*, 31:38–48, 2003.

M. Stolarska and D.L. Chopp. Modeling thermal fatigue cracking in integrated circuits by level sets and the extended finite element method. *International Journal of Engineering Science*, 41:2381–2410, 2003.

M. Stolarska, D. L. Chopp, N. Moës, and T. Belytschko. Modelling crack growth by level set in the extended finite element method. *International Journal for Numerical Methods in Engineering*, 51:943–960, 2001.

T. Strouboulis, L. Zhang, D. Wang, and I. Babuka. A posteriori error estimation for generalized finite element methods. *Computer Methods in Applied Mechanics and Engineering*, 195:852–879, 2006.

T. Strouboulis, L. Zhang, and I. Babuka. Assessment of the cost and accuracy of the generalized fem. *International Journal for Numerical Methods in Engineering*, 69:250–283, 2007.

N. Sukumar and J.H. Prévost. Modeling quasi-static crack growth with the extended finite element method, part i: Computer implementation. *International Journal of Solids and Structures*, 40:7513–7537, 2003.

N. Sukumar, N. Moës, B. Moran, and T. Belytschko. Extended finite element method for three-dimensional crack modelling. *International Journal For Numerical Methods In Engineering*, 48:1549–1570, 2000.

N. Sukumar, D.L. Chopp, N. Moës, and T. Belytschko. Modeling holes and inclusions by level sets in the extended finite-element method. *Computer Methods in Applied Mechanics and Engineering*, 190:6183–6200, 2001.

N. Sukumar, D.L. Chopp, and B. Moran. Extended finite element method and fast marching method for three-dimensional fatigue crack propagation. *Engineering Fracture Mechanics*, 70:29–48, 2003.

N. Sukumar, D.L. Chopp, E. Béchet, and N. Moës. Three-dimensional non-planar crack growth by a coupled extended finite element and fast marching method. *International Journal For Numerical Methods In Engineering*, 76:727–748, 2008.

M. Sussman and E. Fatemi. An efficient interface-preserving level set redistancing algorithm and its application to interfacial incompressible fluid flow. *SIAM Journal on Scientific Computing*, 20:1165–1191, 1999.

M. Sussman, P. Smereka, and S. Osher. A level set approach for computing solutions to incompressible two-phase flow. *Journal of Computational Physics*, 114:146–159, 1994. doi: 10.1006/jcph.1994.1155.

M. Sussmann, E. Fatemi, P. Smereka, and S. Osher. An improved level set method for incompressible two-phase flows. *Computers and Fluids*, 27:663–680, 1998.

J.E. Tarancón, A. Vercher, E. Giner, and F.J. Fuenmayor. Enhanced blending elements for xfem applied to linear elastic fracture mechanics. *International Journal for Numerical Methods in Engineering*, 77:126–148, 2009. doi: 10.1002/nme.2402.

R. Tezaur, L. Zhang, and C. Farhat. A discontinuous enrichment method for capturing evanescent waves in multiscale fluid and fluid/solid problems. *Computer Methods in Applied Mechanics and Engineering*, 197:1680–1698, 2008.

J.F. Unger, S. Eckardt, and C. Könke. Modelling of cohesive crack growth in concrete structures with the extended finite element method. *Computer Methods in Applied Mechanics and Engineering*, 196:4087–4100, 2007.

N. Vajragupta, V. Uthaisangsuk, B. Schmaling, S. Münstermann, A. Hartmaier, and W. Bleck. A micromechanical damage simulation of dual phase steels using xfem. *Computational Materials Science*, 54:271–279, 2012. doi: 10.1016/j.commatsci.2011.10.035.

S.P. Van der Pijl, A. Segal, C. Vuik, and P. Wesseling. A mass-conserving level-set method for modelling of multi-phase flows. *International Journal For Numerical Methods In Fluids*, 47:339–361, 2005.

B.L. Vaughan, B.G. Smith, and D.L. Chopp. A comparison of the extended finite element method with the immersed interface method for elliptic equations with discontinuous coefficients and singular sources. *Communications in Applied Mathematics and Computational Science*, 1:207–228, 2006.

G. Ventura, E. Budyn, and T. Belytschko. Vector level sets for description of propagating cracks in finite elements. *International Journal for Numerical Methods in Engineering*, 58:1571–1592, 2003.

F. J. Vernerey and M. Farsad. An eulerian/xfem formulation for the large deformation of cortical cell membrane. *Computer Methods in Biomechanics and Biomedical Engineering*, 433:14, 2011.

L. Vigneron, R. Boman, L. Noels, J.P. Ponthot, S. Warfield, P. Robe, and J. Verly. Fem and xfem based biomechanical models for advanced image-guided neurosurgery. In *5th European Congress on Computational Methods in Applied Sciences and Engineering (ECCOMAS 2008) June 30 July 5, Venice, Italy*, 2008.

M.V. Vigneron, L. Noels, S.K. Warfield, J.G. Verly, and A. R. Pierre. Serial fem/xfem-based update of preoperative brain images using intraoperative mri. *International Journal of Biomedical Imaging*, 2012, 2011. doi: 10.1155/2012/872783.

G.J. Wagner, N. Moës, W.K. Liu, and T. Belytschko. The extended finite element method for rigid particles in stokes flow. *International Journal for Numerical Methods in Engineering*, 51:293–313, 2001.

G.J. Wagner, S. Ghosal, and W.K. Liu. Particulate flow simulations using lubrication theory solution enrichment. *International Jour*, 56:1261–1289, 2003.

N. Watanabe and O. Kolditz. Mechanically enriched fracture elements for a hydromechanical problem in fractured rocks. In *The 2nd International Conference on the Extended Finite Element Method (XFEM2011), Cardiff, UK*, 2011.

F. M. White. *Fluid Mechanics*. McGraw-Hill Coorperation, 2006.

E. Wyart, D. Coulon, M. Duflot, T. Pardoen, J.F. Remacle, and F. Lani. A substructured fe-shell/xfe 3d method for crack analysis in thin walled structures. *International Journal for Numerical Methods in Engineering*, 72:757–779, 2007. doi: 10.1002/nme.2029.

E. Wyart, M. Duflot, D. Coulon, P. Martiny, T. Pardoen, J.F. Remacle, and F. Lani. Substructuring fe-xfe approaches applied to three-dimensional crack propagation. *Journal of Computational and Applied Mathematics*, 215:626–638, 2008.

Q.Z. Xiao and B.L. Karihaloo. Direct evaluation of accurate coefficients of the linear elastic crack tip asymptotic field. *Fatigue and Fracture of Engineering Materials and Structures*, 26:719–729, 2003.

Q.Z. Xiao and B.L. Karihaloo. Improving the accuracy of xfem crack tip fields using higher order quadrature and statically admissible stress recovery. *International Journal for Numerical Methods in Engineering*, 66:1378–1410, 2006.

Q.Z. Xiao and B.L. Karihaloo. Implementation of hybrid crack element on a general finite element mesh and in combination with xfem. *Computer Methods in Applied Mechanics and Engineering*, 196:1864–1873, 2007.

P.S. Yang, J.Y. Liou, and J.C. Sung. Infinite sequence of parallel cracks in an anisotropic piezoelectric solid. *Computer Methods in Applied Mechanics and Engineering*, 197:3858–3861, 2008.

T.T. Yu. The extended finite element method (xfem) for discontinuous rock masses. *Engineering Computations*, 28:340–369, 2011.

Y. Zhang, W. Zhang, and M. Shi. Gpu accelerated xfem and its applications in the simulation of underground excavation. In *International Conference on Extended Finite Element Methods - XFEM Cardiff, United Kingdom*, 2011.

H.K. Zhao, T. Chan, B. Merriman, and S. Osher. A variational level set approach to multiphase motion. *Journal of Computational Physics*, 127:179–195, 1996.

G. Zi and T. Belytschko. New crack-tip elements for xfem and applications to cohesive cracks. *International Journal for Numerical Methods in Engineering*, 57: 2221–2240, 2003.

O. C. Zienkiewicz and R. L. Taylor. *The Finite Element Method Fluid Dynamics Volume 3*. Butterworth-Heinemann, 2000.

A. Zilian. Modeling and enriched approximations for multi-field problems in engineering applications. In *International Conference on Extended Finite Element Methods - XFEM 2011 June 29 July 1, Cardiff, United Kingdom*, 2011. doi: 10.1080/10255842.2010.531273.

S. Zlotnik and P. Diez. Hierarchical x-fem for n-phase flow (n>2). *Computer Methods in Applied Mechanics and Engineering*, 198:2329–2338, 2009. doi: 10.1016/j.cma.2009.02.025.

S. Zlotnik, P. Díez, M. Fernández, and J. Vergés. Numerical modelling of tectonic plates subduction using x-fem. *Computer Methods in Applied Mechanics and Engineering*, 196:4283–4293, 2007.